5-15-2015

Methane Occurrence in Domestic Wells Overlying the Marcellus Shale

Kayla Christian
Syracuse University

Abstract

This study explores whether spatial parameters (e.g. landscape position, distance to nearest gas well, geologic unit of water extraction) corresponded with the spatial distribution of methane concentrations in domestic drinking water wells overlying the Marcellus Shale in New York State, where unconventional shale gas extraction is currently banned. Domestic groundwater wells (n=204) were sampled across five counties (Broome, Chemung, Chenango, Steuben, and Tioga) in New York from 2012-2014. Based on analysis of water from homeowner wells sampled in 2013 the majority of samples (77%) had low concentrations of methane (< 0.1 mg/L), and only 5% of wells (n=7) had actionable levels of methane (> 10 mg/L), in the absence of shale gas production. Dissolved methane concentrations are not strongly correlated with landscape position, as observed in prior studies, nor other parameters indicative of subsurface planes of weakness (i.e. faults or lineaments). The distribution of elevated methane levels was most strongly correlated with Na-HCO_3 water type. While the majority of all groundwater samples (55%) were classified as Ca-HCO_3-type waters, 93% of those wells have <0.1 mg/L of dissolved methane. The distribution of methane between Ca-HCO_3 (n=76) and Na-HCO_3 (n=23) water types was significantly different ($p<0.001$) with mean methane concentrations of 0.3 and 3.8 mg/L, respectively. Methane isotopic compositions of a subset of samples suggest a thermogenic or mixed origin for methane. Results suggest that shallow groundwater mixing with deeper Na-Cl and Na-HCO_3 type water charged with thermogenic methane from Upper Devonian shales might occur more frequently in the fractured bedrock upland regions than previously suspected.

Methane Occurrence in Domestic Wells Overlying the Marcellus Shale

By

Kayla M. Christian

B.S., University of Illinois at Chicago, 2013

MASTERS THESIS

Submitted in partial fulfillment of the requirements for the degree of
Master of Science in Earth Sciences

Syracuse University

May 2015

Acknowledgements

I'd especially like to thank my advisor Laura Lautz for her encouragement throughout my time here in Syracuse, as well as my committee members Don Siegel and Greg Hoke and chair Zunli Lu for all their advice and support over the past two years. A special thanks to all of the people that assisted in the field work over the past three summers, without whom I would not have this amazing dataset: Max Gade, Karolina Lubecka, Anthony Carrancejie, Sushyne Hummel, Egan Waggoner, and Natalie Teal. Finally, thanks to all of the graduate students and faculty who made my time here at Syracuse so memorable.

Table of Contents

List of Tables

List of Figures

Introduction

The Marcellus shale is a gas-bearing middle Devonian formation deposited in the Appalachian basin and underlies regions of New York (NY), Pennsylvania (PA), Ohio, and West Virginia. Development of unconventional shale gas extraction methods (e.g. directional drilling and high volume hydraulic fracturing), has led to a surge in the number of gas wells completed in the Marcellus shale in recent years (Vidic et al., 2013). One of the largest shale gas plays in the U.S, the Marcellus is estimated to have 141 trillion cubic feet (TCF) of technically recoverable dry thermogenic natural gas (EIA 2012; Kargbo, 2010). To put that volume in perspective, total U.S consumption of natural gas in 2014 was 26.7 TCF (EIA, 2014). Development of the Marcellus has generated millions of dollars in state and federal tax revenue and created tens of thousands of jobs (Considine et al., 2010). Despite the economic benefits, there are societal concerns regarding the impact of unconventional hydraulic fracturing on water resources and water quality that have drawn heightened media attention and influenced political decisions surrounding the issue (Soeder, 2010; Vengosh et al., 2013; Vidic et al., 2013). Unconventional extraction methods are currently used to produce gas from the Marcellus in all of its overlying states, with the exception of NY, where the Marcellus underlies an area of approximately 48,433 km^2 (NYSDEC, 2011). In 2010, the NY state legislature established a moratorium on unconventional gas drilling in the state, which lasted a number of years, before the state's ultimate decision to officially ban the process in 2014. As such, NY provides a unique opportunity to understand the natural occurrence of dissolved methane in the absence of unconventional gas extraction in regions overlying the Marcellus.

Concerns for potential stray gas migration to shallow groundwater aquifers (e.g. Entrekin et al., 2011; Kargbo et al., 2010), which provide water to domestic wells in the region, have prompted numerous studies of the natural variability of groundwater methane concentrations in areas of NY, PA, and West Virginia underlain by the Marcellus shale. In New York, methane occurs naturally in groundwater wells, primarily at low concentrations (< 1 mg/L), but occasionally in amounts which exceed the solubility in water and present an explosive hazard (Kappel, 2013; Kappel & Nystrom, 2012; Heisig & Scott, 2013; McPhillips et al., 2014; Molofksy et al., 2013; and Eltschlager et al, 2001). Gas production may introduce additional stray gas into shallow groundwater aquifers due to faulty seals on gas production wells, or enhanced migration of methane along fracture pathways during the drilling processes (Vidic et al. 2013). The potential for stray gas contamination of shallow groundwater in areas with unconventional gas production creates a need for effective means of distinguishing between natural and anthropogenic methane occurrence, while recognizing the extended history of historical gas production from conventional wells. This necessitates additional baseline water quality information and a greater understating of dissolved methane variability in groundwater prior to unconventional gas extraction, to evaluate allegations of contamination (Davies, 2011; Molofsky et al., 2013). Given the similar regional geology, climate, and land use across areas underlain by the Marcellus, studies in NY can be considered representative of natural methane occurrence prior to high volume hydraulic fracturing in an area with historical and continuous conventional gas development.

Prior work clearly demonstrates there is natural occurrence of methane in shallow groundwater throughout the Marcellus shale play, and specifically in southern NY (Kappel & Nystrom, 2012; Heisig & Scott, 2013; McPhillips et al., 2014; Boyer et al., 2012; Mathes &

White, 2006; and Molofksy et al., 2013). Natural surface seeps of methane have been observed in NY along faults or laterally from swamps (Kappel & Nystrom, 2012), with low levels of dissolved methane present in shallow groundwater throughout the state, and localized occurrences of elevated methane concentrations above 10 and 28 mg/L (Kappel, 2013). In NY, natural gas has been observed in groundwater drawn from upper Devonian bedrock, the Tully limestone, surficial glacial till deposits, and in the Hamilton group above the Marcellus. Isotopes of methane and higher chain hydrocarbons (C_1-C_5) have been used to identify sources of natural gas in groundwater and reflect the geochemistry and thermal maturity of natural gas in the source rock. Upper and middle Devonian formations are less thermally mature in central NY, relative to northeastern PA (Repetski et al., 2008). Methane isotopes from the upper and middle Devonian formations in central NY are, on average, $\delta^{13}C$-CH_4 of -44.7 +/- 3.9 ‰, compared to -36.3 +/- 3.0 ‰ in lower Devonian and Silurian formations (Jenden, 1993).

Prior studies of patterns of elevated methane concentrations in the Marcellus shale region have focused on hydrogeologic setting and environmental drivers, such as well proximity to gas production areas. In PA, NY, and West Virginia, elevated methane concentrations in domestic wells have been linked to topographic position, specifically lowland valleys (Molofsky et al. 2011; Heisig & Scott, 2013; Mathis & White, 2006). However, the correlation between landscape position and methane is not consistently observed, even within similar study areas. Near the PA border, in Susquehanna County, Jackson *et al.* (2013) observed no correlation between elevated methane concentrations and proximity to valley bottoms, but rather cited proximity to gas wells as the primary driver for elevated methane. Conversely, in the same study region, Molofsky *et al.* (2013) observed a significant correlation between topographic position and methane concentration, and found upper range methane concentrations occurred more

frequently in valley versus upland water wells. Analysis of an expansive dataset of groundwater quality data from groundwater wells throughout northeastern PA revealed no relationship between methane concentrations in domestic wells and proximity to existing gas wells (Siegel et al., 2015). Similar to the findings in PA, two studies in southern NY noted contradictory evidence for the importance of landscape position in conjunction with aquifer confinement on the distribution of methane concentrations in domestic wells (Heisig & Scott, 2013; McPhillips, et al., 2014).

Use of publically available water quality data to assess impacts of shale development in the Marcellus are hindered by the presence of pre-existing elevated methane concentrations (Brantley et al., 2014). Understanding the occurrence of dissolved methane levels prior to high volume hydraulic fracturing in aquifers with a history of natural methane occurrence and historical conventional gas drilling is important for evaluating future contamination (Davies, 2011; Molofsky et al., 2013). Prior studies have also noted the need for a larger randomized sampling size and increased sampling density (Davies, 2011; Saba & Orzechowski 2011; McPhillips et al., 2014; Kappel, 2013). The goal of this study is to further interrogate relationships between landscape parameters and natural occurrence of methane in shallow groundwater overlying the Marcellus shale. We build on prior work by expanding the geographic study area, while maintaining a high density of randomly-selected observation sites to provide a comprehensive analysis of natural occurrence of methane in the region. This study also complements similar studies in the region by providing an increased number of isotopic data in upland areas, examining temporal changes in methane concentrations, and evaluating the influence of faults and lineaments on gas levels. Well and spatial proximity parameters addressed

in this study include: well depth, topographic position, geologic setting, stratigraphic unit of water extraction, and distance to nearest road, fault, and active or other gas wells.

Study Area

The study area extends across five counties in NY (Broome, Chemung, Chenango, Steuben, and Tioga counties), which lie along the border of NY and PA (Figure 1). This region is primarily underlain by upper Devonian shale and sandstone, transitioning from the lower Canadaway in the southwestern region of the study area, into the West Falls, Sonyea, Genesee and older middle Devonian Hamilton Group shale towards the northwest. The underlying bedrock is sedimentary rock of Cambrian, Ordovician, Silurian, and Devonian age, which gently dips southward and is overlain by discontinuous glacial till, with an unsorted mixture of clay, silt, sand, and boulders in the uplands and stratified silt, clay, and outwash sand and gravel in the valleys (Williams, 2010).

In the western part of the study region (Steuben and the majority of Chemung County), the Chemung River trends northwest to southeast before merging with the Susquehanna River in northern Pennsylvania. To the west, in Tioga, Broome, and Chenango Counties, the Upper Susquehanna River flows from the northeast into Pennsylvania. In general, throughout the study area, uplands are bedrock overlain by thin layers of glacial till, with thicker layers of glacial till and alluvium lining the river valleys (Miller et al., 1982; McPherson, 1993). The river valleys are lined with glacial material and make up the primary and principal aquifers mapped by the U.S Geologic Survey (USGS). In upland regions the groundwater source is primarily fractured bedrock, and freshwater zones observed to circulate to greater depths in upland areas relative to valleys (Williams, 2014).

Methods

Site Selection

A total of 203 domestic groundwater wells were sampled in the summers of 2012 and 2013 across 5 counties (10,231 km^2) in Southern NY (Broome, Chenango, Chemung, Steuben, and Tioga Counties). Sampling locations were chosen from an online database of domestic wells drilled in the region since 2000, which is collected and maintained by the NY State Department of Environmental Conservation (NYSDEC) and made available from the NY state GIS Clearinghouse (https://gis.ny.gov/). To obtain a large distribution of randomly selected domestic wells, three wells were indiscriminately chosen within each cell of a 7 by 7 km grid overlain across the study area. This process generated approximately 750 candidate wells. We solicited landowner participation in our study by contacting well owners by mail using tax parcel data for the location of the candidate wells. This methodology produced a total sample size of 203 groundwater samples across the study area. In addition to taking water samples, homeowners were also surveyed regarding their well water quality and well construction.

Sample Collection and Analysis

Untreated well water was purged from each well until a stable temperature was reached, which typically took 5-10 minutes. Samples were collected from an indoor or outdoor spigot that bypassed any water treatment systems or, in a few instances, collected directly from the home's pressure tank. Field measurements of pH, temperature, and electrical conductivity were taken with a WTW 340i probe. Groundwater samples were filtered with a 0.45-µm filter into two 125-ml polypropylene bottles, one acidified to a pH less than 2 (3-4 drops nitric acid) and one left un-acidified, to analyze for trace metals and dissolved ions, respectively. Samples were analyzed for major dissolved ions and $\delta D\text{-}H_2O$ and $\delta^{18}O\text{-}H_2O$ isotopes at the Syracuse University Department of Earth Sciences Hydrology Laboratory. Major ions (Na^+, NH_4^+, K^+, Ca^{2+}, Mg^{2+}, F^-, Cl^-, Br^-,

NO_3^-, PO_4^{3-}, SO_4^{2-}) were analyzed using a Dionex ICS-2000 ion chromatograph. Isotopes of water were measured using a Picarro L2130-i Cavity Ringdown Spectrometer. Trace metal analysis for Li, B, Al, P, Mn, Fe, Zn, Sr, Ba, Pb, and Se in water samples were measured using an Elan DRC-e Inductively Coupled Plasma Mass Spectrometer (ICPMS) at the State University of NY College of Environmental Science and Forestry Analytical and Technical Services Laboratory. Halogen analyses for Br and I were done using a Bruker Daltronics Aurora M90 Quadrupole based ICPMS at Syracuse University. A subset of 35 samples was selected for strontium isotopic analysis ($^{86}Sr/^{87}Sr$) by thermal ionization mass spectrometry (TIMS) at the Radiogenic Isotope Laboratory at the Massachusetts Institute of Technology (MIT) and data from this analysis can be found in.

A total of 137 of the samples collected in 2013 were analyzed for dissolved methane. These samples were collected in two 100-mL glass vials with no headspace, one acidified with hydrochloric acid. Dissolved methane concentrations were measured at the University of Rochester by the headspace equilibration technique and gas chromatography (GC), using a Shimadzu GC-14A equipped with a flame ionization detector (FID). The minimum detection limit (MDL) for the method was 0.0001 mg/L; detections below this limit were treated as equal to the MDL. Of these samples, 21 sites were resampled in the summer of 2014 for methane concentration and methane isotopic analysis of $\delta^{13}C\text{-}CH_4$ and $\delta D\text{-}CH_4$. Samples for methane isotope analysis were collected in 60-ml glass vials with silicone lined caps and measured at the University of California at Davis Stable Isotope Facility. Raw data for all chemical constituents and isotopic data evaluated in this study can be can be found in Appendix A.

Spatial Data Analysis

Various well and spatial parameters were compiled for the sampled wells to identify potential correlations with methane concentrations. Similar groundwater studies in NY and PA

have noted a correlation between the topographic position of a well and the dissolved methane concentration in groundwater (Heisig & Scott 2013; Molofsky et al. 2013). In NY, valley wells completed in confined bedrock were shown to have higher dissolved methane concentrations than those in upland settings (Heisig & Scott, 2013). However, multiple methods for the delineation of landscape position have been suggested, including: (1) delineation of valley extent based on a synthetic stream network from a 1/3 arc second 10 meter digital elevation model (DEM, Heisig & Scott 2013) (2) well proximity to major and minor flowlines in the national hydrography dataset (Molofsky et al. 2013); and (3) well position within USGS mapped valley fill aquifers (McPhillips et al. 2014). The first method above, which is based on a synthetic stream network derived from a DEM, is the most comprehensive method of determining valley extent because it takes into account valley slope and topographic relief, but is also time-consuming to implement. To understand how the choice of method affects well classification and associated correlation with methane levels, all three methods are used and compared.

Although much attention has been given to valley setting as an important predictor of elevated methane concentrations, the orientation and size of valleys are controlled primarily by prior glacial activity in southern NY. However, Heisig & Scott (2013) noted that valley orientation can occasionally be a reflection of regional joint, lineament, or fault orientation. Throughout NY State, Jacobi (2002) delineated a large number of faults, some identified by methane detection in the overlying soil, and lineaments. For this reason, in addition to landscape position, we evaluated well proximity to faults (Jacobi, 2002) or lineaments (EARTHSAT, 1997) (Appendix B, Fig S1a).

Potential for gas migration to domestic wells from historical gas production areas was assessed based on domestic well proximity to active (n=125) and presumed inactive (n=245) gas

wells (Appendix B, Fig S1b). from available 2013 NYSDEC data (http://www.dec.ny.gov/energy/1603.html). Gas wells were classified based on the well status as either active or other (all remaining classifications, including inactive, plugged and abandoned, temporarily abandoned, unknown, etc). Well proximity to roads and highways were also examined (Appendix B, Fig S1c). GIS files of New York State (NYS) roads were obtained from the NYS GIS Clearinghouse, with highways classified as major U.S routes and interstate highways.

Geologic Setting

The geologic unit of completion for each groundwater well was determined based on well depth information and contoured maps of the stratigraphic base elevation for the Dunkirk, Java, West Falls, Sonyea, Genesee, and Hamilton formations, as well as isopach maps of the Java, West Falls, Sonyea, Genesee, and Hamilton upper Devonian geologic groups prepared by the Eastern Shale Gas Project (EGSP) and Morgantown Energy Technology Center (METC) (EGSP, 1980). These maps, in conjunction with the location of the surface contact between stratigraphic groups on a geologic map, were used to generate interpolated elevation surfaces of the contacts between geologic groups underlying the study area. The bedrock of well completion was determined based on the elevation of the maximum well depth, relative to the bedrock contact surfaces. When the bedrock unit of completion was ambiguous, due to limited spatial extent of some bedrock surface data, wells were classified as being from one of two potential stratigraphic units. This classification method was compared to classifications based solely on the well location on a geologic map of the study area (Fisher, 1970). A detailed discussion on how to determine the geologic group of well completion can be found in the documentation (Appendix C).

Statistical Analysis of Data

Multiple statistical methods have been used to asses which parameters are the best predictors of variability in methane concentrations in shallow groundwater overlying the Marcellus. Due to the typically skewed distribution of methane concentrations, non-parametric statistical tests are often used. Mann-Whitney U, Kruskal-Wallis, and Tukey's tests, all non-parametric, have been used to determine the significance of observed differences in methane concentrations between discretely grouped wells (McPhillips et al., 2014; Molofsky et al., 2013; Heisig & Scott, 2013; Jackson, 2013). The Mann-Whitney U statistical test evaluates whether two sample sets are drawn from equivalent distributions (a non-parametric analogue to a t-test), while the Kruskall-Wallis test extends to more than two groups (a non-parametric ANOVA). Tukey's tests, provided the distributions are not equal, is used in conjunction with ANOVA to determine which groups significantly differ (Helsel & Hirsch, 2012).

In the case of continuous explanatory variables, rather than discrete groups, Pearson and Spearman correlations (parametric and non-parametric, respectively) have been used to determine the significance of observed relationships between methane and various explanatory variables (Jackson et al., 2013). Pearson correlation coefficients are a measure of the linear correlation between continuous variables and are most appropriate for normally distributed data. The Spearman correlation coefficient is a more robust non-parametric test for a monotonic relationship between variables that is not strongly influenced by outliers. Similar to the Spearman correlation coefficient is the Kendall τ coefficient, which measures the strength of association between two values (Helsel & Hirsh, 2002).

Mann-Whitney U non-parametric tests have been used in NY and Pennsylvania studies to assess differences in dissolved methane concentrations in wells grouped by landscape position (upland or valley) and/or proximity (<1 km or >1 km) to gas wells (McPhillips et al., 2014;

Molofsky et al., 2013). Comparatively, Jackson (2013) used a Kruskall-Wallis test on wells grouped by proximity to natural gas wells using a 1 km threshold and Pearson and Spearman correlations to evaluate the relationship between methane concentrations and well proximity to gas wells and stream valley bottoms. In Heisig & Scott (2013), a Kruskal Wallis test was used to asses significant differences between median methane concentrations for wells grouped by landscape position and well confinement, and those with significant differences were further analyzed using Tukey's test to determine which median concentrations differed among groups.

For this study, significance of continuous relationships between methane concentrations and solute concentrations and proximity parameters (e.g. distances to nearest gas wells, faults) were evaluated using Pearson, Spearman, and Kendall τ coefficients. Statistical tests were performed using non-transformed and log-transformed data for both methane and solute concentrations.

The full dataset of well proximity in relation to the spatial parameters analyzed in this study, as well as the resulting classifications for landscape position and geologic unit of well completion using the described methods can be found in Appendix B.

Results

A majority of the wells sampled in 2013 (n=137) had dissolved methane concentrations <0.001 mg/L CH_4 (n=95). Spatially, the highest methane concentrations occurred predominantly in Steuben County, and to a lesser extent, Chenango County (Fig. 2). The majority of observed methane concentrations were low, with 66% of wells containing <0.1 mg/L CH_4. Seven samples (5.1% of those sampled) had methane concentrations >10 mg/L, with a maximum observed concentration of 28.7 mg/L CH_4 (Fig. 3). This sample was the only to exceed the U.S Office of Surface Mining and Reclamation Enforcement hazard level of 28 mg/L, when gas levels become

potentially explosive (Eltschlager, et al., 2001). Analysis of dissolved methane concentrations in wells sampled in 2013 and 2014 indicates some variability between years (see Appendix A. Figure S1).

The piper diagram (Fig. 4) illustrates that groundwater type throughout the study area is primarily Ca-HCO_3 with relatively elevated methane levels associated with Na-HCO_3 type water. Samples classified by groundwater type based the piper diagram (Fig. 5), indicate that dissolved methane concentrations in 14 samples (or 50%) of Na-HCO_3 or Na-HCO_3-Cl type waters, had above 1 mg/L CH_4. The majority of all samples (55%) were classified as Ca-HCO_3 type waters and 93% of Ca-HCO_3 type waters have < 0.1 mg/L of dissolved methane. The distribution of dissolved methane concentrations between water types ($p<0.001$, Kruskall Wallis) and between Ca-HCO_3 and Na-HCO_3 ($p<0.001$, Mann-Whitney U) were significantly different; with mean methane concentrations of 0.3 and 3.8 mg/L for Ca-HCO_3 and Na-HCO_3 respectively.

Three methods for classifying the topographic position of wells were compared: generation of valley extent using a synthetic stream network derived from a DEM ("DEM-based") (Fig. 6a); proximity to major and minor National Hydrography Data flowlines ("NHD method") (Fig. 6b); and well location ("mapped valley aquifer method") (Fig. 6c). Of the wells sampled for methane (n=137), 55% were classified the same (n=76) across all three methods (Appendix B, Table S3). The mapped aquifer-method classified the topographic position of the majority of wells as upland and the Mann-Whitney U test for significance between methane and landscape position using this method was significant. However, a disproportionately large number of wells were classified as occurring in upland settings (n=117) for the mapped valley aquifer method, relative to either of the other two methods (Fig 6f).

Mann-Whitney U tests show no significant differences between methane concentrations in valleys compared to uplands when classified by the DEM-based method. However the NHD method yielded statistically significant differences ($p=0.04$) with mean methane concentrations slightly higher in upland wells (mean=0.88 and 1.9 mg/L for upland and valley wells, respectively). When wells are classified using the mapped valley aquifer method, differences between methane distributions in valleys versus uplands are significant ($p=0.01$), but concentrations are higher in uplands, contrary to prior findings (Molofsky et al., 2013; Heisig & Scott, 2013). Because a disproportionately large number of wells were classified as in uplands when using the mapped valley aquifer method for classifying landscape position, it is unlikely the differences between the groups are meaningful. Spearman, Pearson and Kendall τ coefficients between methane concentrations and landscape position (expressed as distance to closest major or minor NHD flowlines) were not significant ($p>0.05$).

Two methods were used to determine the geologic group of well completion (Fig. 7). The first was the "bedrock contact interpolation method," which classified wells based on the elevation of the maximum well depth and the interpolated elevations of the underlying bedrock contact surfaces. The second "geologic map" method classified wells based solely on their location on a geologic map. Table 1 shows the contingency table for instances where the bedrock contact interpolation method classified wells the same or differently than the geologic map method. Wells classified differently using the two methods were generally determined to be in the next stratigraphically older (or deeper) unit when classified by the bedrock interpolation method, rather than the geologic map method, or as being in either the same or adjacent group in locations where contact surfaces were unavailable. Wells with "error" classifications reflect instances where the interpolated surface method classified wells as completed in a geologic

group not present at that location (i.e the geologic group outcrops south of the well location). The highest methane concentrations occurred in wells completed in the West Fall group, which underlies the majority of the study area, with a few high methane samples observed in the Sonyea or Genesee formations (Fig 8). The Kruskall-Wallis test for differences in the methane concentrations across geologic units shows no statistically significant differences. However, the bedrock surface interpolation method only considers the total well depth in relation to the interpolated geologic surfaces, and does not attempt to differentiate between those wells classified as above the base of a geologic unit which could be completed in till or glacial sediment.

The distribution of methane concentrations was not affected by well distance to nearest proximity parameter (Fig. 9). Pearson, Spearman, and Kendall τ coefficients between methane concentrations and various proximal variables (distance to nearest faults, lineaments, active and other gas wells, roads and highways) hypothesized to influence methane levels were not significant ($p>0.05$), with the exception of distances to nearest highways (Table 2). However, distances to nearest highways were only weakly, negatively correlated with methane concentrations (coefficients ranged from -0.2 to -0.3) Correlations between methane concentrations and other chemical constituents were significant for Na, NH_4, F, Sr, Ba, Br, and I (Table 3).

Isotopes of methane, $\delta^{13}C\text{-}CH_4$ and $\delta D\text{-}CH_4$, suggest the sources of methane to our sampled wells were primarily thermogenic associated gases (T, T_c), with one sample in the range of non-associated (T_m) dry gases (Fig 10a). Six samples had isotope values indicative of a mixed origin, with very few samples showing a biogenic signature. Isotope values for the highest

methane concentrations (>10 mg/L) clustered between -250 and -270 and -49 and -52 for δD-CH_4 and $\delta^{13}C$-CH_4, respectively. Isotopes of methane for samples with between 0.1 and 1 mg/L CH_4 were scattered between biogenic, mixed, and thermogenic. For comparison, isotopes of methane from samples collected from organic-rich shale from neighboring Allegheny county (D6-D10; Osborn et al, 2010) and samples collected from the Marcellus shale (D60-62; Osborn et al, 2010) and Trenton/Black River Group (O74; Osborn et al, 2010) from Steuben county were used as a first approximation for local shale gas signatures in the region (Fig. 10b).

The methane isotopic signature of groundwater wells (this study) and an additional 60 wells from a USGS study within the same area (Heisig & Scott, 2013), were compared to the methane isotopic signature of gas from local Upper Devonian and Ordovician Trenton-Black River river formation (Osborn & McIntosh, 2010), and regional samples of Marcellus gas from NY and PA (Osborn & McIntosh, 2010; Molofsky et al., 2013). Samples of the Marcellus gas from NY (D60) and PA (D61-62) in Washington County (Osborn & McIntosh, 2010) and free gas from Susquehanna Co. (Molofsky et al., 2013) have different isotopic signatures, reflecting of the variations in the thermal maturity between localities. The isotopic composition of methane samples of the Upper Devonian shales used for comparison were sampled from nearby Allegheny County, and these formations likely outcrop at the surface before entering our study area. Samples taken from local NY formations show a trend in increasing thermally maturity from the Upper Devonian formations to the Ordovician Trenton-Black River group. Groundwater samples fall within the thermogenic range of Upper and Middle Devonian formations, but none of the groundwater samples are as enriched in $\delta^{13}C$-CH_4 as the Trenton-Black River group.

Discussion

As shown in previous studies, occurrence of dissolved methane in shallow groundwater is common in areas overlying the Marcellus shale, with 14% of sampled wells having >1 mg/L CH_4 and 5.1% having >10 mg/L CH_4. Detectable levels of methane (>0.001 mg/L) were found in the majority of wells sampled. Multiple studies have attributed elevated methane concentrations in the region with valley lowlands (Molofsky et al., 2013; Heisig & Scott, 2013) or proximity to existing gas wells (Osborn et al., 2011; Jackson et al., 2013), and with Na-HCO_3 groundwater type (McPhillips et al., 2014; Siegel et al., 2015), although these attributes have had varied success as predictors of high methane concentrations.

The association between landscape position of a well and elevated methane concentrations is based on the conceptual model that valley wells are proximally closer to the interface of fresh groundwater and saline groundwater charged with methane seeping upward through the underlying fractured bedrock (Heisig & Scott, 2013). In PA, methane concentrations in 1,701 predrill samples in Susquehanna County were found to be significantly higher in wells completed in lowlands compared to upland settings using a one-way Mann-Whitney U test (Molofsky et al., 2013). Conversely, a similar study in the same area, although with a smaller sampling density, discerned no correlation between methane concentrations and proximity to valleys (Jackson et al., 2013). Similar contradictory findings have been observed in NY as well. A USGS study that sampled 60 homeowner wells across a large study area (4,687 km^2), equivalent to a sampling density of 1.2 wells per 100 km^2, found topographic position and well confinement to be strong predictors of high methane concentrations (Heisig & Scott, 2013). A higher density study of 113 wells in a smaller study area (2,315 km^2 ; 5 wells per 100 km^2) found methane concentrations in wells were not influenced by topographic position (McPhillips et al, 2014). This study, with the largest study area and a sampling density of 1.3 wells per 100 km^2,

found landscape position provided conflicting results with regard to the significance of methane distributions in wells classified based on topographic position. This study suggests the method chosen to classify the topographic position of a well may influence the significance of this parameter as a mechanism influencing the distribution of elevated methane concentrations. Elevated methane concentrations appear to be isolated geographically and the topographic position of wells with elevated methane is not consistently valley lowlands. This finding does not appear to be an issue of sample size or distribution. This could be in part, that the sampling strategy used in this study was more favorable to upland settings. Efforts to sample a large number of domestic wells over such a large study area was inherently favorable to uplands. One suggestion to overcome this would be to combine data from all prior work in the study area, including data from Heisig and Scott (2013) and McPhillips et al. (2014). However, while this would create a larger database for statistical analysis, difference in well selection criteria may bias the analysis. For example, the Heisig and Scott (2013) study intentionally sampled wells greater than 1 km from an existing gas well, so using the data set in analysis of distance to gas wells could bias results. Furthermore, addition of the McPhillips et al. (2014) data set would result in an oversampling of Chenango County compared to the rest of the study area. The distribution of methane between these datasets may also be different, calling into question the comparability of these different sample populations.

Multiple statistical approaches were used to evaluate the relationship between methane concentrations and landscape position and distance to gas wells, to better understand how the choice of statistical test presented in previous studies might influence the significance of these relationships. Excluding classifications based on the regional aquifer method, which classified a disproportionate number of wells as occurring in upland settings, no statistical difference in the

methane concentrations was observed in wells based on landscape position for Mann-Whitney U test, contradictory to previous studies (Molofsky et al., 2013; Heisig & Scott, 2013). Using a statistical approach similar to Jackson et al (2013), the Pearson, Spearman, and Kendall τ coefficients between methane and proximity to valley bottom streams defined by NHD flowlines were also not significant.

At a linear scale, elevated methane concentrations visually appear to correspond to proximity to fault, lineaments, and gas wells (Fig. 9). Because of the heavily skewed distribution of methane concentration toward lower concentrations, empirical observations of the influence of well distance to proximity parameters must be evaluated using a log scale. Siegel et al. (2015) noted the high percentage of samples at low concentrations presents a visually misleading depiction of the relationship between methane and proximity to oil and gas wells at linear scale. This remains true for all of the proximity parameters investigated in this study. The lack of any relationship between methane concentrations and active or other gas wells in the study area suggests that conventional gas drilling has not influenced that distribution of elevated methane levels in groundwater for this region

As observed in previous studies, the association between elevated methane concentrations and Na-HCO_3 type waters is likely the result of carbonate dissolution in the underlying shale bedrock and subsequent cation exchange between calcium and sodium over long residence times. The evolutionary trend from Ca-Mg-HCO_3 to Na-HCO_3 type waters, and corresponding shift in redox conditions to more reducing, favors methanogenesis (Kreese, 2012). However, isotopes of methane indicate sources are primarily thermogenic or mixed gas sources. The majority of the wells, including those with elevated methane concentrations, were completed in the West Falls group, which contains the organic rich Rhinestreet shale. Gas production in the

Rhinestreet shale is scattered throughout New York, primarily in the western portion of the state. Investigation into gas production from this formation, specifically the Rathborne gas field in Steuben County, demonstrated pockets of sporadic methane production. Methane isotopic data from this formation might prove useful in evaluating thermogenic sources of dissolved groundwater methane in regions overlying the West Falls.

The isotopic composition of several groundwater samples exhibit a signature indicative of potential mixing with a thermogenic gas source such as Upper Devonian shale, or possible fractionation as a result of methane oxidation could that have caused an increased in the $\delta^{13}C$-CH_4 and δD-CH_4 isotope values. The methane isotopic compositions of groundwater samples with the highest concentrations of dissolved methane are not easily distinguishable from the methane isotopic signature of the Upper Devonian samples from Alleghany County. The Marcellus sample (D60) taken from Steuben County also has an isotopic signature within the range of groundwater samples. $\delta^{13}C$-CH_4 and δD-CH_4 isotopes of the more thermally mature Ordovician Trenton/Black River does not fall into the range of isotopes values for groundwater samples. Since the isotope ranges of natural gases are a reflection of the geochemistry and thermal maturity of source rock, which varies with locality, any comparison between the isotopic signatures of methane in groundwater to a proposed source material needs to be local to the study area. Also, without knowing the isotopic range of other gas bearing units underlying the study area it would be difficult to claim a specific source for thermogenic methane for the sampled groundwater. But given the differences between the much lower lying Ordovician Trenton/Black River samples, groundwater samples based on our limited data are similar in methane isotopic composition to thermogenic Devonian gas sources. However, given the similarity of methane isotopic signatures in upper and middle Devonian formations and local groundwater samples,

$\delta^{13}C\text{-}CH_4$ and $\delta D\text{-}CH_4$ will not be enough to distinguish between individual sources and isotopic analysis of $C_2 - C_5$ for both groundwater and local Devonian gas bearing units may be required to distinguish between sources.

Dissolved methane was most strongly correlated with water type and we observed significant differences in the distribution of methane from $Ca\text{-}HCO_3$ and $Na\text{-}HCO_3$ type waters. Prior work has suggested that shallow groundwater mixing with deeper Na-Cl and $Na\text{-}HCO_3$ type groundwater, charged with thermogenic methane from underlying formations, occurs more frequently in valley wells where the distance to these waters is less. However, thermogenically sourced methane from primarily upland wells sampled in this study, might suggest that upland mixing with deeper brine influenced water might me more prevalent that previously considered; and more work is needed to understand migration pathways in upland settings.

Tables

Table 1. Contingency table comparing the Bedrock interpolation Method and the Geologic Map Method for classifying the geologic unit of well completion.

Bedrock Interpolation Method	Geologic Map Method							
	Conneaut	**Canadaway**	**Java**	**West Falls**	**Sonyea**	**Genesee**	**Hamilton**	**Total**
Conneaut	**0**	0	0	0	0	0	0	0
Canadaway	0	**13**	0	0	0	0	0	13
Java	0	**1**	**10**	0	0	0	0	11
West Falls	0	0	**4**	**63**	0	0	0	67
Sonyea	0	0	0	**13**	**6**	0	0	19
Genesee	0	0	0	0	**7**	**18**	0	25
Hamilton	0	0	0	0	0	**1**	**3**	4
Canadaway/Conneaut	**5**	0	0	0	0	0	0	5
West Falls/Sonyea	0	0	0	**5**	0	0	0	5
Sonyea/Genesee	0	0	0	0	**3**	0	0	3
Error	0	0	**6**	**1**	0	0	**4**	11
Total	5	14	20	82	16	19	7	

Table 2**.** Statistical results of Pearson, Spearman, and Kendall correlation between proximity parameters and methane concentration

	Statistical Test for Correlation					
Proximity Parameter	**Pearson**		**Spearman**		**Kendall**	
	p-value	R	p-value	Rho	p-value	Tau
Faults	0.102	-0.140	0.876	-0.013	0.987	-0.001
Lineaments	0.717	-0.031	0.231	0.103	0.251	0.067
Active Gas Wells	0.122	-0.133	0.833	-0.018	0.842	-0.012
Other Gas Wells	0.168	-0.119	0.320	-0.086	0.314	-0.058
Highway	0.118	0.134	0.881	0.013	0.978	0.002
NYS Roads	0.195	-0.111	0.360	-0.079	0.359	-0.053

Table 3. Statistical results of Pearson, Spearman, and Kendall correlation between water chemistry and methane concentration

Chemical Constituent	**Correlation between methane and other chemical constituents**						**Correlation between log methane and log chemical constituents**					
	Pearson		**Spearman**		**Kendall**		**Pearson**		**Spearman**		**Kendall**	
	p-value	R	p-value	Rho	p-value	Tau	p-value	R	p-value	Rho	p-value	Tau
Na (ppm)	<0.0001	0.24	<0.0001	-0.42	<0.0001	-0.29	<0.0001	0.19	<0.0001	-0.42	<0.0001	-0.29
I (ppb)	<0.0001	0.03	<0.0001	0.52	<0.0001	0.36	<0.0001	0.03	<0.0001	0.52	<0.0001	0.36
Ba (ug/L)	<0.0001	0.58	<0.0001	0.49	<0.0001	0.35	<0.0001	0.55	<0.0001	0.49	<0.0001	0.35
Fe (ug/L)	<0.0001	0.14	0.62	0.51	0.70	0.35	0.04	0.20	0.62	0.51	0.70	0.35
F (ppm)	<0.0001	0.07	<0.0001	-0.02	<0.0001	-0.01	<0.0001	-0.02	<0.0001	-0.02	<0.0001	-0.01
Br (ppb)	<0.0001	0.47	<0.0001	-0.04	<0.0001	-0.02	<0.0001	0.17	<0.0001	-0.04	<0.0001	-0.02
Cl (ppm)	<0.0001	0.52	0.07	0.48	0.05	0.34	0.00	0.49	0.07	0.48	0.05	0.34
Sr (ug/L)	<0.0001	0.43	<0.0001	0.16	<0.0001	0.12	<0.0001	0.27	<0.0001	0.16	<0.0001	0.12
NH4 (ppm)	<0.0001	-0.09	<0.0001	-0.17	<0.0001	-0.10	<0.0001	-0.18	<0.0001	-0.17	<0.0001	-0.10
Pb (ug/L)	0.01	-0.06	<0.0001	0.01	<0.0001	0.00	0.05	0.09	<0.0001	0.01	<0.0001	0.00
SO4 (ppm)	0.04	0.07	0.05	0.57	0.06	0.41	0.07	0.11	0.05	0.57	0.06	0.41
Mn (ug/L)	0.10	0.02	<0.0001	-0.16	<0.0001	-0.11	0.02	-0.16	<0.0001	-0.16	<0.0001	-0.11
NO3 (ppm)	0.21	0.15	<0.0001	0.35	<0.0001	0.28	<0.0001	0.14	<0.0001	0.35	<0.0001	0.28
Mg (ppm)	0.28	-0.12	0.05	-0.61	0.07	-0.42	0.03	-0.43	0.05	-0.61	0.07	-0.42
Zn (ug/L)	0.38	0.04	0.00	0.00	0.00	0.00	0.26	-0.02	0.00	0.00	0.00	0.00
Li (ug/L)	0.41	0.54	<0.0001	0.41	<0.0001	0.28	0.22	0.51	<0.0001	0.41	<0.0001	0.28
K (ppm)	0.42	0.52	0.84	0.71	0.84	0.51	0.84	0.61	0.84	0.71	0.84	0.51
P (ug/L)	0.44	-0.08	0.07	-0.03	0.04	-0.02	0.48	-0.10	0.07	-0.03	0.04	-0.02
Al (ug/L)	0.57	0.45	0.81	0.57	0.83	0.41	0.47	0.62	0.81	0.57	0.83	0.41
Se (ug/L)	0.64	0.46	0.97	0.37	0.97	0.26	0.81	0.34	0.97	0.37	0.97	0.26
PO4 (ppm)	0.69	0.43	0.93	0.47	0.96	0.33	0.51	0.45	0.93	0.47	0.96	0.33
B (ug/L)	0.78	-0.08	<0.0001	-0.27	<0.0001	-0.18	0.74	-0.10	<0.0001	-0.27	<0.0001	-0.18
Ca (ppm)	0.86	-0.17	0.07	-0.17	0.06	-0.11	0.07	-0.16	0.07	-0.17	0.06	-0.11

Figures

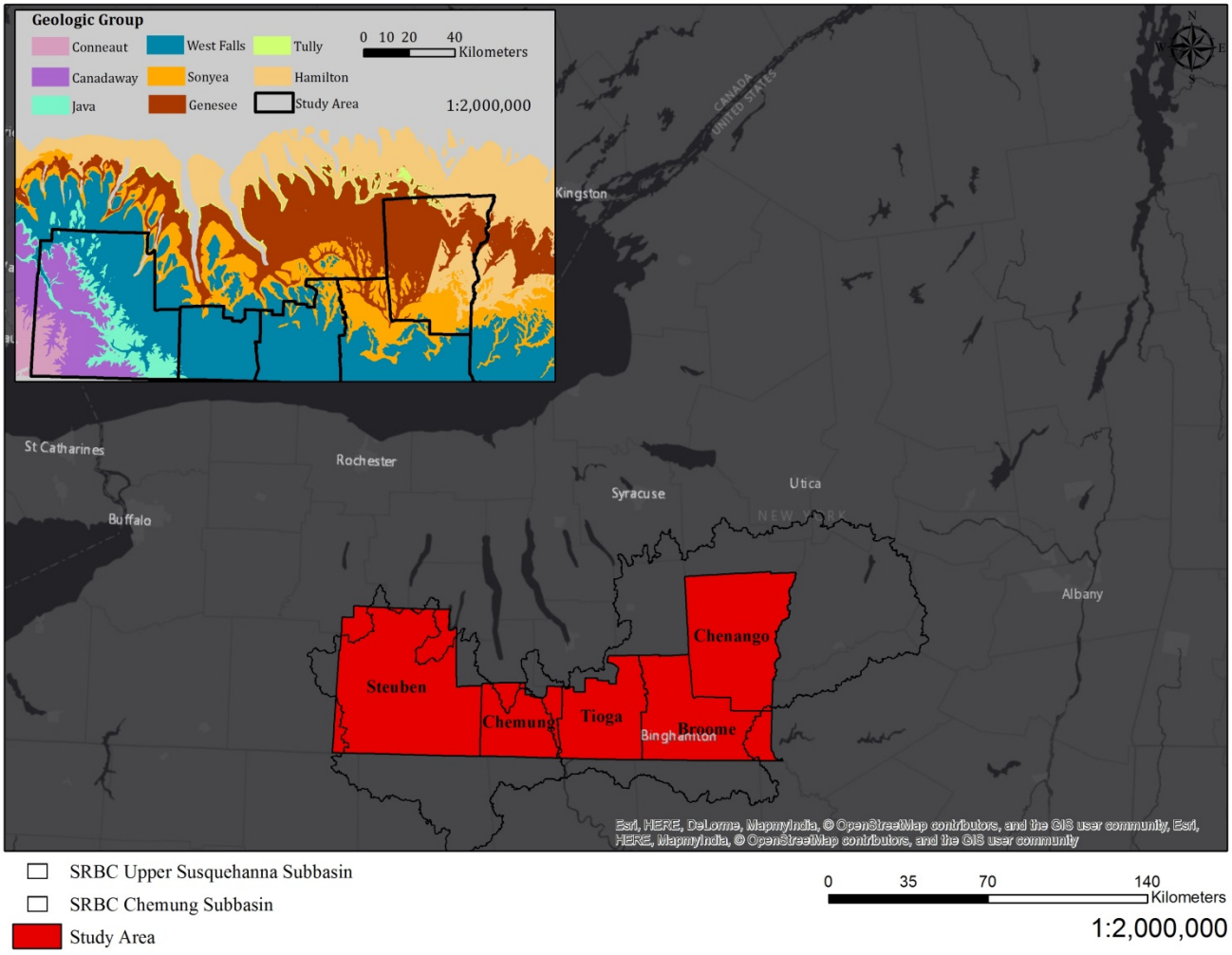

Figure 1. The study area which covers Steuben, Chemung, Tioga, Broome, and Chenango Counties in relation to the outlined extent of the Upper Susquehanna Subbasin (left) and Chemung Subbasin (right). The inset map shows the underlying bedrock across the study area.

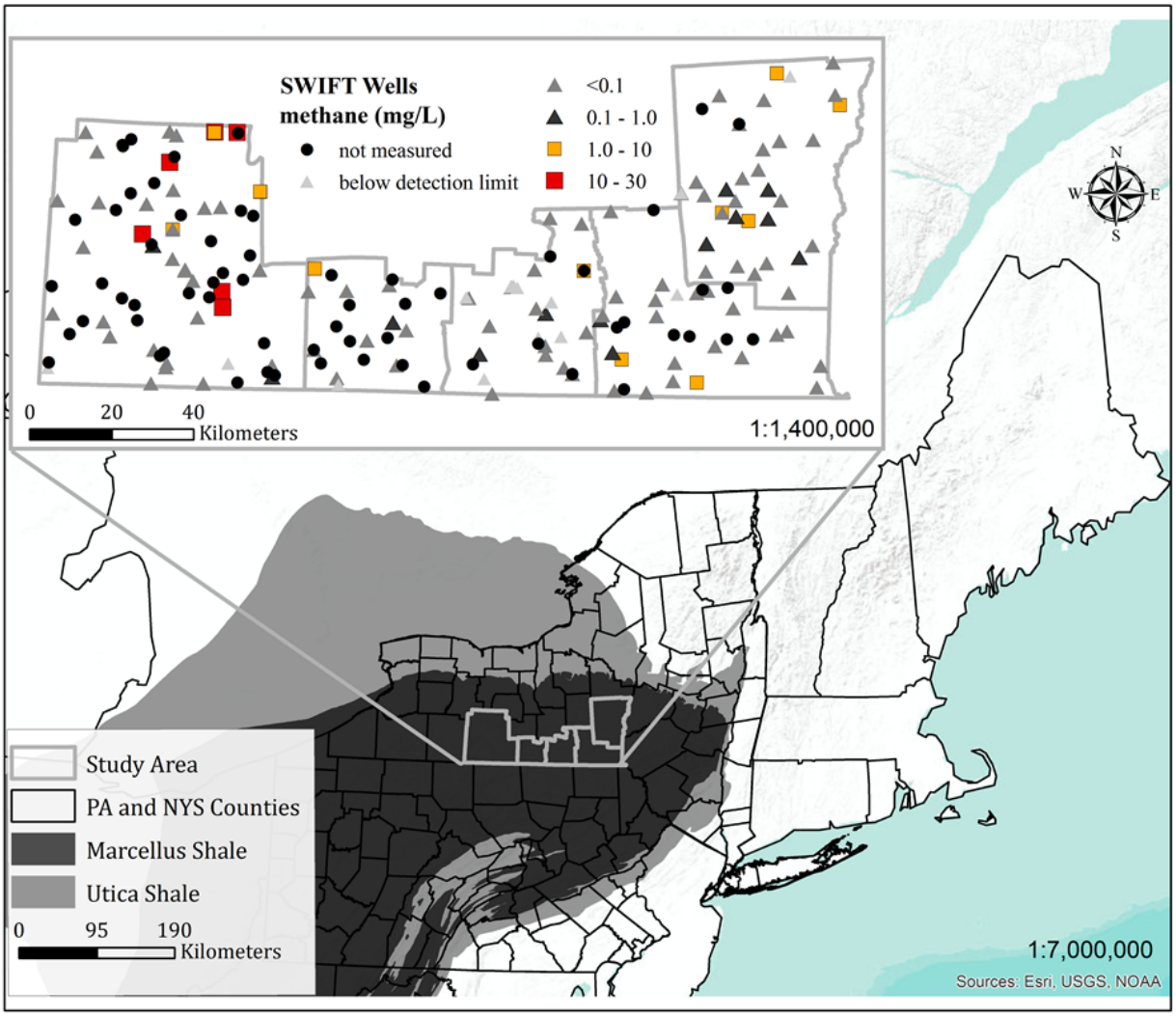

Figure 2. The spatial distribution of methane across the study area in relation to the geologic extent of underlying Utica and Marcellus Shale.

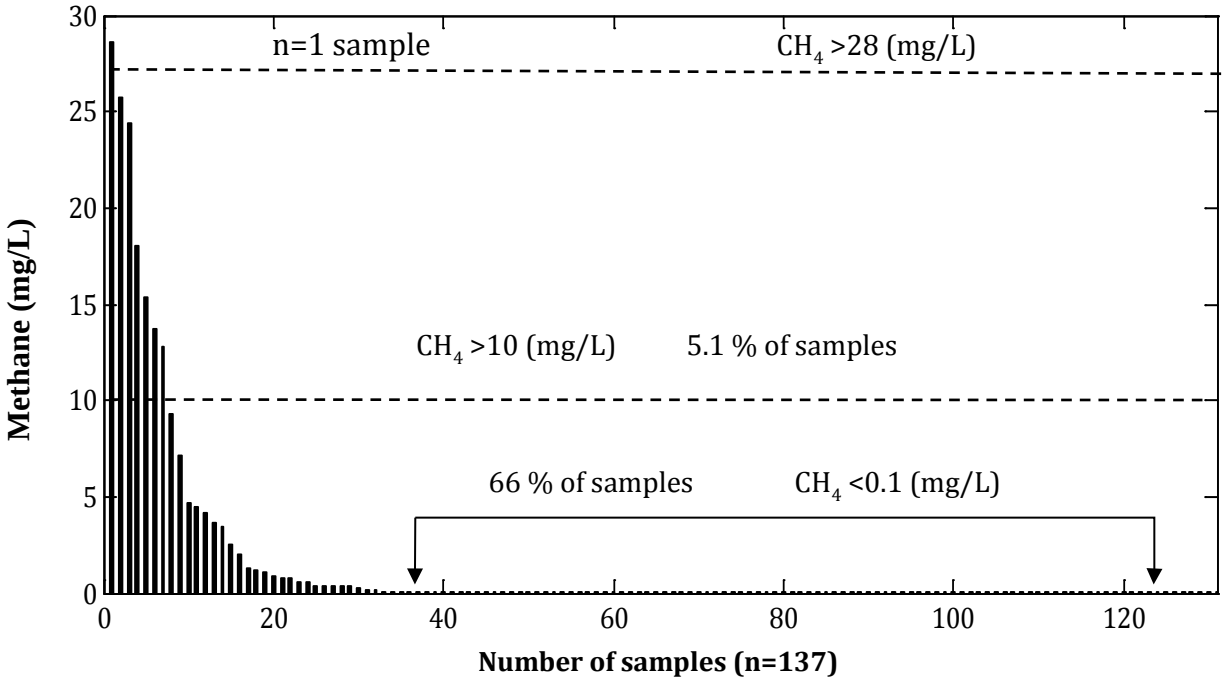

Figure 3. Distribution of methane from (n=137) samples

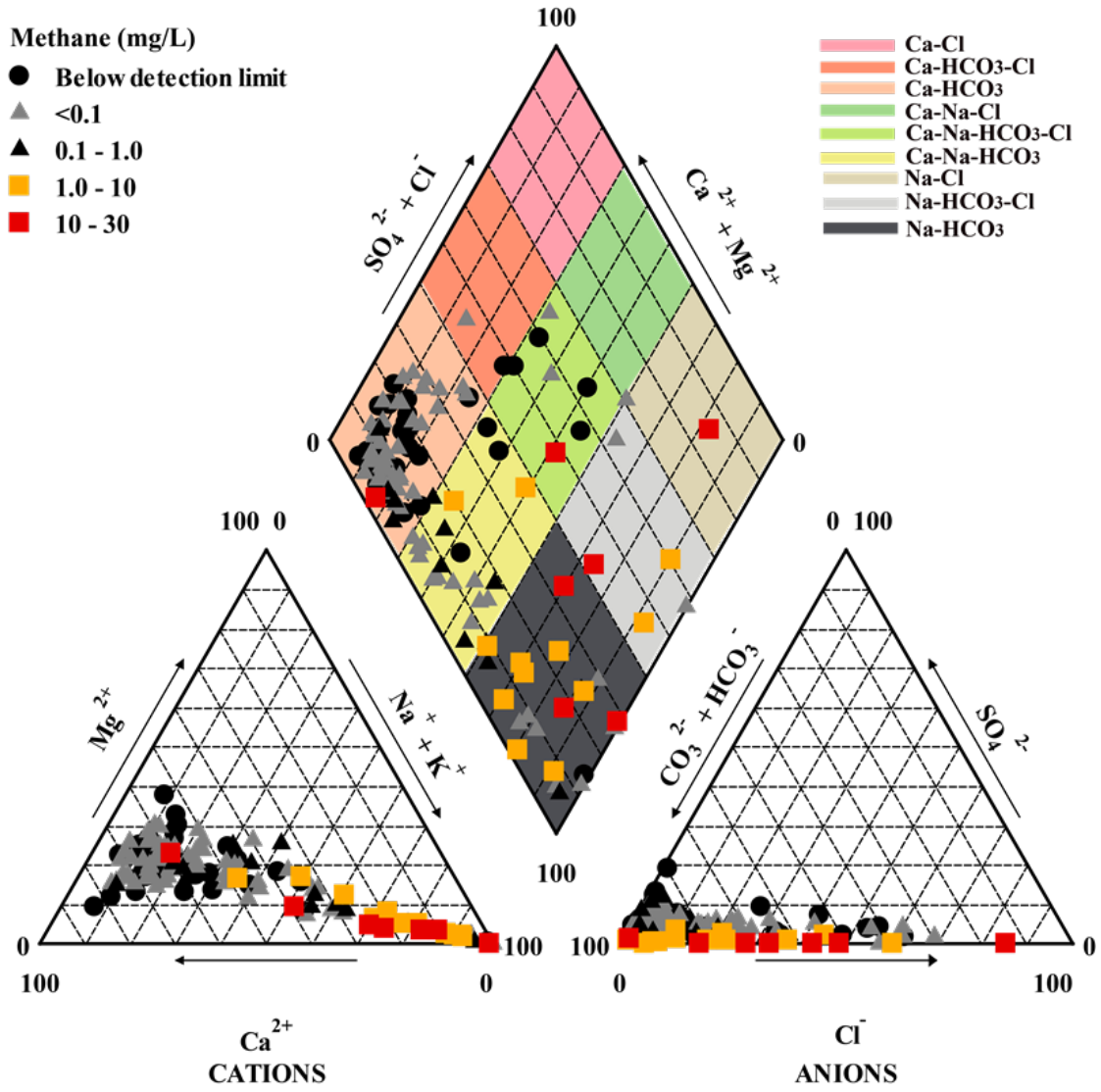

Figure 4. Piper diagram of (n=137) samples classified by water type and symbolized by ,ethane concentration.

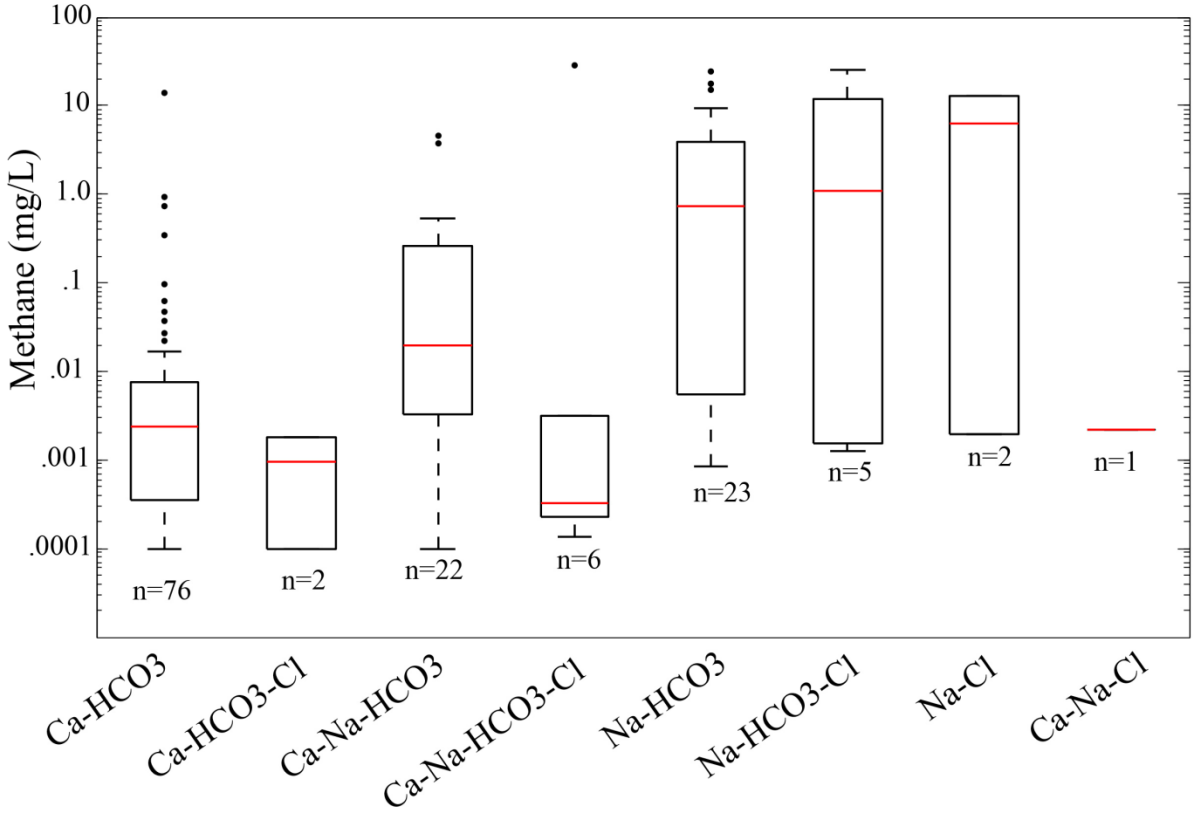

Figure 5. The distribution of methane based on water type classified using the piper diagram

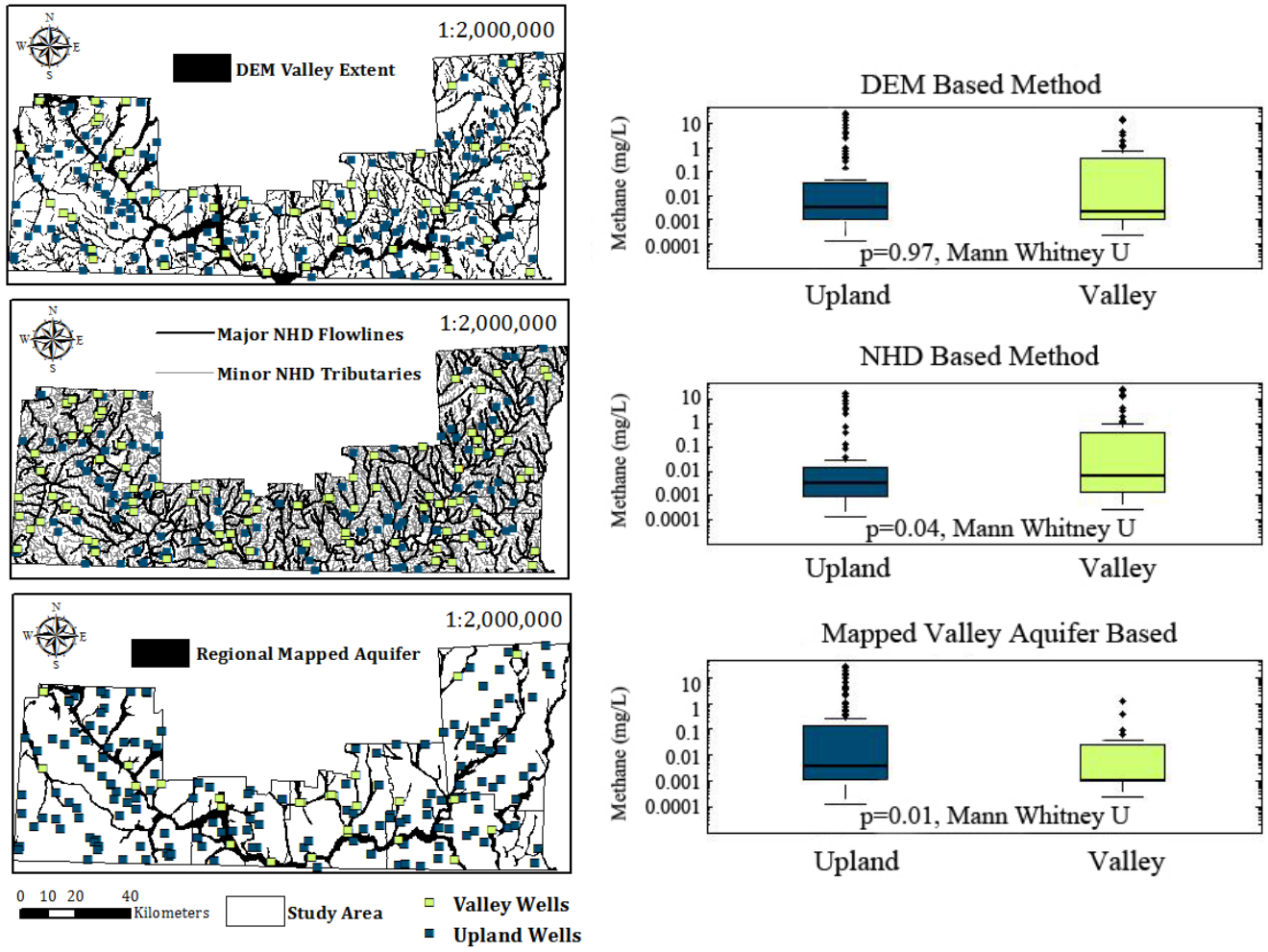

Figure 6. Landscape position of well classified using the DEM based –method (a), the NHD-method (b), and the mapped aquifer method (c). The distribution of methane based on each classification (d-f).

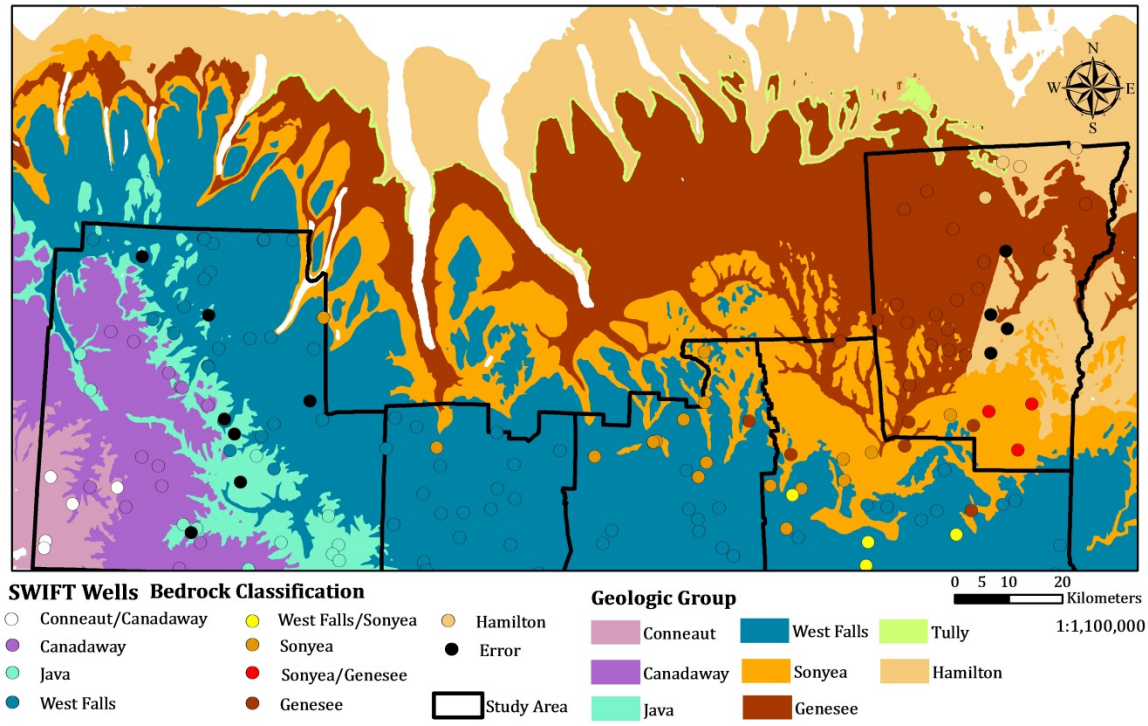

Figure 7. Geologic map of the study area and well classification based on bedrock contact interpolation method compared to a geologic map of the study area (Fisher, 1970).

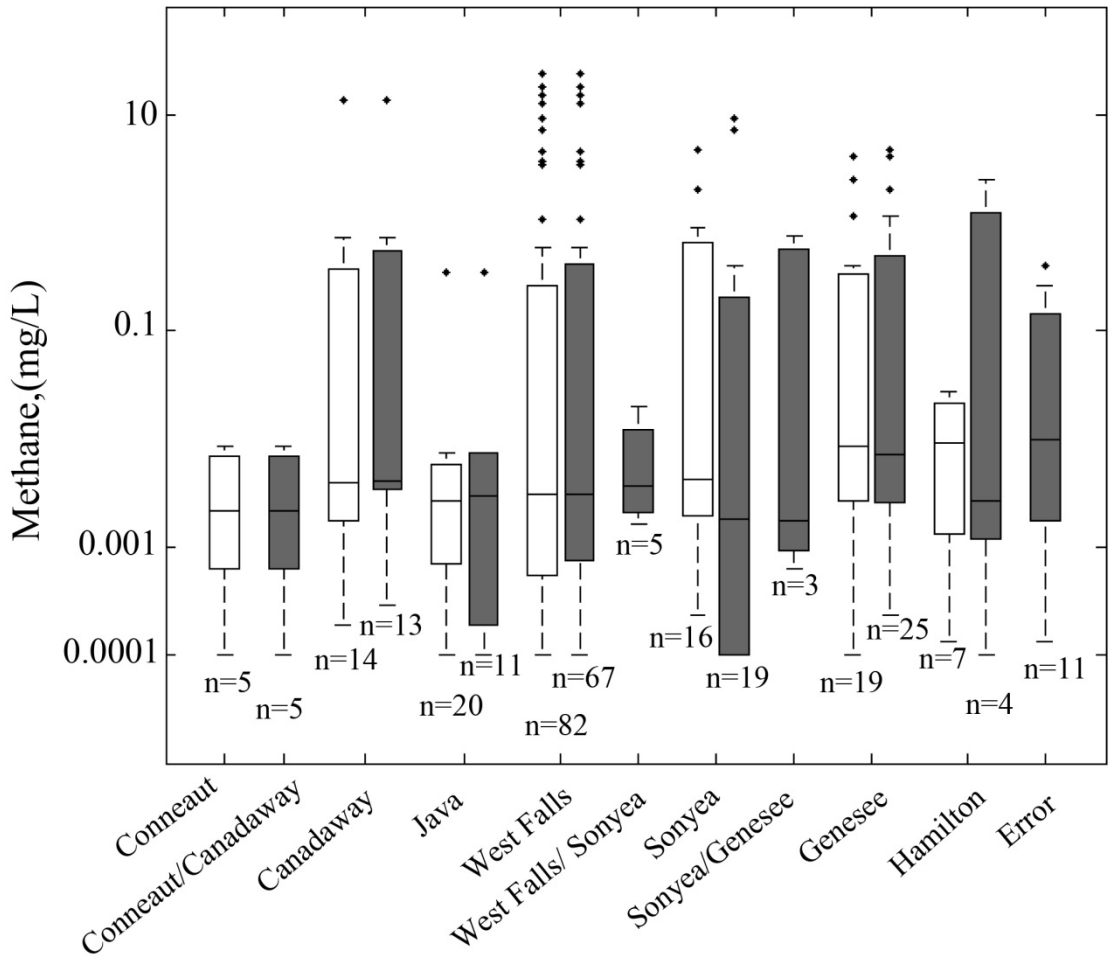

Figure 8. Boxplot distribution of methane concentrations for wells classified using the bedrock contact interpolation method and the geologic map method.

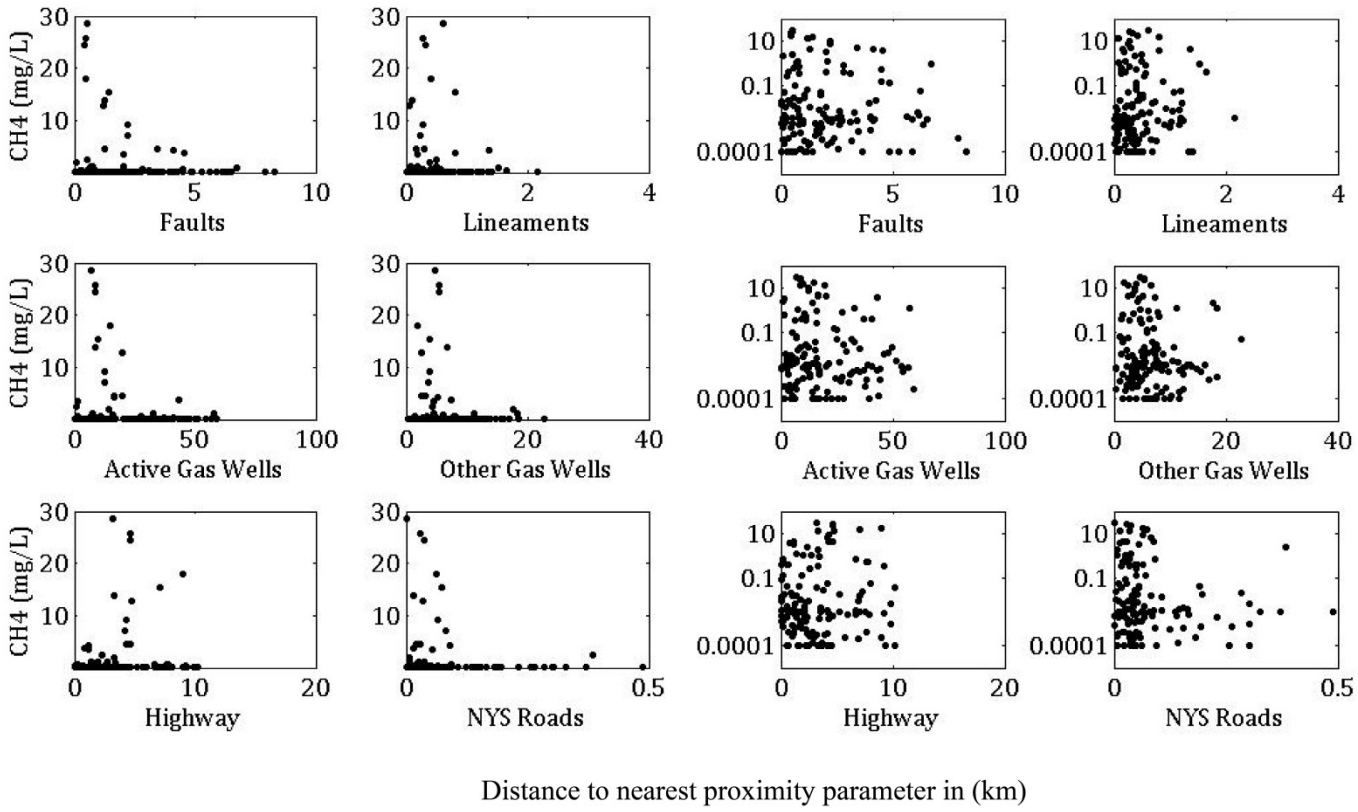

Figure 9. Methane concentration with well proximity to faults, lineaments, active and other gas wells, highways and lineaments at linear and log scale.

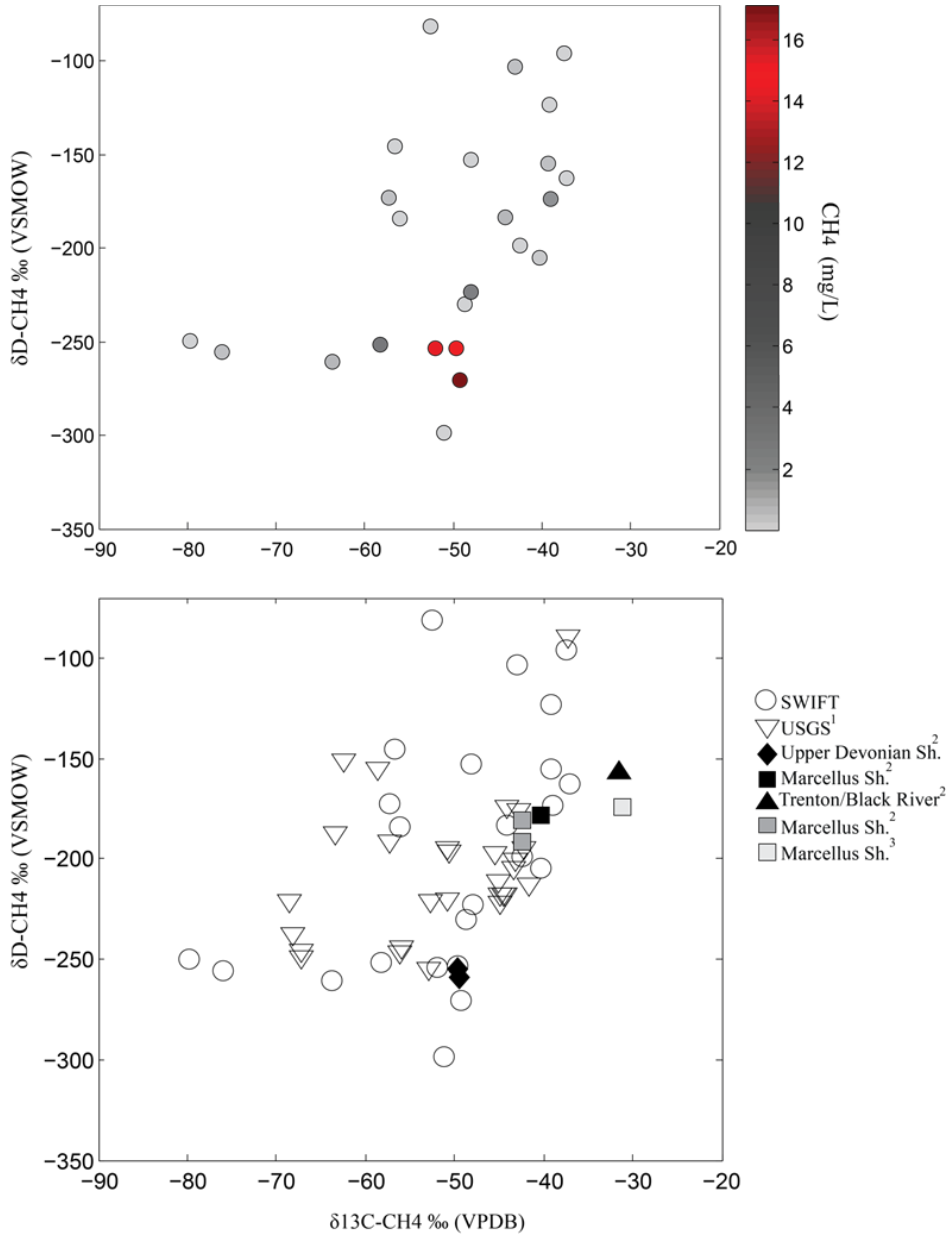

Figure10**.** Schoell plot (1980) of (10a) isotopes δ^{13}C-CH_4 and δD-CH_4 of methane colors based on dissolved methane concentration. (10b) δ^{13}C-CH_4 and δD-CH_4 of NY groundwater SWIFT (this study), USGS (Heisig & Scott, 2013)[1] , NY gas bearing formations (black symbols) Upper Devonian, Marcellus, Trenton/Black River (Osborn & McIntosh, 2010)[2], and PA gas from the Marcellus in Washington Co. (Osborn & McIntosh, 2010)[2] and Susquehanna Co. (Molofksy, 2013)[3].

Table S1. Concentrations of major ions, and dissolved methane data for (n=204) wells sampled from 2012 through 2013

SWIFT ID	Sample ID	Na (ppm)	NH4 (ppm)	K (ppm)	Mg (ppm)	Ca (ppm)	F (ppm)	Cl (ppm)	NO3 (ppm)	PO4 (ppm)	SO4 (ppm)	CH4 (mg/L)
BR01A	BR01A_2013	13.1	b.d.l	0.5	6.0	36.6	0.1	1.8	0.5	n.m	26.2	0.0017
BR09A	BR09A_2013	16.6	n.m	0.6	3.1	9.8	0.1	3.1	1.9	n.m	11.6	0.0035
BR10A	BR10A_2013	83.5	n.m	b.d.l	b.d.l	0.4	0.2	9.6	0.4	0.1	16.3	0.0030
BR12A	BR12A_2013	14.5	b.d.l	0.8	6.1	46.8	0.1	1.4	1.1	0.9	27.7	0.0018
BR13A	BR13A_2012	12.1	b.d.l	1.7	6.9	36.4	0.2	1.8	0.2	n.m	13.7	n.m
BR13B	BR13B_2013	6.1	n.m	0.3	9.3	43.8	b.d.l	1.8	0.5	n.m	8.7	0.0001
BR13C	BR13C_2013	70.7	n.m	n.m	b.d.l	b.d.l	0.1	23.8	2.1	n.m	13.2	0.0018
BR14A	BR14A_2012	8.8	0.1	0.8	8.0	32.4	0.2	0.9	b.d.l	n.m	10.1	n.m
BR14B	BR14B_2013	52.5	0.2	0.7	7.3	27.2	0.2	4.4	n.m	n.m	19.9	0.0180
BR15A	BR15A_2013	17.4	b.d.l	0.6	5.9	29.1	0.1	7.0	0.4	1.6	11.2	0.0007
BR16A	BR16A_2013	7.8	n.m	1.0	2.3	17.7	0.1	13.6	6.9	0.2	12.9	0.0003
BR16B	BR16B_2013	70.1	0.3	0.9	6.1	30.1	0.3	10.6	b.d.l	n.m	14.1	0.3916
BR17A	BR17A_2012	20.3	b.d.l	0.9	14.5	46.0	0.2	32.0	0.1	n.m	6.3	n.m
BR17B	BR17B_2012	37.0	b.d.l	0.9	26.7	72.3	b.d.l	1.2	0.1	n.m	83.2	n.m
BR18A	BR18A_2012	8.8	b.d.l	1.2	10.3	39.8	0.2	0.9	0.4	n.m	12.6	n.m
BR18B	BR18B_2013	93.0	b.d.l	0.7	1.0	7.7	0.2	40.6	b.d.l	b.d.l	15.7	0.0103
BR19A	BR19A_2012	77.9	0.2	1.1	13.4	49.4	0.2	6.7	b.d.l	n.m	105.3	n.m
BR20A	BR20A_2012	8.8	0.2	1.6	8.2	32.5	0.2	0.8	0.3	n.m	11.6	n.m
BR21A	BR21A_2012	79.9	0.1	1.0	2.3	12.7	0.2	44.1	b.d.l	n.m	0.1	n.m
BR22A	BR22A_2013	6.9	n.m	0.8	4.7	21.1	0.1	10.7	0.8	0.8	8.3	0.0022
BR22B	BR22B_2013	11.5	n.m	2.1	13.1	39.1	0.2	3.1	b.d.l	b.d.l	17.8	0.0007
BR26A	BR26A_2013	82.8	b.d.l	1.6	15.2	50.0	0.5	95.4	b.d.l	n.m	5.4	3.6772
BR28A	BR28A_2013	74.8	n.m	0.1	b.d.l	b.d.l	0.1	66.3	0.3	n.m	0.6	0.0016
BR29A	BR29A_2013	80.0	0.3	1.3	2.8	14.4	0.4	6.4	b.d.l	n.m	19.3	0.0119
BR30A	BR30A_2013	63.4	b.d.l	1.0	8.5	34.6	0.2	17.3	b.d.l	b.d.l	15.5	0.0199
BR33A	BR33A_2013	32.6	b.d.l	1.3	6.8	31.6	0.2	1.8	b.d.l	n.m	12.7	0.0031
BR34A	BR34A_2013	8.7	n.m	1.8	22.7	53.6	0.1	21.0	b.d.l	n.m	27.8	0.0001
BR35A	BR35A_2012	24.4	0.2	1.6	16.1	46.0	0.2	1.1	0.1	n.m	17.8	n.m

Table S1. Concentrations of major ions, and dissolved methane data for (n=204) wells sampled from 2012 through 2013

SWIFT ID	Sample ID	Na (ppm)	NH4 (ppm)	K (ppm)	Mg (ppm)	Ca (ppm)	F (ppm)	Cl (ppm)	NO3 (ppm)	PO4 (ppm)	SO4 (ppm)	CH4 (mg/L)
BR36A	BR36A_2013	10.3	n.m	1.0	8.2	23.5	0.1	4.5	1.2	b.d.l	10.2	0.0048
BR36B	BR36B_2013	28.5	b.d.l	2.2	18.1	58.3	0.1	66.5	b.d.l	10.1	17.5	0.0026
BR37A	BR37A_2013	78.8	0.5	1.2	8.5	30.0	0.3	16.9	b.d.l	n.m	1.7	1.2468
BR41A	BR41A_2013	14.3	n.m	0.8	4.5	18.3	0.1	37.6	0.7	n.m	7.7	0.0003
CM01A	CM01A_2013	80.4	0.4	0.8	2.7	16.2	0.3	37.1	b.d.l	n.m	3.8	3.4465
CM02A	CM02A_2012	20.6	b.d.l	1.2	9.6	44.0	0.1	1.4	b.d.l	n.m	10.0	n.m
CM04A	CM04A_2012	14.6	b.d.l	0.6	9.6	35.4	0.2	0.5	0.2	n.m	16.8	n.m
CM06A	CM06A_2013	19.1	b.d.l	1.1	10.3	55.0	0.2	3.4	b.d.l	1.2	25.0	0.0031
CM07A	CM07A_2012	27.5	b.d.l	1.4	50.5	203.9	0.1	433.7	1.0	n.m	24.6	n.m
CM07B	CM07B_2013	51.0	n.m	1.1	11.8	79.2	0.1	122.7	5.1	n.m	13.6	0.0002
CM09A	CM09A_2012	7.3	b.d.l	1.0	8.5	32.5	0.2	1.8	0.1	n.m	10.7	n.m
CM09B	CM09B_2013	8.1	b.d.l	0.6	12.3	58.1	b.d.l	1.4	b.d.l	n.m	16.0	0.0004
CM10A	CM10A_2012	21.8	0.3	0.6	8.7	37.4	0.1	0.9	b.d.l	n.m	23.3	n.m
CM10B	CM10B_2012	8.7	b.d.l	0.6	11.5	44.4	0.2	5.9	b.d.l	n.m	22.2	n.m
CM12A	CM12A_2012	5.6	b.d.l	1.2	11.0	56.1	0.2	9.5	14.3	n.m	34.9	n.m
CM13A	CM13A_2012	15.6	b.d.l	1.3	16.0	94.6	0.1	132.2	0.1	n.m	14.6	n.m
CM14A	CM14A_2013	65.4	0.2	0.7	2.0	12.8	0.2	2.3	0.2	n.m	14.7	0.0030
CM14B	CM14B_2013	125.2	0.2	0.6	2.2	12.4	0.5	44.7	b.d.l	1.2	21.8	0.5847
CM16A	CM16A_2012	n.m	n.m	n.m	n.m	n.m	n.m	n.m	n.m	n.m	n.m	n.m
CM16B	CM16B_2012	8.9	b.d.l	1.9	14.4	58.6	0.2	13.4	0.8	n.m	16.5	n.m
CM16C	CM16C_2013	8.4	n.m	1.0	5.8	85.2	b.d.l	31.4	0.7	0.5	21.5	0.0004
CM17A	CM17A_2012	33.0	0.2	1.1	30.2	98.4	0.2	20.3	b.d.l	n.m	115.8	n.m
CM17B	CM17B_2013	12.2	b.d.l	0.8	8.8	43.4	0.2	5.5	b.d.l	n.m	31.6	0.0012
CM18A	CM18A_2012	96.6	0.3	1.3	1.6	10.6	0.2	1.1	b.d.l	n.m	21.5	n.m
CM19A	CM19A_2012	20.0	b.d.l	0.9	11.6	47.8	0.1	0.6	n.m	n.m	20.7	n.m
CM19B	CM19B_2013	43.4	b.d.l	0.7	9.6	30.0	0.1	2.7	b.d.l	0.1	28.4	0.0565
CM22A	CM22A_2013	48.8	b.d.l	1.2	3.9	29.4	0.1	74.3	2.3	0.6	14.5	0.0004
CM22B	CM22B_2013	6.3	n.m	1.1	6.6	33.4	0.1	1.3	0.3	n.m	15.6	0.0001
CM25A	CM25A_2012	n.m	n.m	n.m	n.m	n.m	n.m	n.m	n.m	n.m	n.m	n.m
CN05A	CN05A_2013	66.3	0.1	0.4	3.2	18.8	0.3	15.5	n.m	n.m	13.6	2.5014
CN06A	CN06A_2013	16.2	b.d.l	1.6	10.4	68.0	b.d.l	27.3	24.5	0.6	9.6	0.0001
CN07A	CN07A_2013	5.6	n.m	0.3	5.3	41.3	0.1	2.3	0.7	b.d.l	23.4	0.0032

Table S1. Concentrations of major ions, and dissolved methane data for (n=204) wells sampled from 2012 through 2013

SWIFT ID	Sample ID	Na (ppm)	NH4 (ppm)	K (ppm)	Mg (ppm)	Ca (ppm)	F (ppm)	Cl (ppm)	NO3 (ppm)	PO4 (ppm)	SO4 (ppm)	CH4 (mg/L)
CN10A	CN10A_2013	4.4	n.m	0.5	6.4	21.2	0.1	0.5	0.6	n.m	8.9	0.0220
CN12A	CN12A_2013	20.9	n.m	0.6	11.0	40.4	0.1	3.3	b.d.l	n.m	15.9	0.0022
CN14A	CN14A_2013	25.0	b.d.l	0.5	9.1	34.9	0.1	0.8	b.d.l	n.m	19.1	0.0033
CN14B	CN14B_2013	76.7	0.3	0.4	2.6	11.5	0.3	2.0	b.d.l	b.d.l	3.1	2.0377
CN18A	CN18A_2013	7.4	b.d.l	0.5	6.0	25.7	0.1	b.d.l	0.2	n.m	12.3	0.0042
CN18B	CN18B_2013	1.5	b.d.l	0.6	2.0	9.5	0.1	0.6	2.0	n.m	3.3	n.m
CN26A	CN26A_2013	18.7	b.d.l	0.7	10.3	38.5	0.1	4.5	0.2	n.m	11.4	0.0032
CN26B	CN26B_2013	7.6	n.m	0.7	9.3	36.0	0.1	0.9	0.7	n.m	8.1	0.0025
CN26C	CN26C_2013	1.9	n.m	0.3	1.4	14.5	0.1	1.4	5.5	n.m	2.7	0.0003
CN27A	CN27A_2013	17.4	n.m	1.1	14.1	57.2	0.1	5.2	1.6	n.m	26.3	0.0027
CN30A	CN30A_2013	4.7	n.m	0.8	3.0	15.7	b.d.l	2.8	8.8	b.d.l	5.8	0.0003
CN30B	CN30B_2013	18.3	n.m	1.3	3.9	38.3	b.d.l	30.7	13.3	n.m	8.9	n.m
CN30C	CN30C_2013	7.7	b.d.l	0.7	7.3	38.4	0.1	2.8	b.d.l	0.3	12.7	0.0031
CN30C Artesian	CN30C Artesian_2013	4.4	n.m	0.9	2.3	15.0	0.1	3.7	7.0	n.m	8.7	0.0001
CN31A	CN31A_2013	15.4	b.d.l	0.7	8.2	44.5	0.1	2.9	b.d.l	n.m	16.3	0.0072
CN31B	CN31B_2013	8.7	b.d.l	0.6	5.1	25.0	0.1	2.1	0.8	n.m	7.1	0.3463
CN32A	CN32A_2013	5.6	b.d.l	1.3	7.8	30.4	b.d.l	2.6	13.0	n.m	8.3	0.0002
CN33A	CN33A_2013	48.6	b.d.l	0.9	5.8	26.1	0.3	21.5	b.d.l	b.d.l	9.5	0.4049
CN37A	CN37A_2013	28.0	0.2	0.8	7.0	33.4	0.1	23.5	b.d.l	0.7	3.0	4.6494
CN37A MILK	CN37AMILK_ 2013	8.5	n.m	0.8	7.7	52.3	0.1	20.2	12.0	0.2	16.1	0.0026
CN38A	CN38A_2013	19.6	0.6	1.0	7.4	43.6	0.1	3.3	b.d.l	0.3	3.6	0.9162
CN38B	CN38B_2013	96.4	0.2	0.7	1.3	5.3	0.3	11.9	n.m	1.8	1.3	4.1413
CN38C	CN38C_2013	24.9	b.d.l	0.7	6.3	34.7	0.1	2.9	b.d.l	n.m	10.5	0.0197
CN39A	CN39A_2013	37.6	0.2	0.9	3.5	21.2	0.2	3.4	b.d.l	0.7	2.5	0.2637
CN39B	CN39B_2013	19.6	n.m	0.7	7.3	39.0	0.1	2.9	b.d.l	n.m	15.6	0.0010
CN43A	CN43A_2013	50.8	0.3	0.9	3.7	19.9	0.1	4.7	b.d.l	n.m	9.1	0.1274
CN46A	CN46A_2013	29.6	n.m	0.7	2.1	17.6	0.1	3.9	3.3	0.2	23.4	0.0044
CN49A	CN49A_2013	9.1	b.d.l	0.6	6.8	38.1	0.1	3.9	b.d.l	n.m	10.9	0.0012
CN50A	CN50A_2013	6.8	n.m	0.8	4.3	33.5	0.1	18.8	10.1	b.d.l	14.4	0.0142
CN50B	CN50B_2013	30.7	0.2	0.6	5.6	28.9	0.2	2.7	n.m	n.m	13.1	0.0277

Table S1. Concentrations of major ions, and dissolved methane data for (n=204) wells sampled from 2012 through 2013

SWIFT ID	Sample ID	Na (ppm)	NH4 (ppm)	K (ppm)	Mg (ppm)	Ca (ppm)	F (ppm)	Cl (ppm)	NO3 (ppm)	PO4 (ppm)	SO4 (ppm)	CH4 (mg/L)
CN51A	CN51A_2013	7.4	n.m	0.6	5.5	25.1	0.2	1.6	b.d.l	n.m	9.5	0.0006
CN52A	CN52A_2013	80.8	0.2	0.6	b.d.l	2.8	0.2	3.6	n.m	0.4	11.1	0.7478
CN53A	CN53A_2013	9.3	n.m	1.1	4.0	19.1	0.1	2.0	7.0	n.m	13.9	0.0017
ST01A	ST01A_2013	29.9	b.d.l	1.4	12.6	86.5	0.1	56.5	b.d.l	b.d.l	29.0	0.0950
ST03A	ST03A_2012	108.4	0.3	1.1	1.9	11.4	0.6	53.7	b.d.l	n.m	2.8	n.m
ST04A	ST04A_2013	86.8	n.m	6.0	6.6	41.4	b.d.l	159.2	4.2	n.m	10.9	0.0020
ST04B	ST04B_2013	3.5	n.m	0.5	5.8	32.9	0.1	3.7	4.2	b.d.l	14.8	0.0032
ST04C	ST04C_2013	86.6	n.m	1.6	5.7	35.6	0.1	132.2	1.2	1.4	10.3	0.0013
ST05A	ST05A_2013	66.8	0.7	1.8	3.2	18.3	0.5	8.0	n.m	b.d.l	0.3	4.5022
ST05B	ST05B_2013	413.9	1.5	3.1	9.6	63.0	0.7	664.2	b.d.l	b.d.l	n.m	12.7982
ST06A	ST06A_2012	48.0	0.6	1.3	13.9	49.4	0.2	25.1	b.d.l	n.m	12.4	n.m
ST06C	ST06C_2013	183.7	0.7	1.0	4.0	19.6	0.6	58.5	n.m	n.m	0.1	17.9937
ST09A	ST09A_2013	6.5	n.m	0.9	14.2	60.4	0.1	14.8	2.2	b.d.l	31.9	0.0044
ST10A	ST10A_2012	10.0	b.d.l	1.5	10.5	41.4	b.d.l	31.1	27.5	n.m	15.7	n.m
ST10B	ST10B_2012	7.7	b.d.l	1.1	8.1	29.1	b.d.l	14.2	18.1	n.m	16.0	n.m
ST12A	ST12A_2012	45.5	0.3	1.3	5.2	26.2	0.2	11.0	b.d.l	n.m	0.5	n.m
ST12B	ST12B_2013	152.4	0.6	0.8	b.d.l	0.7	0.3	66.1	n.m	n.m	0.1	15.3230
ST19A	ST19A_2012	29.2	b.d.l	0.9	4.4	22.1	0.1	6.3	b.d.l	n.m	1.8	n.m
ST19B	ST19B_2012	6.6	b.d.l	2.3	8.8	41.4	0.1	8.3	4.9	n.m	11.0	n.m
ST20A	ST20A_2013	79.3	n.m	2.1	13.2	47.9	0.1	153.2	1.9	n.m	12.2	0.0001
ST23B	ST23B_2013	141.7	n.m	1.1	2.2	12.8	0.7	53.6	b.d.l	n.m	17.5	9.3039
ST23C	ST23C_2013	224.4	n.m	1.0	1.9	11.7	0.9	164.9	n.m	n.m	19.6	7.1298
ST24B	ST24B_2013	9.9	b.d.l	1.4	18.8	92.9	0.1	16.0	4.4	0.4	28.1	0.0102
ST25A	ST25A_2012	11.4	b.d.l	1.9	24.6	95.6	0.1	19.0	0.1	n.m	140.7	n.m
ST25B	ST25B_2013	12.5	n.m	1.5	7.4	51.3	0.2	6.2	0.4	n.m	13.3	0.0040
ST26A	ST26A_2012	144.9	0.4	2.1	3.4	15.7	0.3	57.3	b.d.l	n.m	1.2	n.m
ST27A	ST27A_2013	12.6	n.m	1.5	7.6	48.7	b.d.l	22.0	7.1	n.m	12.5	0.0058
ST28A	ST28A_2012	n.m	n.m	n.m	n.m	n.m	n.m	n.m	n.m	n.m	n.m	n.m
ST29A	ST29A_2013	21.8	b.d.l	1.2	18.1	85.1	0.2	95.8	b.d.l	n.m	33.2	0.0018
ST30A	ST30A_2012	55.2	b.d.l	2.0	13.4	52.6	0.3	4.7	3.3	n.m	69.9	n.m
ST30B	ST30B_2013	10.9	b.d.l	1.1	13.8	72.8	0.1	15.2	b.d.l	0.1	31.6	0.0013
ST31A	ST31A_2012	6.2	b.d.l	1.0	17.3	45.6	0.2	3.4	3.5	n.m	31.1	n.m

Table S1. Concentrations of major ions, and dissolved methane data for (n=204) wells sampled from 2012 through 2013

SWIFT ID	Sample ID	Na (ppm)	NH4 (ppm)	K (ppm)	Mg (ppm)	Ca (ppm)	F (ppm)	Cl (ppm)	NO3 (ppm)	PO4 (ppm)	SO4 (ppm)	CH4 (mg/L)
ST33A	ST33A_2013	16.4	b.d.l	1.5	11.8	68.7	0.1	6.1	0.2	n.m	31.2	0.0074
ST35A	ST35A_2012	11.6	b.d.l	2.3	16.0	86.7	0.1	0.8	0.1	n.m	93.9	n.m
ST35B	ST35B_2013	30.1	0.2	1.6	21.6	93.7	0.1	4.1	b.d.l	b.d.l	9.0	13.7646
ST35C	ST35C_2013	10.6	b.d.l	2.1	9.5	80.0	0. 1	3.3	b.d.l	14.7	53.9	0.7281
ST36B	ST36B_2013	8.0	n.m	2.4	8.5	44.6	0.1	1.3	1.2	n.m	12.3	0.0006
ST36C	ST36C_2013	202.6	0.3	1.5	2.3	14.3	0.3	207.4	n.m	0.7	2.0	1.0740
ST37A	ST37A_2012	38.1	b.d.l	1.1	8.3	36.2	0.1	17.6	0.2	n.m	5.3	n.m
ST44A	ST44A_2013	9.1	n.m	1.8	9.7	80.6	0.2	34.2	5.5	b.d.l	29.8	0.0039
ST45A	ST45A_2012	8.3	b.d.l	0.9	6.5	45.6	b.d.l	1.5	0.5	n.m	10.0	n.m
ST46A	ST46A_2012	23.1	b.d.l	1.3	15.8	66.0	b.d.l	42.2	8.3	n.m	16.7	n.m
ST46B	ST46B_2012	9.0	b.d.l	0.9	6.5	41.3	0.1	0.4	b.d.l	n.m	6.8	n.m
ST46C	ST46C_2013	4.8	n.m	1.4	4.3	31.0	b.d.l	3.8	1.4	n.m	11.7	0.0025
ST47A	ST47A_2012	10.3	b.d.l	1.2	9.7	42.7	0.1	0.9	0.1	n.m	14.1	n.m
ST47B	ST47B_2013	13.1	b.d.l	0.6	6.0	26.5	0.2	25.9	b.d.l	n.m	13.3	0.0103
ST49A	ST49A_2012	17.2	b.d.l	2.1	16.9	47.0	0.2	0.8	0.1	n.m	9.1	n.m
ST49B	ST49B_2013	19.4	n.m	1.1	5.7	27.5	0.1	57.8	9.9	n.m	11.4	0.0022
ST51A	ST51A_2012	131.0	0.3	2.5	2.7	13.5	0.5	52.4	0.1	n.m	b.d.l	n.m
ST51B	ST51B_2012	12.6	b.d.l	1.4	9.0	44.4	0.1	12.8	b.d.l	n.m	10.3	n.m
ST52A	ST52A_2012	67.4	0.2	2.6	17.1	98.2	0.1	109.3	b.d.l	n.m	16.2	n.m
ST53A	ST53A_2013	64.6	n.m	5.8	10.1	70.7	b.d.l	138.9	n.m	n.m	26.4	0.0032
ST53B	ST53B_2013	9.8	n.m	1.0	9.7	66.0	0.1	40.9	1.8	n.m	7.7	0.0274
ST54A	ST54A_2012	35.3	b.d.l	1.4	7.6	74.5	0.1	103.7	1.3	n.m	9.9	n.m
ST54B	ST54B_2012	13.9	b.d.l	1.3	7.0	49.7	0.1	1.4	0.1	n.m	4.9	n.m
ST55A	ST55A_2013	138.8	0.4	1.9	4.9	42.9	0.2	101.9	b.d.l	n.m	n.m	24.3748
ST55A_2	ST55A_2_2013	158.5	0.5	2.3	4.5	40.9	0.3	141.6	n.m	n.m	n.m	25.7118
ST55B	ST55B_2013	116.6	0.2	0.7	11.0	77.0	0.3	168.7	n.m	b.d.l	b.d.l	28.6485
ST59A	ST59A_2012	17.0	b.d.l	2.0	35.4	60.9	0.1	0.7	0.1	n.m	48.8	n.m
ST60A	ST60A_2012	19.5	0.1	2.3	23.6	57.4	0.1	3.0	0.3	n.m	35.7	n.m
ST61A	ST61A_2013	18.8	n.m	2.5	15.0	80.9	0.2	47.5	3.4	b.d.l	34.4	0.0166
ST61B	ST61B_2013	7.9	n.m	2.0	14.4	47.0	0.2	20.1	0.4	n.m	19.9	0.0085
ST62A	ST62A_2012	33.3	b.d.l	2.6	18.3	138.9	b.d.l	119.4	4.1	n.m	25.1	n.m
ST64A	ST64A_2013	16.6	0.2	2.2	15.2	61.5	0.1	2.4	b.d.l	0.5	20.8	0.0162

Table S1. Concentrations of major ions, and dissolved methane data for (n=204) wells sampled from 2012 through 2013

SWIFT ID	Sample ID	Na (ppm)	NH4 (ppm)	K (ppm)	Mg (ppm)	Ca (ppm)	F (ppm)	Cl (ppm)	NO3 (ppm)	PO4 (ppm)	SO4 (ppm)	CH4 (mg/L)
ST69A	ST69A_2012	21.2	0.2	1.7	6.1	21.3	0.2	2.0	0.2	n.m	11.0	n.m
ST72A	ST72A_2013	31.2	b.d.l	3.1	18.0	75.1	0.2	2.0	b.d.l	n.m	53.2	0.0055
ST73A	ST73A_2012	39.8	0.3	2.0	11.4	50.2	0.1	40.9	b.d.l	n.m	1.5	n.m
ST73B	ST73B_2012	17.8	b.d.l	1.4	10.0	48.2	0.1	2.8	0.2	n.m	14.4	n.m
ST73C	ST73C_2013	13.9	n.m	2.2	10.2	64.5	b.d.l	28.7	1.2	n.m	15.4	0.0003
ST73D	ST73D_2013	12.0	n.m	0.8	5.8	53.0	0.1	20.2	7.3	n.m	13.2	0.0004
ST75A	ST75A_2013	15.1	b.d.l	2.7	22.3	96.8	0.2	5.3	1.6	n.m	80.0	0.0001
ST76A	ST76A_2012	43.0	b.d.l	1.5	8.2	53.7	b.d.l	93.9	3.3	n.m	10.8	n.m
ST76B	ST76B_2013	12.1	n.m	1.9	17.1	65.3	0.1	10.9	0.3	n.m	22.5	0.0004
ST77A	ST77A_2013	42.0	b.d.l	2.6	12.9	44.7	0.2	20.6	b.d.l	n.m	12.2	0.4058
ST79A	ST79A_2013	7.9	n.m	1.6	11.1	30.0	0.1	1.5	0.5	n.m	16.5	0.0001
ST82A	ST82A_2013	29.3	b.d.l	1.7	12.3	31.1	0.2	1.5	b.d.l	n.m	22.3	0.0033
ST84A	ST84A_2013	7.5	n.m	3.4	16.9	88.9	0.1	16.9	2.3	0.1	46.4	0.0002
ST85A	ST85A_2012	4.6	b.d.l	1.8	25.4	61.0	0.2	1.3	0.2	n.m	46.6	n.m
ST86A	ST86A_2012	5.2	b.d.l	2.0	14.3	60.1	0.2	4.6	1.1	n.m	15.6	n.m
ST86B	ST86B_2013	23.8	b.d.l	1.9	11.2	57.7	0.2	3.6	b.d.l	b.d.l	21.6	0.3502
ST87A	ST87A_2012	69.7	0.4	3.8	8.8	22.3	0.2	2.7	b.d.l	n.m	3.0	n.m
TI01A	TI01A_2013	10.4	b.d.l	0.4	8.2	34.8	0.1	0.7	b.d.l	n.m	12.7	0.0009
TI02A	TI02A_2013	7.2	b.d.l	0.6	7.2	28.7	0.2	2.9	b.d.l	n.m	17.1	0.0466
TI07A	TI07A_2013	50.1	n.m	1.8	17.1	61.5	b.d.l	82.4	11.4	n.m	12.7	0.0001
TI10A	TI10A_2012	14.0	0.5	1.2	8.9	36.5	0.2	34.1	b.d.l	n.m	10.1	n.m
TI10B	TI10B_2013	58.1	n.m	0.8	12.9	45.1	0.1	3.4	0.5	n.m	74.7	0.0002
TI11A	TI11A_2013	37.7	b.d.l	0.5	2.2	8.9	0.2	9.6	b.d.l	n.m	2.9	1.1548
TI11B	TI11B_2013	1.2	b.d.l	3.9	0.9	3.7	0.1	3.3	b.d.l	b.d.l	1.7	n.m
TI12A	TI12A_2013	10.4	b.d.l	0.7	13.5	54.8	b.d.l	7.8	b.d.l	n.m	10.1	0.0620
TI14A	TI14A_2013	11.6	n.m	0.5	11.6	37.8	0.1	3.5	0.6	b.d.l	15.1	0.0001
TI14B	TI14B_2013	23.5	n.m	0.6	17.8	68.7	0.1	56.5	n.m	b.d.l	21.5	0.0378
TI14C	TI14C_2013	9.1	n.m	0.4	4.7	21.3	b.d.l	8.7	5.4	n.m	8.1	0.0001
TI14D	TI14D_2013	17.2	n.m	1.3	18.4	79.0	b.d.l	16.9	26.5	n.m	13.3	0.0001
TI15A	TI15A_2013	63.6	b.d.l	0.5	1.5	9.7	0.3	2.8	b.d.l	n.m	20.4	0.0038
TI15B	TI15B_2013	15.7	n.m	2.0	10.1	59.5	b.d.l	24.6	12.4	n.m	10.5	0.0001
TI18D	TI18D_2013	14.0	b.d.l	0.8	8.9	41.3	0.1	1.9	2.0	b.d.l	8.3	0.0009

Table S1. Concentrations of major ions, and dissolved methane data for (n=204) wells sampled from 2012 through 2013

SWIFT ID	Sample ID	Na (ppm)	NH4 (ppm)	K (ppm)	Mg (ppm)	Ca (ppm)	F (ppm)	Cl (ppm)	NO3 (ppm)	PO4 (ppm)	SO4 (ppm)	CH4 (mg/L)
TI18E	TI18E_2013	17.8	b.d.l	0.8	10.9	50.0	0.1	5.1	0.5	n.m	9.2	0.0470
TI18F	TI18F_2013	8.6	n.m	1.1	14.8	53.1	0.1	10.6	0.6	n.m	14.9	0.0076
TI20A	TI20A_2013	53.4	b.d.l	1.1	17.9	38.8	0.3	1.2	b.d.l	0.8	46.4	0.1388
TI20B	TI20B_2013	9.8	n.m	0.6	11.0	47.1	0.1	24.4	19.8	b.d.l	13.9	0.0001
TI20C	TI20C_2013	18.0	n.m	1.4	9.4	41.6	0.1	26.6	3.8	n.m	8.7	n.m
TI21A	TI21A_2013	10.7	b.d.l	0.9	5.0	15.5	b.d.l	24.1	2.1	n.m	11.6	0.0001
TI21B	TI21B_2013	97.3	b.d.l	4.0	1.1	3.7	0.2	4.2	n.m	b.d.l	15.2	0.0020
TI22A	TI22A_2012	14.1	b.d.l	2.2	18.7	54.2	0.2	61.3	0.2	n.m	13.3	n.m
TI22B	TI22B_2013	43.0	0.2	0.8	7.1	26.4	0.2	6.6	b.d.l	n.m	4.5	n.m
TI22C	TI22C_2013	10.3	n.m	0.9	10.8	38.2	0.2	1.2	b.d.l	n.m	8.3	n.m
TI23A	TI23A_2013	46.4	0.2	1.0	20.7	61.4	0.2	8.3	n.m	b.d.l	78.6	0.5246
TI26A	TI26A_2013	36.5	b.d.l	0.9	31.7	111.2	0.1	4.0	b.d.l	n.m	179.4	0.0005
TI28A	TI28A_2013	40.1	n.m	0.9	8.2	42.1	0.1	53.5	10.1	n.m	13.5	0.0001
TI28B	TI28B_2013	32.8	0.3	1.4	10.6	41.6	0.2	4.0	b.d.l	n.m	14.1	0.0033
TI30A	TI30A_2013	147.2	b.d.l	1.1	b.d.l	1.3	0.2	3.9	n.m	0.2	76.3	0.0008
TI31A	TI31A_2012	32.2	0.2	2.0	9.5	39.4	0.2	4.6	b.d.l	n.m	9.9	n.m
TI31B	TI31B_2013	33.4	0.3	1.0	10.2	40.1	0.2	3.7	b.d.l	n.m	10.1	0.0375

b.d.l = below detection; n.m = not measured

Table S2. Concentrations of trace metals, bromide, and iodide

SWIFT ID	Sample ID	Li (ug/L)	B (ug/L)	Al (ug/L)	P (ug/L)	Mn (ug/L)	Fe (ug/L)	Zn (ug/L)	Sr (ug/L)	Ba (ug/L)	Pb (ug/L)	Se (ug/L)	Br (ppb)	I (ppb)
BR01A	BR01A_2013	13.2	b.d.l	b.d.l	b.d.l	11.1	93.3	5.9	373.0	97.4	0.1	b.d.l	8.6	2.6
BR09A	BR09A_2013	11.6	b.d.l	128.7	b.d.l	7.4	26.0	6.5	132.0	151.9	0.2	b.d.l	5.6	1.8
BR10A	BR10A_2013	1708.9	10747.0	120.0	b.d.l	5.1	237.6	235.3	39.3	b.d.l	0.1	b.d.l	5.6	4.9
BR12A	BR12A_2013	14.9	b.d.l	b.d.l	b.d.l	17.4	113.5	b.d.l	613.0	131.4	b.d.l	b.d.l	4.4	2.4
BR13A	BR13A_2012	7.5	27.8	n.m	b.d.l	3.2	n.m	12.3	234.2	31.7	0.5	b.d.l	b.d.l	6.2
BR13B	BR13B_2013	b.d.l	b.d.l	b.d.l	b.d.l	b.d.l	125.0	b.d.l	80.8	15.7	0.1	b.d.l	6.0	1.5
BR13C	BR13C_2013	b.d.l	b.d.l	b.d.l	b.d.l	b.d.l	b.d.l	b.d.l	b.d.l	b.d.l	b.d.l	b.d.l	11.4	2.2
BR14A	BR14A_2012	11.4	75.7	n.m	b.d.l	79.5	n.m	b.d.l	561.9	144.4	0.3	b.d.l	b.d.l	6.3
BR14B	BR14B_2013	54.4	b.d.l	b.d.l	b.d.l	67.4	70.3	b.d.l	631.8	105.8	b.d.l	b.d.l	9.6	3.1
BR15A	BR15A_2013	11.9	b.d.l	b.d.l	b.d.l	9.8	73.0	5.1	402.5	99.0	0.2	b.d.l	5.9	2.8
BR16A	BR16A_2013	b.d.l	b.d.l	10.1	b.d.l	109.5	50.3	9.5	41.8	75.9	0.2	b.d.l	2.1	0.5
BR16B	BR16B_2013	45.5	b.d.l	b.d.l	b.d.l	97.0	86.1	18.4	636.5	233.1	b.d.l	b.d.l	69.1	15.0
BR17A	BR17A_2012	10.1	64.8	n.m	b.d.l	70.2	n.m	6.5	255.9	211.9	0.0	b.d.l	b.d.l	17.3
BR17B	BR17B_2012	19.0	78.1	n.m	b.d.l	79.0	n.m	b.d.l	1128.4	54.6	1.3	b.d.l	b.d.l	13.5
BR18A	BR18A_2012	10.1	66.2	n.m	b.d.l	b.d.l	n.m	6.2	563.4	107.6	1.1	0.0	b.d.l	3.7
BR18B	BR18B_2013	39.7	b.d.l	b.d.l	b.d.l	2.9	25.0	4.2	161.1	47.0	b.d.l	b.d.l	13.9	5.1
BR19A	BR19A_2012	45.7	169.2	n.m	b.d.l	126.4	n.m	18.8	611.2	33.0	0.2	b.d.l	b.d.l	19.8
BR20A	BR20A_2012	14.0	74.0	n.m	b.d.l	22.7	n.m	b.d.l	862.4	117.4	0.3	b.d.l	b.d.l	2.6
BR21A	BR21A_2012	63.3	145.8	n.m	b.d.l	51.1	n.m	b.d.l	293.8	326.7	0.1	b.d.l	393.1	36.5
BR22A	BR22A_2013	b.d.l	b.d.l	b.d.l	b.d.l	4.9	61.4	31.8	147.1	54.2	0.9	b.d.l	b.d.l	0.6
BR22B	BR22B_2013	21.2	b.d.l	b.d.l	b.d.l	23.2	77.3	b.d.l	131.4	41.0	0.1	b.d.l	3.4	1.5
BR26A	BR26A_2013	61.0	b.d.l	b.d.l	b.d.l	16.6	114.2	b.d.l	924.1	215.5	b.d.l	b.d.l	446.1	27.7
BR28A	BR28A_2013	b.d.l	b.d.l	b.d.l	b.d.l	5.3	b.d.l	b.d.l	6.5	b.d.l	1.0	b.d.l	17.3	1.2
BR29A	BR29A_2013	46.7	b.d.l	b.d.l	b.d.l	17.9	39.9	b.d.l	397.0	77.0	b.d.l	b.d.l	13.5	9.6
BR30A	BR30A_2013	15.5	b.d.l	b.d.l	b.d.l	546.2	140.5	b.d.l	205.2	20.2	b.d.l	b.d.l	108.5	17.3
BR33A	BR33A_2013	34.9	b.d.l	b.d.l	b.d.l	6.0	70.4	b.d.l	373.3	93.2	b.d.l	b.d.l	15.9	6.2
BR34A	BR34A_2013	18.5	b.d.l	b.d.l	b.d.l	b.d.l	127.6	8.2	403.0	162.7	0.1	b.d.l	7.8	1.8
BR35A	BR35A_2012	22.4	102.6	n.m	b.d.l	384.2	n.m	11.0	611.4	68.3	0.3	b.d.l	b.d.l	7.6
BR36A	BR36A_2013	b.d.l	b.d.l	b.d.l	b.d.l	b.d.l	51.7	6.1	133.4	105.9	0.2	b.d.l	5.0	0.9
BR36B	BR36B_2013	44.3	b.d.l	b.d.l	b.d.l	209.7	140.1	5.0	1645.5	102.2	b.d.l	b.d.l	8.0	2.2
BR37A	BR37A_2013	79.7	b.d.l	b.d.l	b.d.l	48.5	76.2	b.d.l	1537.4	890.1	b.d.l	b.d.l	102.8	27.5
BR41A	BR41A_2013	b.d.l	b.d.l	b.d.l	b.d.l	b.d.l	61.3	8.8	45.7	119.9	0.2	b.d.l	11.3	0.6

Table S2. Concentrations of trace metals, bromide, and iodide

CM01A	CM01A_2013	46.6	b.d.l	b.d.l	b.d.l	61.9	117.5	b.d.l	444.4	478.1	b.d.l	b.d.l	241.5	14.5
CM02A	CM02A_2012	n.m	n.m	n.m	n.m	n.m	n.m	n.m	n.m	n.m	n.m	n.m	b.d.l	7.8
CM04A	CM04A_2012	13.8	82.7	n.m	b.d.l	13.3	n.m	12.1	630.0	101.2	0.1	b.d.l	b.d.l	4.9
CM06A	CM06A_2013	12.4	b.d.l	b.d.l	b.d.l	11.8	132.6	b.d.l	377.3	85.7	b.d.l	b.d.l	8.7	4.8
CM07A	CM07A_2012	46.4	108.2	n.m	b.d.l	135.9	n.m	13.2	3324.8	599.0	1.1	0.1	205.6	63.4
CM07B	CM07B_2013	b.d.l	b.d.l	b.d.l	b.d.l	b.d.l	234.7	48.5	128.8	82.7	0.6	b.d.l	8.1	0.5
CM09A	CM09A_2012	6.6	b.d.l	n.m	b.d.l	15.6	n.m	7.3	140.4	177.5	0.5	b.d.l	b.d.l	4.6
CM09B	CM09B_2013	b.d.l	b.d.l	b.d.l	b.d.l	291.7	209.3	b.d.l	228.5	290.6	b.d.l	b.d.l	6.6	1.3
CM10A	CM10A_2012	8.4	30.4	n.m	b.d.l	12.7	n.m	b.d.l	498.4	105.7	0.6	b.d.l	b.d.l	3.2
CM10B	CM10B_2012	14.7	103.0	n.m	b.d.l	18.1	n.m	b.d.l	610.5	58.3	0.3	b.d.l	b.d.l	6.8
CM12A	CM12A_2012	5.2	22.6	n.m	b.d.l	b.d.l	n.m	14.0	113.5	30.9	0.2	0.1	b.d.l	2.1
CM13A	CM13A_2012	10.1	b.d.l	n.m	b.d.l	b.d.l	n.m	9.1	324.5	302.6	0.6	0.0	50.4	13.1
CM14A	CM14A_2013	31.5	b.d.l	b.d.l	b.d.l	4.6	36.2	b.d.l	409.4	98.5	b.d.l	b.d.l	10.8	4.5
CM14B	CM14B_2013	32.9	b.d.l	b.d.l	b.d.l	56.2	44.5	b.d.l	152.4	128.3	b.d.l	b.d.l	289.8	42.5
CM16A	CM16A_2012	20.0	55.8	n.m	b.d.l	14.8	n.m	11.5	465.4	61.7	0.8	b.d.l	n.m	n.m
CM16B	CM16B_2012	12.3	26.5	n.m	b.d.l	b.d.l	n.m	46.5	222.2	167.7	0.3	0.1	b.d.l	4.7
CM16C	CM16C_2013	b.d.l	b.d.l	b.d.l	b.d.l	b.d.l	192.8	b.d.l	157.3	108.3	0.1	b.d.l	82.6	1.1
CM17A	CM17A_2012	44.0	232.8	n.m	15.9	1375.5	n.m	5.8	618.9	38.4	b.d.l	b.d.l	b.d.l	23.2
CM17B	CM17B_2013	15.5	b.d.l	b.d.l	b.d.l	139.4	92.7	5.4	414.2	80.8	0.1	b.d.l	8.8	4.1
CM18A	CM18A_2012	67.0	245.3	n.m	16.1	8.1	n.m	b.d.l	590.5	115.8	b.d.l	0.1	b.d.l	4.8
CM19A	CM19A_2012	n.m	n.m	n.m	n.m	n.m	n.m	n.m	n.m	n.m	n.m	n.m	b.d.l	5.0
CM19B	CM19B_2013	b.d.l	b.d.l	b.d.l	b.d.l	269.1	250.7	b.d.l	266.3	31.1	b.d.l	b.d.l	n.m	n.m
CM22A	CM22A_2013	17.7	b.d.l	b.d.l	b.d.l	24.6	107.3	16.5	408.1	420.3	0.3	b.d.l	284.6	18.1
CM22B	CM22B_2013	b.d.l	b.d.l	b.d.l	b.d.l	b.d.l	78.9	11.1	87.9	23.1	0.3	b.d.l	8.3	1.6
CM25A	CM25A_2012	472.0	637.1	n.m	54.6	59.2	n.m	b.d.l	1168.7	895.4	0.1	0.0	n.m	n.m
CN05A	CN05A_2013	102.0	435.3	b.d.l	b.d.l	13.9	38.0	b.d.l	508.6	105.7	b.d.l	b.d.l	110.4	5.6
CN06A	CN06A_2013	b.d.l	b.d.l	b.d.l	b.d.l	b.d.l	187.5	6.4	101.8	23.2	0.2	b.d.l	15.2	2.0
CN07A	CN07A_2013	10.5	b.d.l	b.d.l	b.d.l	b.d.l	107.5	8.9	469.7	87.2	0.2	b.d.l	n.m	n.m
CN10A	CN10A_2013	b.d.l	b.d.l	b.d.l	b.d.l	b.d.l	46.4	12.8	80.5	63.4	0.1	b.d.l	3.4	0.9
CN12A	CN12A_2013	15.0	b.d.l	b.d.l	b.d.l	12.1	99.1	21.6	409.7	82.3	0.1	b.d.l	7.4	2.0
CN14A	CN14A_2013	15.8	b.d.l	b.d.l	b.d.l	142.6	86.2	b.d.l	558.7	78.4	0.4	b.d.l	3.7	1.5
CN14B	CN14B_2013	42.4	365.6	b.d.l	b.d.l	11.7	25.2	b.d.l	369.9	143.9	0.1	b.d.l	7.9	1.6
CN18A	CN18A_2013	b.d.l	b.d.l	b.d.l	b.d.l	96.0	116.7	6.5	167.1	79.4	b.d.l	b.d.l	0.5	1.5

Table S2. Concentrations of trace metals, bromide, and iodide

CN18B	CN18B_2013	b.d.l	b.d.l	11.7	b.d.l	10.7	63.8	b.d.l	20.6	24.6	b.d.l	b.d.l	4.3	2.0
CN26A	CN26A_2013	16.8	b.d.l	b.d.l	b.d.l	b.d.l	93.2	30.4	1071.8	172.9	1.6	b.d.l	11.6	2.0
CN26B	CN26B_2013	b.d.l	b.d.l	b.d.l	b.d.l	4.0	80.2	12.2	123.9	75.8	0.2	b.d.l	2.0	2.0
CN26C	CN26C_2013	b.d.l	b.d.l	19.0	b.d.l	b.d.l	36.2	11.0	29.9	52.6	1.6	b.d.l	6.5	0.9
CN27A	CN27A_2013	10.9	b.d.l	b.d.l	b.d.l	54.5	142.5	4.1	335.1	117.6	b.d.l	0.1	19.7	3.8
CN30A	CN30A_2013	b.d.l	b.d.l	b.d.l	b.d.l	b.d.l	14.6	148.7	18.5	17.8	0.9	0.0	6.7	1.0
CN30B	CN30B_2013	b.d.l	b.d.l	b.d.l	b.d.l	b.d.l	104.3	8.7	67.3	24.1	0.1	b.d.l	13.5	0.8
CN30C	CN30C_2013	10.0	b.d.l	b.d.l	b.d.l	44.1	112.0	12.9	239.2	123.4	0.1	0.0	4.1	3.4
CN30C Artesian	CN30CArtesian_2013	11.7	b.d.l	b.d.l	b.d.l	b.d.l	22.7	5.3	41.5	15.7	b.d.l	b.d.l	6.6	1.0
CN31A	CN31A_2013	19.4	b.d.l	b.d.l	b.d.l	22.1	60.4	84.1	301.3	279.3	0.2	b.d.l	3.9	1.3
CN31B	CN31B_2013	21.8	b.d.l	b.d.l	b.d.l	171.1	259.5	b.d.l	439.9	127.4	b.d.l	0.0	3.2	2.9
CN32A	CN32A_2013	15.5	b.d.l	b.d.l	b.d.l	b.d.l	53.5	b.d.l	144.7	97.3	0.2	b.d.l	13.1	2.0
CN33A	CN33A_2013	50.8	367.2	b.d.l	b.d.l	11.7	47.3	10.1	1081.2	366.4	0.1	0.2	20.9	6.8
CN37A	CN37A_2013	33.7	b.d.l	b.d.l	b.d.l	38.4	74.9	b.d.l	750.3	1713.6	b.d.l	b.d.l	157.0	9.4
CN37A MILK	CN37AMILK_2013	16.1	b.d.l	b.d.l	b.d.l	b.d.l	101.6	b.d.l	109.5	281.3	0.2	0.0	7.4	1.6
CN38A	CN38A_2013	22.4	b.d.l	b.d.l	b.d.l	186.3	261.2	b.d.l	630.7	522.1	b.d.l	b.d.l	4.4	5.4
CN38B	CN38B_2013	74.7	b.d.l	b.d.l	b.d.l	3.4	b.d.l	b.d.l	125.3	154.7	b.d.l	b.d.l	11.2	1.1
CN38C	CN38C_2013	24.1	b.d.l	b.d.l	b.d.l	115.1	347.7	8.3	370.6	422.0	b.d.l	b.d.l	4.6	11.9
CN39A	CN39A_2013	36.2	253.6	b.d.l	b.d.l	86.2	45.7	5.3	1137.7	899.3	0.1	b.d.l	22.7	4.2
CN39B	CN39B_2013	15.8	b.d.l	b.d.l	b.d.l	1.5	86.0	b.d.l	167.1	83.4	0.8	b.d.l	3.7	6.0
CN43A	CN43A_2013	51.9	350.5	b.d.l	b.d.l	32.1	53.2	b.d.l	502.0	405.6	b.d.l	b.d.l	18.6	6.6
CN46A	CN46A_2013	33.1	b.d.l	b.d.l	b.d.l	b.d.l	29.4	13.7	239.8	241.3	0.1	0.5	7.1	0.9
CN49A	CN49A_2013	22.2	b.d.l	b.d.l	b.d.l	148.7	77.8	14.8	851.3	137.0	0.1	b.d.l	3.8	1.6
CN50A	CN50A_2013	14.7	b.d.l	b.d.l	b.d.l	2.0	67.7	42.8	79.8	33.6	0.3	0.1	12.1	0.9
CN50B	CN50B_2013	33.3	b.d.l	b.d.l	b.d.l	61.4	56.8	b.d.l	605.5	116.4	b.d.l	b.d.l	6.7	4.5
CN51A	CN51A_2013	15.9	b.d.l	b.d.l	b.d.l	1.8	49.3	13.3	149.2	74.1	0.4	0.1	2.8	1.1
CN52A	CN52A_2013	72.6	b.d.l	b.d.l	b.d.l	12.8	b.d.l	b.d.l	100.6	52.5	b.d.l	b.d.l	8.2	1.7
CN53A	CN53A_2013	18.8	b.d.l	b.d.l	b.d.l	b.d.l	36.8	5.0	367.1	34.9	0.2	0.0	3.5	1.0
ST01A	ST01A_2013	17.7	b.d.l	b.d.l	b.d.l	170.8	297.0	5.9	171.9	108.6	b.d.l	b.d.l	9.9	0.8
ST03A	ST03A_2012	49.8	294.7	n.m	b.d.l	20.4	n.m	b.d.l	262.0	256.6	b.d.l	b.d.l	510.8	30.1
ST04A	ST04A_2013	12.3	b.d.l	b.d.l	b.d.l	b.d.l	100.7	30.7	80.5	44.8	1.6	0.1	7.5	0.3
ST04B	ST04B_2013	14.2	b.d.l	b.d.l	b.d.l	b.d.l	68.2	4.4	56.2	14.8	0.1	0.2	3.8	0.4

Table S2. Concentrations of trace metals, bromide, and iodide

ST04C	ST04C_2013	12.8	b.d.l	b.d.l	b.d.l	3.5	85.5	15.2	55.6	28.9	0.1	0.1	28.3	1.5
ST05A	ST05A_2013	83.3	506.4	b.d.l	b.d.l	34.3	41.1	b.d.l	499.8	134.9	b.d.l	b.d.l	10.8	1.0
ST05B	ST05B_2013	216.6	527.7	b.d.l	b.d.l	47.1	116.9	b.d.l	3422.4	1080.2	b.d.l	0.1	4416.8	71.8
ST06A	ST06A_2012	51.0	300.2	n.m	b.d.l	63.4	n.m	b.d.l	1757.9	471.9	b.d.l	b.d.l	b.d.l	14.8
ST06C	ST06C_2013	77.1	550.5	b.d.l	b.d.l	35.2	51.3	b.d.l	734.6	569.3	b.d.l	0.0	370.2	21.1
ST09A	ST09A_2013	b.d.l	b.d.l	b.d.l	b.d.l	b.d.l	132.4	9.9	135.5	36.1	0.2	0.1	10.5	1.1
ST10A	ST10A_2012	b.d.l	b.d.l	n.m	b.d.l	b.d.l	n.m	13.4	80.2	45.1	0.1	0.2	b.d.l	2.2
ST10B	ST10B_2012	b.d.l	b.d.l	n.m	17.9	b.d.l	n.m	b.d.l	55.5	17.4	0.1	0.1	b.d.l	n.m
ST12A	ST12A_2012	23.1	142.0	n.m	b.d.l	40.8	n.m	b.d.l	579.3	767.5	b.d.l	b.d.l	111.9	11.7
ST12B	ST12B_2013	60.2	b.d.l	b.d.l	b.d.l	b.d.l	b.d.l	b.d.l	b.d.l	5.4	b.d.l	b.d.l	508.4	27.7
ST19A	ST19A_2012	17.2	133.0	n.m	21.6	63.3	n.m	b.d.l	238.7	181.4	b.d.l	b.d.l	55.4	8.8
ST19B	ST19B_2012	b.d.l	24.1	n.m	b.d.l	54.6	n.m	b.d.l	151.5	118.5	b.d.l	0.1	b.d.l	6.4
ST20A	ST20A_2013	b.d.l	b.d.l	b.d.l	b.d.l	3.8	144.8	50.5	174.5	245.3	n.m	b.d.l	9.7	1.2
ST23B	ST23B_2013	79.7	345.6	b.d.l	b.d.l	41.5	36.2	9.5	325.3	95.3	b.d.l	0.1	407.6	25.9
ST23C	ST23C_2013	132.8	441.4	b.d.l	b.d.l	8.2	31.0	5.8	391.6	222.1	b.d.l	b.d.l	157.2	20.9
ST24B	ST24B_2013	b.d.l	b.d.l	b.d.l	b.d.l	88.6	223.6	6.1	128.9	253.0	b.d.l	b.d.l	13.2	2.5
ST25A	ST25A_2012	41.0	69.1	n.m	b.d.l	89.1	n.m	6.1	4508.2	750.7	0.1	0.0	b.d.l	3.5
ST25B	ST25B_2013	b.d.l	b.d.l	b.d.l	b.d.l	29.9	112.3	5.4	115.7	138.4	0.3	0.1	7.9	4.9
ST26A	ST26A_2012	73.6	234.8	n.m	b.d.l	11.3	n.m	b.d.l	260.1	469.3	0.1	b.d.l	497.0	41.5
ST27A	ST27A_2013	b.d.l	b.d.l	b.d.l	b.d.l	5.8	109.2	5.9	124.2	282.2	0.1	b.d.l	7.9	0.8
ST28A	ST28A_2012	b.d.l	b.d.l	n.m	b.d.l	5.6	n.m	b.d.l	71.4	49.4	b.d.l	0.1	n.m	n.m
ST29A	ST29A_2013	b.d.l	b.d.l	b.d.l	b.d.l	161.2	237.8	6.2	241.3	137.0	b.d.l	0.1	7.4	0.7
ST30A	ST30A_2012	58.0	307.3	n.m	b.d.l	4.9	n.m	11.8	1605.9	61.3	b.d.l	0.1	b.d.l	3.6
ST30B	ST30B_2013	b.d.l	b.d.l	b.d.l	b.d.l	7.5	169.1	10.2	145.7	48.0	0.1	b.d.l	0.3	0.1
ST31A	ST31A_2012	13.8	b.d.l	n.m	b.d.l	12.1	n.m	b.d.l	83.6	29.7	0.0	0.4	b.d.l	1.4
ST33A	ST33A_2013	b.d.l	b.d.l	b.d.l	b.d.l	14.0	157.5	5.1	265.7	223.1	b.d.l	0.1	11.2	1.0
ST35A	ST35A_2012	18.6	36.6	n.m	b.d.l	40.1	n.m	13.1	204.4	34.7	0.5	b.d.l	b.d.l	4.7
ST35B	ST35B_2013	b.d.l	b.d.l	b.d.l	b.d.l	301.3	418.3	b.d.l	558.9	2128.2	38.7	0.1	9.7	2.5
ST35C	ST35C_2013	13.7	b.d.l	b.d.l	b.d.l	153.4	168.6	b.d.l	318.2	131.4	4.0	b.d.l	11.2	3.6
ST36B	ST36B_2013	b.d.l	b.d.l	b.d.l	b.d.l	4.8	100.9	30.6	98.8	95.2	0.2	b.d.l	6.0	1.6
ST36C	ST36C_2013	98.4	297.7	b.d.l	b.d.l	11.4	37.9	b.d.l	359.5	161.3	b.d.l	0.1	1154.9	60.7
ST37A	ST37A_2012	8.9	74.6	n.m	b.d.l	88.3	n.m	30.9	213.7	446.4	b.d.l	0.0	90.9	8.2
ST44A	ST44A_2013	10.2	b.d.l	b.d.l	b.d.l	2.4	182.6	11.7	174.9	48.2	0.3	0.0	41.7	3.3

Table S2. Concentrations of trace metals, bromide, and iodide

ST45A	ST45A_2012	5.4	b.d.l	n.m	b.d.l	2.1	n.m	b.d.l	106.1	85.4	0.2	0.0	b.d.l	5.7
ST46A	ST46A_2012	b.d.l	26.7	n.m	b.d.l	b.d.l	n.m	b.d.l	135.0	130.9	0.1	0.1	b.d.l	3.4
ST46B	ST46B_2012	5.4	b.d.l	n.m	b.d.l	11.4	n.m	10.7	109.9	719.5	0.1	0.0	b.d.l	3.9
ST46C	ST46C_2013	b.d.l	b.d.l	b.d.l	b.d.l	b.d.l	70.5	55.9	57.5	38.8	0.3	0.1	4.7	0.5
ST47A	ST47A_2012	8.7	40.4	n.m	b.d.l	14.4	n.m	11.3	334.5	88.6	0.3	b.d.l	b.d.l	3.5
ST47B	ST47B_2013	b.d.l	b.d.l	b.d.l	b.d.l	1098.3	385.2	5.7	75.8	56.8	0.1	0.0	15.1	1.2
ST49A	ST49A_2012	14.5	49.1	n.m	b.d.l	312.3	n.m	b.d.l	342.4	167.5	0.0	b.d.l	b.d.l	8.5
ST49B	ST49B_2013	b.d.l	b.d.l	b.d.l	b.d.l	b.d.l	67.6	6.8	58.0	235.5	0.4	0.0	17.1	0.7
ST51A	ST51A_2012	53.9	133.1	n.m	18.4	45.7	n.m	b.d.l	179.8	139.7	0.1	b.d.l	495.9	43.4
ST51B	ST51B_2012	n.m	n.m	n.m	n.m	n.m	n.m	n.m	n.m	n.m	n.m	n.m	108.5	11.2
ST52A	ST52A_2012	29.6	73.5	n.m	b.d.l	266.1	n.m	b.d.l	647.2	2102.9	0.5	b.d.l	368.8	32.3
ST53A	ST53A_2013	b.d.l	b.d.l	b.d.l	b.d.l	13.1	172.7	8.5	209.7	644.6	0.6	0.1	12.5	1.1
ST53B	ST53B_2013	b.d.l	b.d.l	b.d.l	b.d.l	36.7	156.6	b.d.l	204.9	1345.8	b.d.l	0.1	21.7	3.1
ST54A	ST54A_2012	b.d.l	b.d.l	n.m	b.d.l	19.9	n.m	b.d.l	146.3	287.7	b.d.l	0.1	307.0	24.2
ST54B	ST54B_2012	9.7	41.2	n.m	b.d.l	58.2	n.m	5.4	284.6	837.4	b.d.l	b.d.l	b.d.l	6.6
ST55A	ST55A_2013	89.3	322.0	b.d.l	b.d.l	169.4	113.4	9.3	1080.6	1105.8	b.d.l	0.1	719.2	34.1
ST55A_2	ST55A_2_ 2013	97.8	372.8	b.d.l	b.d.l	79.8	110.6	b.d.l	1385.5	1477.4	b.d.l	0.0	626.4	28.4
ST55B	ST55B_2013	b.d.l	b.d.l	b.d.l	b.d.l	501.5	3158.9	16.0	1050.1	1063.7	0.1	b.d.l	n.m	n.m
ST59A	ST59A_2012	23.6	59.1	n.m	b.d.l	10.2	n.m	b.d.l	469.9	30.4	0.1	0.1	b.d.l	6.5
ST60A	ST60A_2012	21.0	75.8	n.m	b.d.l	404.6	n.m	b.d.l	700.2	84.4	0.3	b.d.l	b.d.l	6.2
ST61A	ST61A_2013	10.1	b.d.l	b.d.l	b.d.l	2.7	198.1	71.1	314.2	53.8	0.1	0.0	7.6	0.3
ST61B	ST61B_2013	17.5	b.d.l	b.d.l	b.d.l	b.d.l	105.4	8.8	720.0	109.1	0.2	0.0	8.8	0.2
ST62A	ST62A_2012	13.0	31.2	n.m	b.d.l	56.5	n.m	21.6	317.6	583.7	b.d.l	0.1	68.5	21.9
ST64A	ST64A_2013	21.1	b.d.l	b.d.l	b.d.l	60.2	150.9	5.4	597.2	116.6	b.d.l	0.0	10.4	4.3
ST69A	ST69A_2012	12.1	67.1	n.m	b.d.l	22.0	n.m	b.d.l	553.7	79.9	0.2	b.d.l	b.d.l	3.0
ST72A	ST72A_2013	28.7	b.d.l	b.d.l	b.d.l	150.2	215.0	b.d.l	339.9	47.9	b.d.l	b.d.l	13.7	5.2
ST73A	ST73A_2012	n.m	n.m	n.m	n.m	n.m	n.m	n.m	n.m	n.m	n.m	n.m	361.2	32.7
ST73B	ST73B_2012	12.3	71.0	n.m	b.d.l	3.1	n.m	5.8	190.4	169.3	0.5	0.1	56.4	5.6
ST73C	ST73C_2013	15.3	b.d.l	b.d.l	b.d.l	1.5	151.0	24.2	367.0	181.8	0.2	b.d.l	88.9	6.5
ST73D	ST73D_2013	b.d.l	b.d.l	b.d.l	b.d.l	5.9	143.0	6.5	83.0	97.9	9.0	0.0	9.7	5.7
ST75A	ST75A_2013	23.5	b.d.l	b.d.l	b.d.l	7.2	233.6	6.3	481.5	23.5	b.d.l	0.0	16.0	3.6
ST76A	ST76A_2012	5.7	b.d.l	n.m	b.d.l	3.1	n.m	b.d.l	212.7	108.8	0.1	0.1	b.d.l	5.5
ST76B	ST76B_2013	14.2	b.d.l	b.d.l	b.d.l	7.9	161.1	15.2	180.1	20.2	0.2	0.1	16.9	4.6

Table S2. Concentrations of trace metals, bromide, and

ST77A	ST77A_2013	45.9	b.d.l	b.d.l	b.d.l	63.1	102.8	13.9	673.5	2357.5	0.1	b.d.l	95.4	8.2
ST79A	ST79A_2013	15.6	b.d.l	b.d.l	b.d.l	b.d.l	66.4	11.1	226.7	52.1	0.2	b.d.l	8.0	0.9
ST82A	ST82A_2013	25.9	b.d.l	b.d.l	b.d.l	20.3	167.6	7.8	673.8	63.6	b.d.l	0.1	12.0	3.9
ST84A	ST84A_2013	16.7	b.d.l	b.d.l	b.d.l	b.d.l	206.8	56.2	237.3	119.4	0.2	b.d.l	15.4	1.2
ST85A	ST85A_2012	14.7	b.d.l	n.m	b.d.l	b.d.l	n.m	b.d.l	96.8	73.7	0.0	0.1	b.d.l	1.8
ST86A	ST86A_2012	11.1	b.d.l	n.m	b.d.l	b.d.l	n.m	b.d.l	118.4	64.3	2.5	0.1	b.d.l	3.2
ST86B	ST86B_2013	22.4	b.d.l	b.d.l	b.d.l	137.5	134.1	4.8	415.9	249.6	0.1	b.d.l	20.2	4.5
ST87A	ST87A_2012	81.4	234.4	n.m	b.d.l	7.4	n.m	b.d.l	1185.8	812.1	b.d.l	b.d.l	b.d.l	7.9
TI01A	TI01A_2013	b.d.l	b.d.l	b.d.l	b.d.l	18.3	79.0	b.d.l	496.4	101.5	0.1	0.0	10.7	3.3
TI02A	TI02A_2013	b.d.l	b.d.l	b.d.l	b.d.l	684.1	119.3	27.0	96.9	207.9	b.d.l	b.d.l	8.1	1.4
TI07A	TI07A_2013	b.d.l	b.d.l	b.d.l	b.d.l	b.d.l	165.4	13.1	89.4	101.8	b.d.l	b.d.l	16.2	1.0
TI10A	TI10A_2012	9.0	30.7	n.m	b.d.l	261.8	n.m	7.4	364.6	189.7	0.4	b.d.l	b.d.l	16.9
TI10B	TI10B_2013	33.7	b.d.l	b.d.l	b.d.l	b.d.l	79.2	b.d.l	342.0	28.1	b.d.l	0.1	6.5	9.1
TI11A	TI11A_2013	25.6	b.d.l	b.d.l	b.d.l	41.9	231.9	b.d.l	131.6	204.0	0.2	b.d.l	7.4	0.9
TI11B	TI11B_2013	b.d.l	b.d.l	b.d.l	b.d.l	45.7	167.2	19.5	15.4	9.0	0.2	b.d.l	0.5	0.5
TI12A	TI12A_2013	b.d.l	b.d.l	b.d.l	b.d.l	4.8	133.9	179.8	144.9	142.3	b.d.l	0.0	8.8	3.6
TI14A	TI14A_2013	14.7	b.d.l	b.d.l	b.d.l	b.d.l	88.2	4.0	478.2	89.4	0.1	0.0	18.6	3.1
TI14B	TI14B_2013	16.7	b.d.l	b.d.l	b.d.l	165.6	163.5	b.d.l	426.4	316.8	b.d.l	0.0	204.7	19.1
TI14C	TI14C_2013	b.d.l	b.d.l	b.d.l	b.d.l	b.d.l	49.1	9.0	39.2	16.6	0.1	b.d.l	3.5	1.0
TI14D	TI14D_2013	b.d.l	b.d.l	b.d.l	b.d.l	b.d.l	188.5	b.d.l	113.7	112.2	b.d.l	0.1	15.9	2.6
TI15A	TI15A_2013	51.0	354.5	b.d.l	b.d.l	1.7	21.9	b.d.l	276.4	72.0	b.d.l	0.0	3.2	6.2
TI15B	TI15B_2013	b.d.l	b.d.l	b.d.l	b.d.l	b.d.l	186.4	b.d.l	101.8	55.8	0.2	b.d.l	4.9	9.1
TI18D	TI18D_2013	10.7	b.d.l	b.d.l	b.d.l	2.8	114.9	4.3	496.9	224.6	b.d.l	0.0	4.7	3.0
TI18E	TI18E_2013	13.0	b.d.l	b.d.l	b.d.l	90.0	143.8	b.d.l	753.0	240.9	b.d.l	b.d.l	10.7	3.5
TI18F	TI18F_2013	b.d.l	b.d.l	b.d.l	b.d.l	14.8	151.6	4.4	239.9	137.1	0.1	b.d.l	10.9	1.4
TI20A	TI20A_2013	b.d.l	b.d.l	b.d.l	b.d.l	601.9	524.8	13.5	282.9	13.8	b.d.l	b.d.l	15.6	12.0
TI20B	TI20B_2013	b.d.l	b.d.l	b.d.l	b.d.l	b.d.l	142.8	b.d.l	71.6	60.4	0.1	0.1	6.4	0.6
TI20C	TI20C_2013	b.d.l	b.d.l	b.d.l	b.d.l	2.8	124.2	b.d.l	73.5	50.0	b.d.l	0.1	13.1	1.1
TI21A	TI21A_2013	b.d.l	b.d.l	b.d.l	b.d.l	20.2	84.1	31.5	85.2	56.5	0.8	0.1	6.1	0.2
TI21B	TI21B_2013	10.6	b.d.l	b.d.l	b.d.l	49.8	10.9	b.d.l	21.0	5.0	b.d.l	b.d.l	12.0	5.5
TI22A	TI22A_2012	18.0	52.4	n.m	b.d.l	17.2	n.m	5.5	600.5	227.5	0.1	0.0	56.6	13.0
TI22B	TI22B_2013	21.3	b.d.l	b.d.l	b.d.l	20.4	76.1	b.d.l	480.1	508.6	b.d.l	b.d.l	72.5	1.2
TI22C	TI22C_2013	b.d.l	b.d.l	b.d.l	b.d.l	192.4	114.6	5.5	216.1	231.3	b.d.l	b.d.l	40.3	5.3

Table S2. Concentrations of trace metals, bromide, and

TI23A	TI23A_2013	25.3	b.d.l	b.d.l	b.d.l	293.0	181.6	5.4	422.5	24.5	b.d.l	b.d.l	6.9	2.3
TI26A	TI26A_2013	b.d.l	b.d.l	b.d.l	b.d.l	755.7	407.9	7.3	262.7	24.6	b.d.l	b.d.l	6.9	6.6
TI28A	TI28A_2013	b.d.l	b.d.l	b.d.l	b.d.l	3.0	132.6	4.2	61.8	38.9	0.1	0.3	17.6	2.2
TI28B	TI28B_2013	30.0	b.d.l	b.d.l	b.d.l	93.7	124.2	b.d.l	682.5	125.9	b.d.l	b.d.l	26.1	7.1
TI30A	TI30A_2013	b.d.l	b.d.l	b.d.l	b.d.l	6.6	11.9	b.d.l	9.7	b.d.l	b.d.l	b.d.l	10.2	5.7
TI31A	TI31A_2012	22.9	154.7	n.m	b.d.l	81.2	n.m	b.d.l	775.9	13.6	0.1	b.d.l	b.d.l	12.8
TI31B	TI31B_2013	22.4	b.d.l	b.d.l	b.d.l	91.2	116.3	7.1	1004.2	181.9	0.2	b.d.l	14.5	6.4
b.d.l = below detection; n.m = not measured														

Table S3. Methane Isotope data for groundwater wells sampled in 2014

Sample	2014 Sample ID	d^2H_{VSMOW}	$d^{13}C_{VPDB}$
1	TI20A	-123.1	-39.15
2	CN33A	-75.5	-35.13
3	CN38B	-173.6	-39.00
5	CN39A	-298.4	-51.12
6	CM14B	-155.0	-39.24
7	BR26A	-153.0	-48.06
9	TI11A	-183.3	-44.12
10	ST23C	-230.0	-48.72
11	ST55A_2	-253.8	-51.99
12	CN05A	-198.8	-42.43
13	ST01A	-162.3	-37.16
14	CM01A	-255.4	-76.06
15	ST12B	-270.3	-49.24
16	ST86B	-103.2	-42.97
17	ST55A	-253.4	-49.63
18	CN38A	-249.8	-79.72
19	CN37A Milk	-205.1	-40.25
20	TI23A	-184.0	-56.05
21	ST36C_2	-172.8	-57.30
23	CN43A	-81.3	-52.53
24	ST23B	-223.2	-47.99
25	ST06C	-260.9	-63.70
26	ST35B	-251.7	-58.23
27	ST77A	-145.7	-56.65
28	ST39A Basswood	-96.1	-37.52

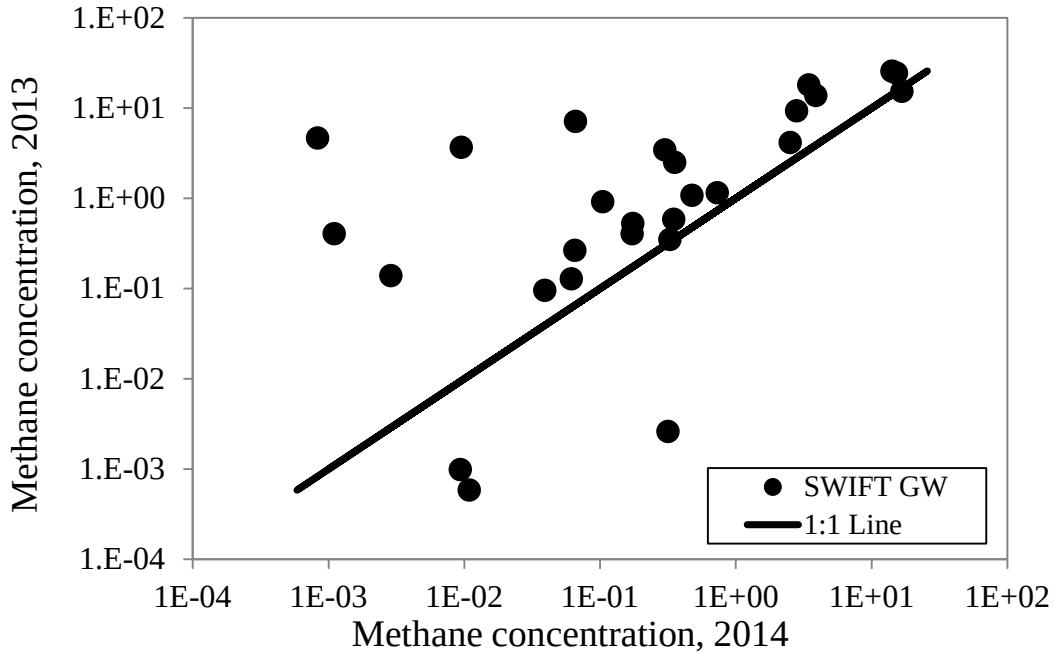

Figure S1. Comparison of dissolved methane concentrations from 2013 and 2014 against a 1:1 line of methane concentrations from 2013.

Table S5. Strontium Isotope data for groundwater wells

Sample Number	Sample ID	Sr (ppb)	87/86	Std Err %	2 SE
1	ST36C	359.456	0.711379	0.0007	0.000010
2	ST73C	367.046	0.711397	0.0006	0.000009
3	TI22A	600.457	0.711390	0.0007	0.000010
4	ST55A	1080.633	0.710975	0.0005	0.000007
5	ST55A_2	1385.470	0.711402	0.0007	0.000010
6	ST05B	3422.411	0.711391	0.0006	0.000009
7	ST53A	209.705	0.711391	0.0006	0.000009
8	CM13A	324.482	0.711384	0.0006	0.000009
9	ST23C	391.591	0.711393	0.0007	0.000010
10	BR36B	1645.482	0.711406	0.0006	0.000009
11	BR34A	403.011	0.711394	0.0008	0.000011
12	ST77A	673.457	0.713667	0.0006	0.000009
13	CN33A	1081.189	0.711399	0.0005	0.000007
14	ST35A	204.355	0.711396	0.0007	0.000010
15	CN39A	1137.654	0.711388	0.0006	0.000009
16	BR14B	631.828	0.711388	0.0006	0.000009

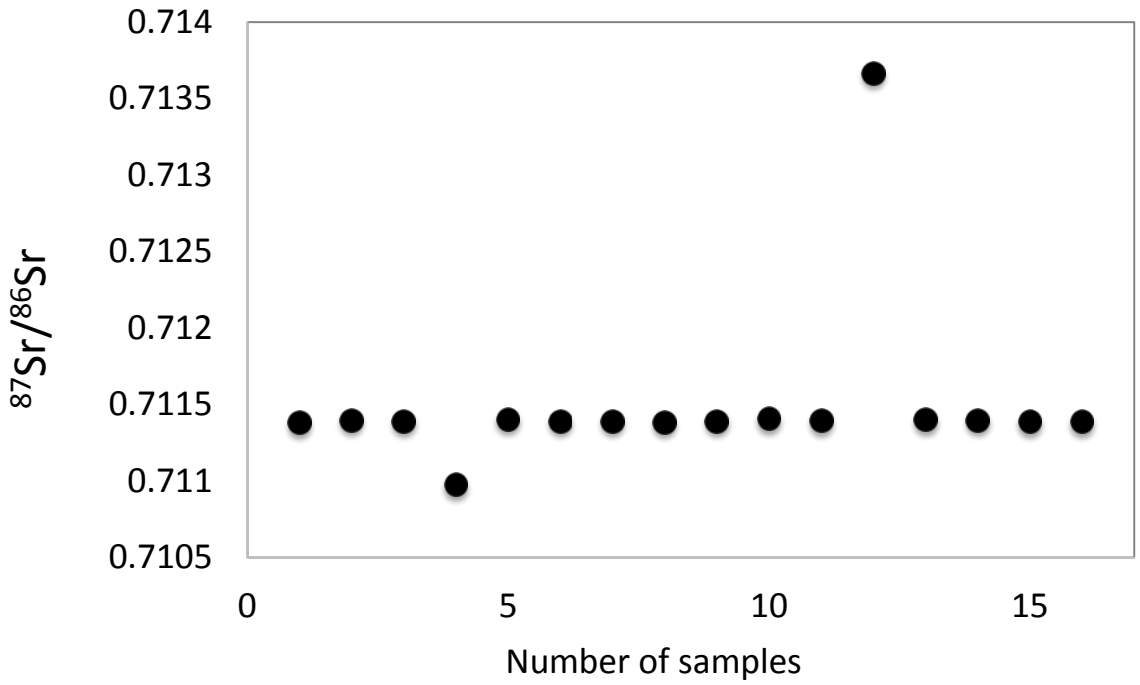

Figure S2. Range of strontium isotopes for groundwater samples

Table S1. Well distance to proximity parameters and landscape positon classification

SWIFT ID	Distance to Parameter in (km)						Distance to NHD Flowline (Ft)		Landscape Position		
	Fault	Lineament	Active Gas Well	Other Gas Well	Highways	Roads	Major Flowline	Minor Flowline	Mapped Valley Aquifer	NHD Based Method	DEM Based Method
BR01A	6.34	0.28	32.03	15.61	4.29	0.03	2035.1	2074.6	Upland	Upland	Upland
BR09A	2.48	0.13	39.03	13.72	0.11	0.11	575.0	1148.9	Upland	Valley	Valley
BR10A	2.16	0.10	40.91	12.97	0.92	0.14	2456.9	1821.8	Valley	Upland	Upland
BR12A	0.53	0.13	43.11	11.62	2.34	0.23	213.4	1906.0	Upland	Valley	Upland
BR13A	1.13	0.28	35.53	8.47	0.12	0.12	1426.1	955.8	Upland	Upland	Valley
BR13B	4.83	1.40	39.25	9.98	1.55	0.26	284.9	334.3	Upland	Valley	Valley
BR13C	1.56	0.17	36.86	8.46	0.60	0.01	836.8	1192.9	Valley	Valley	Valley
BR14A	3.16	0.30	33.39	8.41	0.21	0.13	3935.1	1365.1	Upland	Upland	Upland
BR14B	0.02	0.74	35.34	7.76	1.40	0.08	4612.6	491.9	Upland	Upland	Upland
BR15A	1.70	0.25	38.07	4.85	0.19	0.19	6760.7	426.3	Upland	Upland	Upland
BR16A	0.11	0.43	37.60	7.55	1.10	0.01	4579.1	1861.1	Upland	Upland	Upland
BR16B	0.30	0.21	37.07	6.34	0.05	0.05	1517.4	1127.0	Upland	Upland	Upland
BR17A	0.83	0.24	42.86	9.10	3.71	0.05	1449.2	2473.4	Upland	Upland	Upland
BR17B	0.14	0.45	41.16	6.96	2.04	0.35	2597.0	2609.0	Upland	Upland	Upland
BR18A	1.06	0.12	48.41	3.68	1.22	0.26	1102.0	4678.4	Upland	Upland	Upland
BR18B	2.02	0.33	46.35	8.90	2.45	0.01	3488.4	2045.7	Upland	Upland	Upland
BR19A	0.57	0.52	47.32	0.59	2.65	0.38	1398.7	471.8	Upland	Upland	Upland
BR20A	0.42	0.10	45.82	5.04	3.95	0.05	6583.6	1919.7	Upland	Upland	Upland
BR21A	0.73	0.11	45.27	9.73	0.03	0.03	126.8	1611.6	Valley	Valley	Valley
BR22A	3.13	0.19	44.47	14.81	2.06	0.07	4024.3	3489.5	Upland	Upland	Upland
BR22B	0.89	0.27	44.07	17.10	1.12	0.26	3617.2	2283.3	Upland	Upland	Upland
BR26A	4.54	0.80	43.31	7.41	0.81	0.01	4041.1	747.2	Upland	Upland	Upland
BR28A	0.80	0.91	54.67	3.99	3.44	0.03	181.5	543.6	Upland	Valley	Valley
BR29A	0.56	0.22	47.96	6.23	1.78	0.01	392.4	1558.0	Upland	Valley	Upland
BR30A	0.83	0.42	49.79	10.69	0.35	0.05	1889.2	294.1	Upland	Upland	Upland

Table S1. Well distance to proximity parameters and landscape positon classification

SWIFT ID	Distance to Parameter in (km)						Distance to NHD Flowline (Ft)		Landscape Position		
	Fault	Lineament	Active Gas Well	Other Gas Well	Highways	Roads	Major Flowline	Minor Flowline	Mapped Valley Aquifer	NHD Based Method	DEM Based Method
BR33A	4.17	0.29	54.19	13.88	1.96	0.01	38.8	4180.7	Upland	Valley	Upland
BR34A	0.89	0.06	43.90	10.24	3.71	0.14	2488.5	1080.6	Upland	Upland	Upland
BR35A	0.68	0.84	45.98	12.24	1.45	0.06	3429.0	1131.7	Upland	Upland	Upland
BR36A	1.87	0.53	51.37	10.58	3.59	0.15	2059.8	1699.2	Upland	Upland	Upland
BR36B	1.02	0.28	56.74	7.52	6.74	0.05	1439.0	188.9	Upland	Upland	Upland
BR37A	0.78	0.20	57.58	11.22	1.36	0.04	116.6	1939.8	Valley	Valley	Valley
BR41A	1.18	0.33	59.04	12.35	2.60	0.01	529.8	3067.2	Upland	Valley	Valley
CM01A	2.05	0.19	1.23	4.45	1.16	0.05	302.1	1118.9	Upland	Valley	Valley
CM02A	3.98	0.62	1.44	3.55	5.17	0.02	579.6	1980.2	Upland	Valley	Upland
CM04A	1.93	0.08	5.47	3.71	3.19	0.04	4265.7	655.0	Upland	Upland	Upland
CM06A	6.52	0.01	2.32	4.21	1.00	0.08	1677.3	307.7	Upland	Upland	Upland
CM07A	1.44	0.43	1.65	5.63	3.09	0.02	2684.4	1968.3	Valley	Upland	Upland
CM07B	1.32	0.01	3.27	5.85	5.68	0.03	1390.1	2626.7	Valley	Upland	Valley
CM09A	3.93	0.13	3.15	4.88	5.05	0.05	797.0	2226.8	Upland	Valley	Upland
CM09B	2.40	0.07	4.14	2.93	2.79	0.02	3237.0	247.9	Upland	Upland	Valley
CM10A	0.18	0.09	3.53	3.47	1.34	0.14	4680.0	702.8	Upland	Upland	Upland
CM10B	0.18	0.09	3.53	3.47	1.34	0.14	4680.0	702.8	Upland	Upland	Upland
CM12A	3.85	0.42	3.77	3.77	1.68	0.06	4837.9	1704.5	Upland	Upland	Upland
CM13A	2.59	0.22	2.03	2.03	5.73	0.07	5651.3	1950.3	Upland	Upland	Upland
CM14A	2.28	0.18	2.26	2.26	9.27	0.05	9941.3	744.9	Upland	Upland	Upland
CM14B	0.58	0.14	1.55	1.55	7.65	0.03	2523.4	144.6	Upland	Upland	Upland
CM16A	0.14	0.22	1.62	3.84	2.32	0.04	5073.9	1349.3	Upland	Upland	Upland
CM16B	3.55	0.72	0.83	1.69	4.20	0.02	3069.6	1111.6	Upland	Upland	Upland
CM16C	0.14	0.22	1.62	3.85	2.32	0.03	5067.0	1352.3	Upland	Upland	Upland
CM17A	0.58	1.34	6.03	3.50	3.61	0.06	138.0	2701.1	Upland	Valley	Valley

Table S1. Well distance to proximity parameters and landscape positon classification

SWIFT ID	Distance to Parameter in (km)						Distance to NHD Flowline (Ft)		Landscape Position		
	Fault	Lineament	Active Gas Well	Other Gas Well	Highways	Roads	Major Flowline	Minor Flowline	Mapped Valley Aquifer	NHD Based Method	DEM Based Method
CM17B	1.67	0.99	3.52	1.54	1.79	0.05	565.9	2032.0	Upland	Valley	Upland
CM18A	0.10	1.71	2.18	2.30	0.72	0.01	183.5	3859.2	Valley	Valley	Valley
CM19A	7.37	0.61	8.16	2.81	7.14	0.38	11386.7	1257.2	Upland	Upland	Upland
CM19B	6.21	1.18	6.78	2.44	8.05	0.01	8800.7	123.4	Upland	Upland	Valley
CM22A	7.93	0.03	4.07	3.68	0.71	0.02	1557.3	853.6	Upland	Upland	Upland
CM22B	8.31	1.40	4.67	3.89	2.20	0.01	2647.6	435.4	Upland	Upland	Upland
CM25A	1.59	0.02	15.22	10.20	1.44	0.14	901.2	335.4	Valley	Valley	Valley
CN05A	0.53	0.49	0.93	4.33	2.30	0.38	1257.9	1018.4	Upland	Upland	Upland
CN06A	0.63	0.03	1.61	6.19	0.67	0.06	1293.5	1497.8	Valley	Upland	Valley
CN07A	0.11	0.09	12.23	13.25	5.19	0.37	4721.9	1925.8	Upland	Upland	Upland
CN10A	0.32	0.45	8.99	7.32	0.89	0.29	1207.1	2294.7	Upland	Upland	Upland
CN12A	0.20	1.03	0.37	0.46	4.68	0.14	1969.0	317.1	Upland	Upland	Upland
CN14A	0.83	0.17	12.54	16.21	2.15	0.01	7500.1	480.3	Upland	Upland	Upland
CN14B	0.10	0.38	14.40	17.77	3.32	0.01	612.7	1693.4	Upland	Valley	Valley
CN18A	6.15	0.18	5.42	5.57	1.19	0.17	2823.4	263.5	Upland	Upland	Upland
CN18B	6.15	0.18	5.42	5.57	1.19	0.17	2823.4	263.5	Upland	Upland	Upland
CN26A	0.49	0.09	4.62	4.62	1.45	0.06	4440.7	1359.3	Upland	Upland	Upland
CN26B	2.15	1.25	0.28	0.28	5.96	0.17	4649.7	1401.0	Upland	Upland	Upland
CN26C	2.27	0.41	6.72	0.41	1.06	0.04	1235.7	1390.9	Upland	Upland	Upland
CN27A	4.12	1.20	12.34	12.50	1.16	0.02	4024.6	606.3	Upland	Upland	Upland
CN30A	3.15	0.76	15.80	9.17	3.93	0.05	3002.7	1385.8	Upland	Upland	Upland
CN30B	1.89	0.32	13.21	11.79	0.02	0.02	744.7	710.3	Valley	Valley	Valley
CN30C	5.89	0.23	20.37	5.36	1.59	0.04	2642.2	1465.2	Upland	Upland	Upland
CN30CArtesian	5.89	0.23	20.37	5.36	1.59	0.04	2642.2	1465.2	Upland	Upland	Upland
CN31A	2.62	1.04	15.94	5.49	1.21	0.02	1508.3	2282.5	Upland	Upland	Upland

Table S1. Well distance to proximity parameters and landscape positon classification

SWIFT ID	Distance to Parameter in (km)						Distance to NHD Flowline (Ft)		Landscape Position		
	Fault	Lineament	Active Gas Well	Other Gas Well	Highways	Roads	Major Flowline	Minor Flowline	Mapped Valley Aquifer	NHD Based Method	DEM Based Method
CN31B	0.81	0.13	11.12	4.75	3.27	0.02	185.6	373.7	Upland	Valley	Upland
CN32A	0.15	0.42	3.99	2.08	2.94	0.18	6580.0	1714.2	Upland	Upland	Upland
CN33A	2.02	0.14	9.37	1.29	0.56	0.05	142.6	1403.6	Upland	Valley	Upland
CN37A	3.41	0.30	16.42	3.15	4.29	0.02	1597.2	1872.0	Upland	Upland	Upland
CN37AMILK	3.41	0.30	16.42	3.15	4.29	0.02	1597.2	1872.0	Upland	Upland	Upland
CN38A	6.71	1.53	16.02	6.19	3.42	0.02	2009.2	256.7	Upland	Upland	Upland
CN38B	4.13	1.37	16.46	5.19	1.13	0.09	4643.5	610.2	Upland	Upland	Upland
CN38C	4.25	0.12	12.42	5.47	5.19	0.20	760.5	3175.5	Upland	Valley	Valley
CN39A	0.26	0.55	16.23	4.89	2.54	0.05	1431.8	295.3	Upland	Upland	Upland
CN39B	1.59	0.35	12.87	4.46	1.81	0.05	995.3	1839.7	Upland	Upland	Valley
CN43A	4.87	0.40	24.92	5.91	0.17	0.07	2841.2	12.2	Upland	Upland	Upland
CN46A	0.83	0.05	26.10	11.45	3.50	0.03	1005.9	85.4	Upland	Upland	Valley
CN49A	0.07	0.11	31.15	12.38	2.19	0.05	4504.6	1750.9	Upland	Upland	Upland
CN50A	0.06	0.31	29.35	4.89	0.11	0.11	1195.0	1206.5	Upland	Upland	Upland
CN50B	1.02	0.50	27.75	7.62	3.74	0.05	1342.1	1246.1	Upland	Upland	Upland
CN51A	1.58	0.53	26.90	1.17	1.22	0.09	2522.7	1680.9	Upland	Upland	Upland
CN52A	2.82	0.57	27.60	7.80	0.23	0.03	342.0	2003.8	Upland	Valley	Valley
CN53A	2.59	1.16	34.96	9.82	1.44	0.03	1512.8	2251.8	Upland	Upland	Upland
ST01A	0.63	0.39	5.32	5.89	0.05	0.03	4201.8	2550.2	Valley	Upland	Valley
ST03A	0.44	0.10	13.22	3.83	2.58	0.00	5095.8	11.4	Upland	Valley	Upland
ST04A	1.77	0.09	17.22	3.23	0.00	0.00	2867.4	98.7	Upland	Upland	Valley
ST04B	2.61	1.18	16.69	3.58	0.64	0.01	6672.8	662.1	Upland	Upland	Upland
ST04C	1.83	0.02	17.16	3.19	0.06	0.06	3099.2	267.1	Upland	Upland	Valley
ST05A	1.28	0.17	19.92	2.52	4.60	0.03	411.5	745.0	Upland	Valley	Valley
ST05B	1.20	0.07	19.83	2.58	4.71	0.03	542.5	711.2	Upland	Valley	Valley

Table S1. Well distance to proximity parameters and landscape positon classification

SWIFT ID	Distance to Parameter in (km)						Distance to NHD Flowline (Ft)		Landscape Position		
	Fault	Lineament	Active Gas Well	Other Gas Well	Highways	Roads	Major Flowline	Minor Flowline	Mapped Valley Aquifer	NHD Based Method	DEM Based Method
ST06A	0.71	0.30	14.43	1.69	8.72	0.17	16912.3	1400.6	Upland	Upland	Upland
ST06C	0.46	0.41	14.62	1.90	8.96	0.06	16320.3	1421.4	Upland	Upland	Upland
ST09A	0.12	0.03	6.72	7.93	1.15	0.15	828.8	1639.4	Upland	Valley	Upland
ST10A	1.92	0.88	10.77	6.27	1.35	0.09	9713.2	205.6	Upland	Valley	Upland
ST10B	1.63	0.59	10.62	6.28	1.06	0.07	9949.8	117.6	Upland	Valley	Upland
ST12A	0.01	0.15	11.60	2.96	5.65	0.13	434.3	401.6	Upland	Valley	Valley
ST12B	1.44	0.81	9.93	3.88	7.05	0.07	396.5	307.9	Upland	Valley	Valley
ST19A	3.06	2.00	4.34	9.27	2.01	0.02	523.6	4780.5	Upland	Valley	Upland
ST19B	2.70	0.53	6.54	6.92	3.13	0.20	2965.3	318.6	Upland	Valley	Upland
ST20A	2.57	0.11	4.87	7.53	2.81	0.04	7850.4	834.7	Upland	Upland	Upland
ST23B	2.22	0.28	12.39	3.80	4.25	0.07	22388.1	1966.2	Upland	Upland	Upland
ST23C	2.18	0.24	12.46	3.74	4.19	0.08	22606.0	1738.1	Upland	Upland	Upland
ST24B	0.19	0.02	10.39	7.43	0.04	0.03	2113.1	1093.4	Upland	Upland	Valley
ST25A	1.94	0.37	10.99	1.07	0.98	0.04	810.5	2179.3	Upland	Upland	Upland
ST25B	2.66	0.04	5.83	4.87	2.13	0.03	5996.7	579.5	Upland	Upland	Upland
ST26A	0.06	0.69	9.29	2.48	0.34	0.06	3069.4	844.0	Upland	Upland	Upland
ST27A	6.11	0.64	2.56	7.55	2.07	0.04	1689.1	1196.9	Upland	Upland	Upland
ST28A	1.67	0.62	6.49	6.08	0.97	0.03	5159.7	1118.6	Upland	Upland	Upland
ST29A	0.97	0.58	11.50	6.28	1.42	0.07	455.8	1015.8	Upland	Valley	Valley
ST30A	1.10	0.25	10.62	8.82	3.36	0.06	9992.4	1392.7	Upland	Upland	Upland
ST30B	0.45	0.22	13.08	5.55	0.14	0.04	1865.5	561.9	Upland	Upland	Valley
ST31A	2.07	0.06	7.73	8.25	2.27	0.09	6591.7	1813.8	Upland	Upland	Upland
ST33A	0.75	1.18	5.11	5.28	1.26	0.04	3779.7	61.8	Valley	Upland	Upland
ST35A	0.37	0.13	10.44	3.77	6.34	0.17	1868.2	4174.4	Upland	Upland	Upland
ST35B	1.24	0.10	8.61	6.68	3.35	0.01	2713.0	1678.0	Upland	Upland	Upland

Table S1. Well distance to proximity parameters and landscape positon classification

SWIFT ID	Distance to Parameter in (km)						Distance to NHD Flowline (Ft)		Landscape Position		
	Fault	Lineament	Active Gas Well	Other Gas Well	Highways	Roads	Major Flowline	Minor Flowline	Mapped Valley Aquifer	NHD Based Method	DEM Based Method
ST35C	0.81	0.28	10.62	3.50	6.68	0.09	2505.3	3529.7	Upland	Upland	Upland
ST36B	0.55	0.08	7.45	4.76	1.86	0.15	867.7	599.3	Upland	Upland	Upland
ST36C	0.72	0.08	7.61	4.64	1.94	0.03	986.0	125.6	Upland	Upland	Valley
ST37A	4.71	0.04	7.27	1.23	0.72	0.13	279.3	1184.6	Valley	Valley	Valley
ST44A	4.01	0.09	14.20	4.20	6.65	0.02	2239.0	1292.6	Upland	Upland	Upland
ST45A	2.37	1.28	6.13	2.23	3.83	0.25	3250.5	937.9	Upland	Upland	Upland
ST46A	1.66	0.63	2.87	2.08	0.63	0.03	295.1	327.7	Valley	Valley	Valley
ST46B	0.09	0.76	2.12	2.42	2.10	0.11	3959.0	984.3	Upland	Upland	Upland
ST46C	2.75	0.78	10.04	5.22	7.91	0.04	2575.5	2976.0	Upland	Upland	Upland
ST47A	1.77	1.13	1.47	1.64	4.56	0.03	6676.2	2416.8	Upland	Upland	Upland
ST47B	1.30	0.21	2.39	1.28	6.87	0.05	417.0	822.2	Valley	Upland	Valley
ST49A	3.16	0.25	4.71	3.03	6.69	0.11	430.0	225.9	Upland	Valley	Upland
ST49B	2.27	0.29	2.92	3.88	0.02	0.02	1442.7	243.6	Upland	Upland	Upland
ST51A	2.02	0.27	6.41	0.33	0.06	0.05	604.8	1029.2	Upland	Valley	Valley
ST51B	0.64	0.02	10.19	3.19	2.19	0.01	286.8	630.0	Upland	Valley	Valley
ST52A	3.28	0.76	12.46	3.56	4.12	0.02	415.5	170.2	Upland	Valley	Valley
ST53A	0.27	0.24	11.22	7.02	7.58	0.33	3059.1	2439.2	Upland	Upland	Upland
ST53B	0.56	0.53	11.13	7.25	7.27	0.00	3467.8	2559.4	Upland	Upland	Upland
ST54A	2.32	0.46	12.33	2.30	10.22	0.01	3438.8	3025.2	Upland	Upland	Upland
ST54B	0.59	0.23	9.62	5.98	6.47	0.23	4580.9	1349.7	Upland	Upland	Upland
ST55A	0.43	0.33	8.89	5.50	4.68	0.04	362.4	1236.8	Upland	Valley	Upland
ST55A_2	0.50	0.27	8.83	5.44	4.62	0.03	250.0	1323.5	Upland	Valley	Upland
ST55B	0.50	0.61	7.06	4.80	3.17	0.00	3375.3	12.7	Upland	Upland	Upland
ST59A	0.19	0.06	5.46	5.51	0.81	0.04	2873.3	330.5	Upland	Valley	Upland
ST60A	1.79	0.11	0.93	4.34	0.94	0.03	5574.0	96.1	Upland	Valley	Upland

Table S1. Well distance to proximity parameters and landscape positon classification

SWIFT ID	Distance to Parameter in (km)						Distance to NHD Flowline (Ft)		Landscape Position		
	Fault	Lineament	Active Gas Well	Other Gas Well	Highways	Roads	Major Flowline	Minor Flowline	Mapped Valley Aquifer	NHD Based Method	DEM Based Method
ST61A	0.40	0.70	7.46	7.19	0.99	0.04	9131.2	1893.5	Upland	Upland	Upland
ST61B	0.76	0.94	4.45	3.28	2.21	0.05	1799.3	3753.0	Upland	Upland	Upland
ST62A	1.19	1.68	12.70	0.57	3.90	0.01	6671.7	1712.3	Upland	Upland	Upland
ST64A	3.93	1.23	15.33	2.36	7.06	0.04	1460.3	3593.9	Upland	Upland	Upland
ST69A	1.52	0.15	5.90	2.46	1.77	0.02	5885.0	352.1	Upland	Valley	Upland
ST72A	3.25	0.49	6.70	3.74	0.57	0.07	953.5	995.0	Upland	Valley	Upland
ST73A	1.62	2.06	7.28	1.35	0.55	0.07	623.7	2814.7	Upland	Valley	Valley
ST73B	1.28	1.73	6.10	2.54	1.26	0.28	2365.2	2916.0	Upland	Upland	Upland
ST73C	1.04	0.05	6.10	3.18	3.15	0.04	2675.4	1314.1	Upland	Upland	Upland
ST73D	1.82	0.65	5.47	4.15	4.10	0.06	1117.5	394.9	Upland	Upland	Valley
ST75A	0.46	0.45	13.90	5.38	4.52	0.04	4391.6	1611.1	Upland	Upland	Upland
ST76A	1.42	0.65	4.55	3.56	4.65	0.03	2522.3	2316.3	Upland	Upland	Upland
ST76B	0.36	0.29	6.10	2.23	7.60	0.05	4709.9	1630.5	Upland	Upland	Upland
ST77A	2.83	1.66	40.81	4.71	0.71	0.06	974.1	1156.5	Valley	Upland	Valley
ST79A	0.45	1.34	5.47	2.69	2.49	0.30	3208.0	940.0	Upland	Upland	Upland
ST82A	4.02	0.35	2.33	8.50	7.02	0.49	2756.9	1664.3	Upland	Upland	Upland
ST84A	1.26	0.38	14.33	8.55	6.90	0.04	1348.0	2240.3	Upland	Upland	Upland
ST85A	1.74	1.37	14.70	10.41	7.35	0.00	2928.8	1164.5	Upland	Upland	Upland
ST86A	1.60	0.39	7.08	3.56	7.53	0.04	1336.4	1655.5	Upland	Upland	Upland
ST86B	3.09	0.56	6.17	2.82	9.17	0.04	4123.5	105.8	Upland	Upland	Valley
ST87A	2.84	0.30	5.41	2.02	9.40	0.17	2667.1	1339.0	Upland	Upland	Upland
TI01A	4.00	0.59	27.44	18.48	1.79	0.03	6432.2	800.9	Upland	Upland	Upland
TI02A	0.13	0.24	31.48	22.80	0.56	0.19	248.4	942.2	Upland	Valley	Upland
TI07A	1.42	0.31	6.38	1.47	3.63	0.01	253.9	424.2	Valley	Valley	Valley
TI10A	2.87	0.38	24.59	16.38	4.88	0.11	656.0	656.8	Valley	Valley	Valley

Table S1. Well distance to proximity parameters and landscape positon classification

SWIFT ID	Distance to Parameter in (km)						Distance to NHD Flowline (Ft)		Landscape Position		
	Fault	Lineament	Active Gas Well	Other Gas Well	Highways	Roads	Major Flowline	Minor Flowline	Mapped Valley Aquifer	NHD Based Method	DEM Based Method
TI10B	2.08	0.21	20.49	11.79	9.03	0.06	4074.3	574.3	Upland	Upland	Upland
TI11A	2.05	0.49	32.61	18.38	2.70	0.01	1052.5	102.8	Upland	Upland	Valley
TI11B	2.05	0.49	32.61	18.38	2.70	0.01	1052.5	102.8	Upland	Upland	Valley
TI12A	1.18	0.39	6.88	0.98	4.19	0.03	1118.7	88.3	Valley	Upland	Valley
TI14A	0.39	0.08	16.92	6.47	9.35	0.04	531.4	776.1	Valley	Valley	Valley
TI14B	1.04	0.52	15.39	6.86	10.17	0.02	980.1	1058.9	Valley	Upland	Valley
TI14C	1.16	0.44	15.87	7.04	10.18	0.04	756.2	572.0	Valley	Valley	Valley
TI14D	1.06	0.51	15.38	6.88	10.19	0.02	954.2	1020.8	Valley	Upland	Valley
TI15A	5.63	0.42	21.56	4.98	4.18	0.09	6101.1	746.3	Upland	Upland	Upland
TI15B	3.66	0.37	25.48	9.00	3.36	0.06	576.2	131.5	Valley	Valley	Valley
TI18D	1.70	0.07	10.00	2.62	9.83	0.30	3805.8	842.0	Upland	Upland	Upland
TI18E	1.78	1.08	25.11	1.81	1.66	0.06	777.8	2566.6	Upland	Valley	Upland
TI18F	1.70	0.07	10.00	2.62	9.83	0.30	3805.8	842.0	Upland	Upland	Upland
TI20A	4.52	0.89	23.73	7.08	1.90	0.05	1673.1	661.2	Upland	Upland	Upland
TI20B	5.27	0.31	22.29	5.31	0.55	0.05	156.3	661.6	Valley	Valley	Valley
TI20C	5.00	0.17	22.62	3.90	0.73	0.03	215.5	396.2	Valley	Valley	Valley
TI21A	0.27	0.69	27.77	7.57	3.70	0.09	3997.3	507.4	Upland	Upland	Upland
TI21B	0.02	0.29	33.75	3.79	4.52	0.09	12743.8	1280.5	Upland	Upland	Upland
TI22A	3.73	0.24	12.16	9.06	5.54	0.04	3655.8	1100.1	Upland	Upland	Upland
TI22B	9.31	0.17	28.27	5.23	0.35	0.12	585.0	795.2	Upland	Valley	Valley
TI22C	9.31	0.17	28.27	5.23	0.35	0.12	585.0	795.2	Upland	Valley	Valley
TI23A	4.52	0.40	11.15	8.01	7.78	0.02	238.8	1876.1	Upland	Valley	Upland
TI26A	1.54	0.37	30.37	2.87	2.28	0.12	2783.4	1117.6	Upland	Upland	Upland
TI28A	0.01	0.08	16.73	11.68	4.21	0.01	1127.2	1214.8	Valley	Upland	Valley
TI28B	2.00	2.16	20.75	9.29	3.60	0.07	6252.3	1584.8	Upland	Upland	Upland

Table S1. Well distance to proximity parameters and landscape positon classification

SWIFT ID	Distance to Parameter in (km)						Distance to NHD Flowline (Ft)		Landscape Position		
	Fault	Lineament	Active Gas Well	Other Gas Well	Highways	Roads	Major Flowline	Minor Flowline	Mapped Valley Aquifer	NHD Based Method	DEM Based Method
TI30A	3.48	0.60	24.31	3.59	1.04	0.00	1689.2	4612.0	Upland	Upland	Upland
TI31A	1.80	0.48	32.85	1.68	3.16	0.07	2099.2	1658.7	Upland	Upland	Upland
TI31B	1.80	0.47	32.87	1.67	3.15	0.05	2095.7	1634.0	Upland	Upland	Upland

Table S2. Bedrock Classification using the bedrock interpolation method and the geologic map method

SWIFT ID	Bedrock Classification	
	Bedrock Interpolation Method	Geologic Map Method
BR01A		
BR09A		
BR10A	Genesee	Sonyea
BR12A	Sonyea	West Falls
BR13A	Genesee	Sonyea
BR13B	Sonyea	Sonyea
BR13C		
BR14A		
BR14B		
BR15A	West Falls	West Falls
BR16A		
BR16B	Sonyea	West Falls
BR17A	Sonyea	West Falls
BR17B	West Falls/Sonyea	West Falls
BR18A	West Falls	West Falls
BR18B	Sonyea	West Falls
BR19A	West Falls	West Falls
BR20A	West Falls	West Falls
BR21A	Genesee	Sonyea
BR22A	West Falls	West Falls
BR22B	West Falls	West Falls
BR26A	West Falls	West Falls
BR28A	West Falls/Sonyea	West Falls
BR29A	West Falls	West Falls
BR30A	West Falls/Sonyea	West Falls
BR33A	West Falls	West Falls
BR34A	West Falls	West Falls
BR35A	West Falls	West Falls
BR36A	West Falls/Sonyea	West Falls
BR36B	West Falls/Sonyea	West Falls
BR37A		
BR41A	West Falls	West Falls
CM01A	West Falls	West Falls
CM02A	West Falls	West Falls

Table S2. Bedrock Classification using the bedrock interpolation method and the geologic map method

SWIFT ID	Bedrock Classification	
	Bedrock Interpolation Method	Geologic Map Method
CM04A	West Falls	West Falls
CM06A	West Falls	West Falls
CM07A	West Falls	West Falls
CM07B	Sonyea	West Falls
CM09A	West Falls	West Falls
CM09B		
CM10A	West Falls	West Falls
CM10B	West Falls	West Falls
CM12A	West Falls	West Falls
CM13A	West Falls	West Falls
CM14A	West Falls	West Falls
CM14B	West Falls	West Falls
CM16A	West Falls	West Falls
CM16B	West Falls	West Falls
CM16C		
CM17A	West Falls	West Falls
CM17B	West Falls	West Falls
CM18A	West Falls	West Falls
CM19A	West Falls	West Falls
CM19B		
CM22A	West Falls	West Falls
CM22B	West Falls	West Falls
CM25A	West Falls	West Falls
CN05A	Hamilton	Hamilton
CN06A	Hamilton	Hamilton
CN07A	Hamilton	Hamilton
CN10A	Genesee	Genesee
CN12A	Hamilton	Genesee
CN14A		
CN14B	Genesee	Genesee
CN18A	Genesee	Genesee
CN18B		
CN26A	Error	Hamilton
CN26B	Genesee	Genesee
CN26C	Genesee	Genesee
CN27A	Genesee	Genesee

Table S2. Bedrock Classification using the bedrock interpolation method and the geologic map method

SWIFT ID	Bedrock Classification	
	Bedrock Interpolation Method	Geologic Map Method
CN30A	Genesee	Genesee
CN30B	Genesee	Genesee
CN30C	Genesee	Sonyea
CN30CArtesian		
CN31A	Genesee	Genesee
CN31B	Genesee	Genesee
CN32A	Genesee	Genesee
CN33A	Error	Hamilton
CN37A	Genesee	Genesee
CN37AMILK	Genesee	Genesee
CN38A	Genesee	Genesee
CN38B	Genesee	Genesee
CN38C	Genesee	Genesee
CN39A	Error	Hamilton
CN39B	Error	Hamilton
CN43A	Genesee	Genesee
CN46A		
CN49A	Genesee	Sonyea
CN50A	Genesee	Sonyea
CN50B	Sonyea	Sonyea
CN51A	Genesee/Sonyea	Sonyea
CN52A	Genesee/Sonyea	Sonyea
CN53A	Genesee/Sonyea	Sonyea
ST01A	West Falls	West Falls
ST03A		
ST04A	West Falls	West Falls
ST04B	West Falls	West Falls
ST04C	West Falls	West Falls
ST05A	West Falls	West Falls
ST05B	West Falls	West Falls
ST06A		
ST06C	West Falls	West Falls
ST09A		
ST10A	Error	Java
ST10B		
ST12A	West Falls	West Falls

Table S2. Bedrock Classification using the bedrock interpolation method and the geologic map method

SWIFT ID	Bedrock Classification	
	Bedrock Interpolation Method	Geologic Map Method
ST12B	West Falls	West Falls
ST19A	West Falls	West Falls
ST19B	West Falls	Java
ST20A	Error	Java
ST23B	Sonyea	West Falls
ST23C	Sonyea	West Falls
ST24B		
ST25A	Java	Java
ST25B	Canadaway	Canadaway
ST26A	Canadaway	Canadaway
ST27A	West Falls	Java
ST28A	West Falls	West Falls
ST29A	West Falls	West Falls
ST30A		
ST30B	West Falls	West Falls
ST31A	West Falls	West Falls
ST33A	Java	Java
ST35A	Canadaway	Canadaway
ST35B	Canadaway	Canadaway
ST35C	Canadaway	Canadaway
ST36B	West Falls	West Falls
ST36C	West Falls	West Falls
ST37A		
ST44A	Canadaway	Canadaway
ST45A	West Falls	West Falls
ST46A	West Falls	West Falls
ST46B		
ST46C	Error	Java
ST47A	Error	West Falls
ST47B	West Falls	West Falls
ST49A		
ST49B	Canadaway/Conneaut	Conneaut
ST51A		
ST51B	Canadaway	Canadaway
ST52A	Canadaway	Canadaway
ST53A	West Falls	Java

Table S2. Bedrock Classification using the bedrock interpolation method and the geologic map method

SWIFT ID	Bedrock Classification	
	Bedrock Interpolation Method	Geologic Map Method
ST53B	Error	Java
ST54A	West Falls	Java
ST54B	Java	Java
ST55A	West Falls	West Falls
ST55A_2		
ST55B		
ST59A	Canadaway/Conneaut	Conneaut
ST60A	Canadaway	Canadaway
ST61A	Canadaway	Canadaway
ST61B	Canadaway/Conneaut	Conneaut
ST62A	Canadaway	Canadaway
ST64A	Error	Java
ST69A	Canadaway/Conneaut	Conneaut
ST72A	Java	Java
ST73A	Java	Java
ST73B	Error	Java
ST73C	Canadaway	Canadaway
ST73D		
ST75A	Java	Java
ST76A	Java	Java
ST76B	Java	Java
ST77A	Sonyea	West Falls
ST79A	Canadaway/Conneaut	Conneaut
ST82A	Canadaway	Canadaway
ST84A	Java	Canadaway
ST85A		
ST86A	Java	Java
ST86B	Java	Java
ST87A		
TI01A	Sonyea	West Falls
TI02A		
TI07A	Sonyea	West Falls
TI10A	Sonyea	Sonyea
TI10B	Sonyea	West Falls
TI11A	Genesee	Sonyea
TI11B		

Table S2. Bedrock Classification using the bedrock interpolation method and the geologic map method

SWIFT ID	Bedrock Classification	
	Bedrock Interpolation Method	Geologic Map Method
TI12A		
TI14A		
TI14B	Sonyea	Sonyea
TI14C	Sonyea	Sonyea
TI14D	Sonyea	Sonyea
TI15A	West Falls	West Falls
TI15B	Sonyea	West Falls
TI18D		
TI18E	West Falls	West Falls
TI18F		
TI20A	Sonyea	West Falls
TI20B	West Falls	West Falls
TI20C		
TI21A	West Falls	West Falls
TI21B		
TI22A	West Falls	West Falls
TI22B	Genesee	Genesee
TI22C		
TI23A	West Falls	West Falls
TI26A	West Falls	West Falls
TI28A		
TI28B		
TI30A	West Falls	West Falls
TI31A	West Falls	West Falls
TI31B	West Falls	West Falls

a

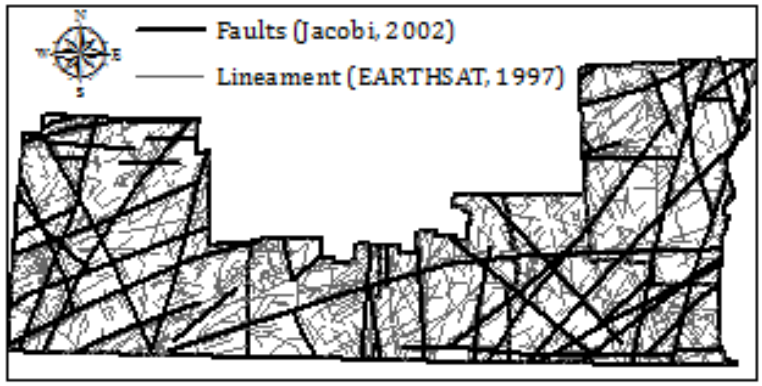

b

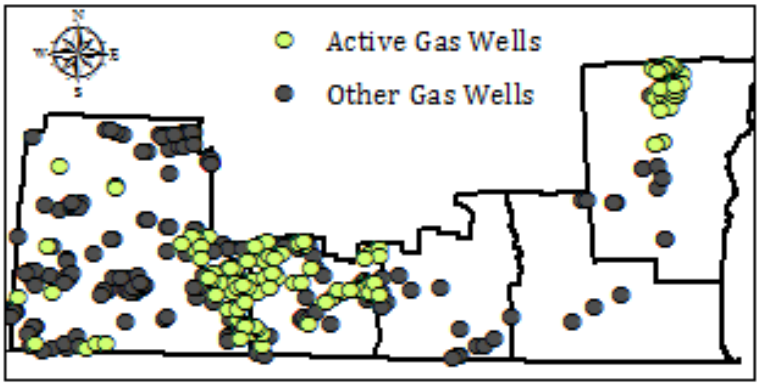

c

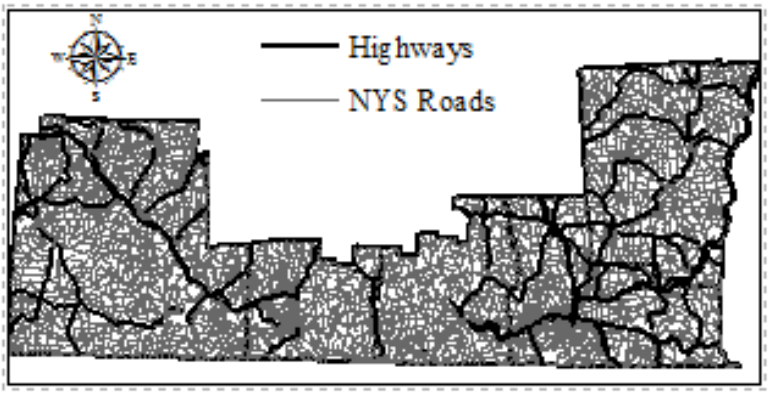

Figure S1 (a) The distribution of inferred faults(Jacobi, 2002) and lineaments (EARTHSAT, 1997). (b) Well location of active and other gas wells in NYS in 2013. (c) Highway and roads in the study area.

Methodology of Bedrock Classification using interpolation method

Contoured maps of the base elevation for the Dunkirk, Java, West Falls, Sonyea, Genesee, and Hamilton and isopach maps of the Java, West Falls, Sonyea, Genesee, and Hamilton upper Devonian geologic groups prepared by the Eastern Shale Gas Project (EGSP) and Morgantown Energy Technology Center (METC) (citation) were converted into tagged image file formats and imported into ESRI ArcGIS software. The contours for each base and isopach map were digitized and used to create a surface of triangular irregular networks (TIN) to represent the base and thickness of each aforementioned geologic group. Points representing the base elevation for the Dunkirk, Java, West Falls, Sonyea, Genesee, and Hamilton were constructed from line contours and polygons of the buried extent of each group were generated in reference to locations where the base outcropped at the surface. The spatial intersection of the base points with the buried extent with the respective geologic group was selected and exported to represent the buried surfacial extent for each formation, which was combined with the TIN isopach surface to determine the group thickness at each point location. The surface elevation of each group was calculated by adding the thickness to the base elevation at that point to create a TIN surface of the buried surface. The resulting surfaces of the base and buried surficial extent of the Java, West Falls, Sonyea, Genesee, and Hamilton and base of the Dunkirk were used to extrapolate the surface and base elevation for each group at the location of each SWIFT well.

To refine the classifications new base surfaces were created to eliminate areas of no data by determining the elevation at the contact between the base and surface of a group. An inverse weighted distance surface was created from the point elevations of the base contours generated

from EGSP maps and the contact between the base and surface of a group on a geologic map. The geologic group of well completion for each groundwater well was determined based on the elevation of the well depth as greater or less than the elevation of the surface or base geologic group. Those classified as between the base and surface of the same formation was classified as being within that formation. Wells that were missing data above a certain geologic group were classified as being above either the surface of base of the last geologic group there was information for. Using a geologic map the bedrock was determined at the location for wells missing data. Those wells identified as being above the base of a unit and classified on a geologic map as being within the same group were identified as completed in that group. Wells classified as being above the base or surface of a unit and classified on a geologic map as being within a stratigrpahically younger group were identified as every possible younger group to the outcropping bedrock. Wells above a group's surface and in the sequentially younger stratigraphic group on a geologic map were classified as in the younger unit.

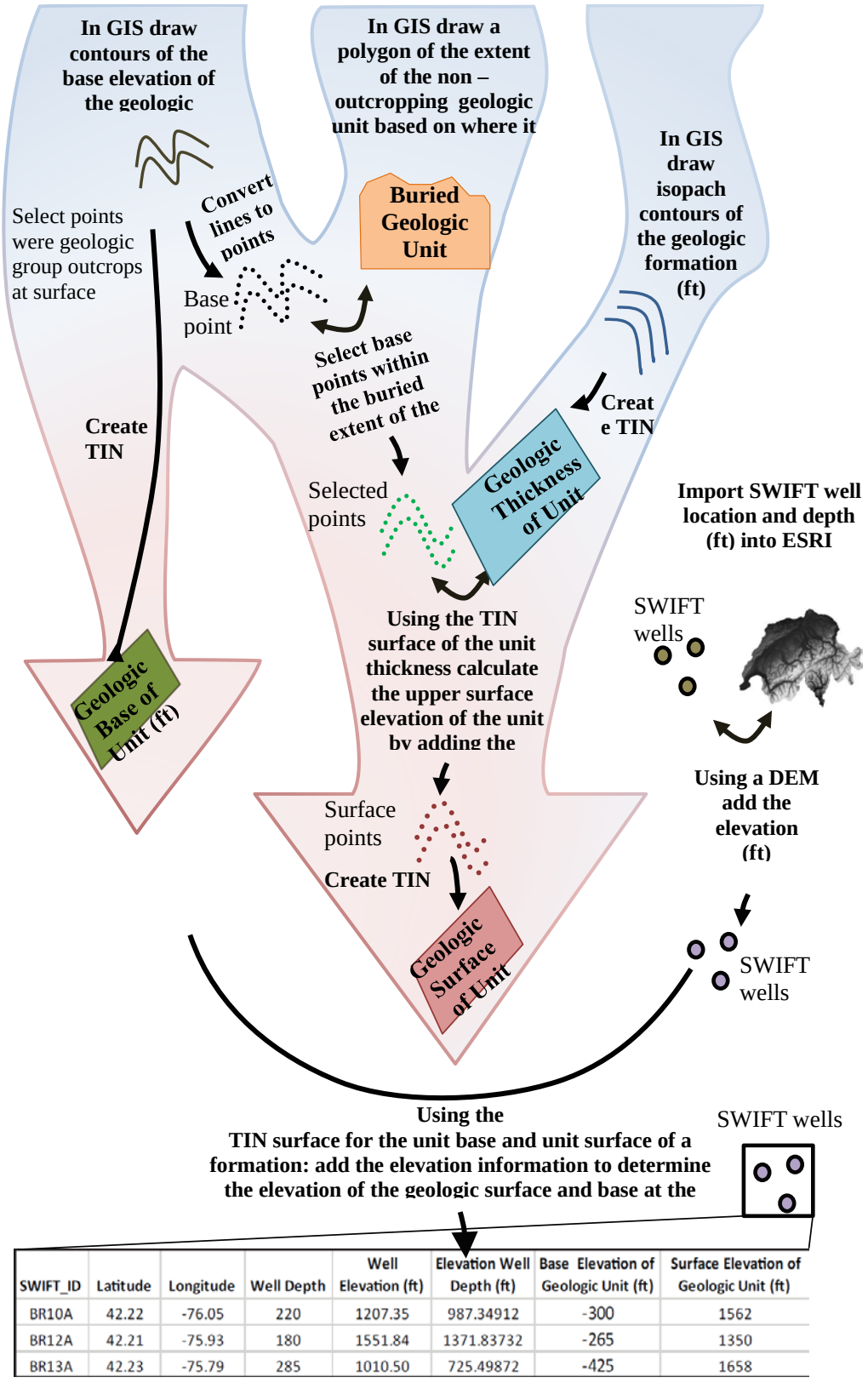

SWIFT_ID	Latitude	Longitude	Well Depth	Well Elevation (ft)	Elevation Well Depth (ft)	Base Elevation of Geologic Unit (ft)	Surface Elevation of Geologic Unit (ft)
BR10A	42.22	-76.05	220	1207.35	987.34912	-300	1562
BR12A	42.21	-75.93	180	1551.84	1371.83732	-265	1350
BR13A	42.23	-75.79	285	1010.50	725.49872	-425	1658

Figure S1. Flow chart of Bedrock Interpolation method to generate geologic surfaces

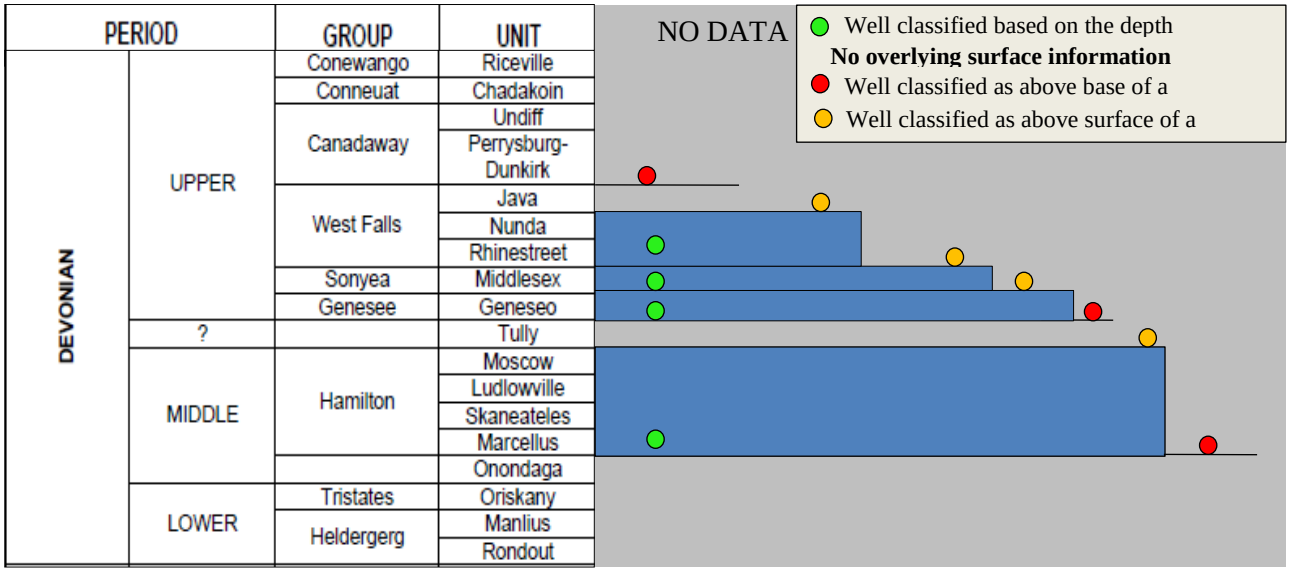

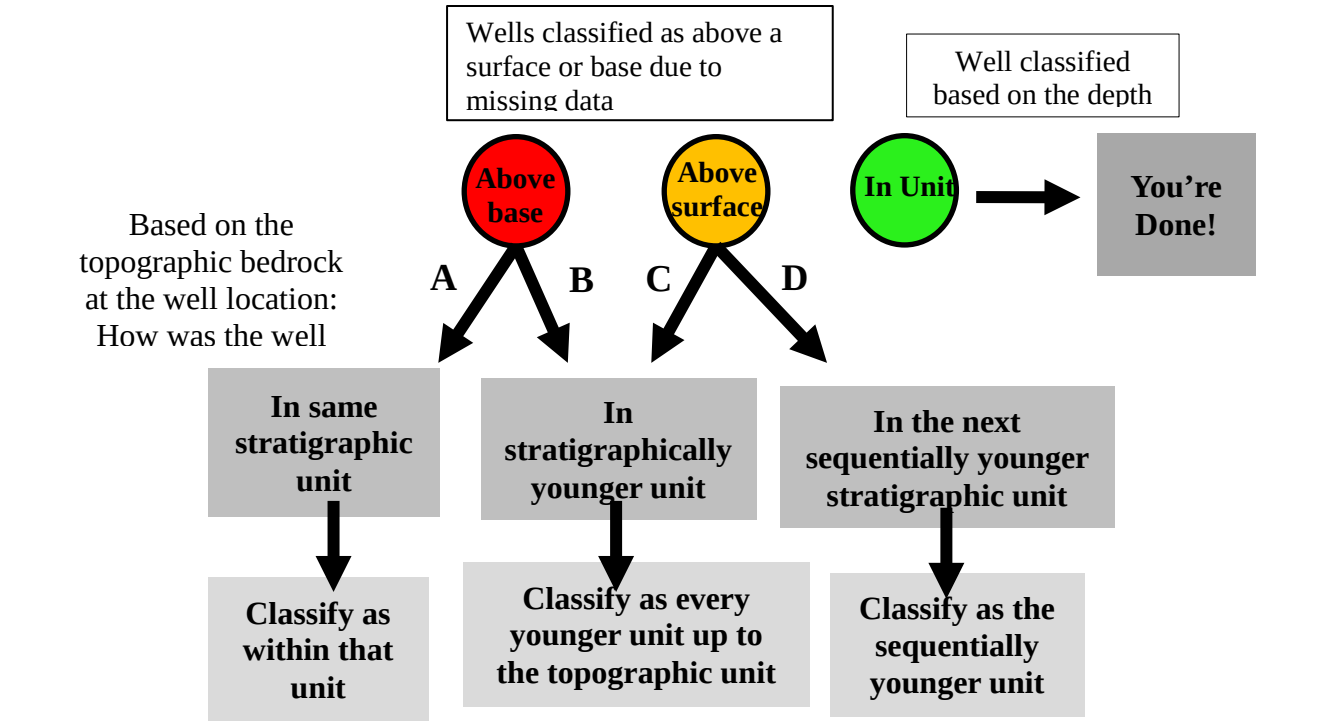

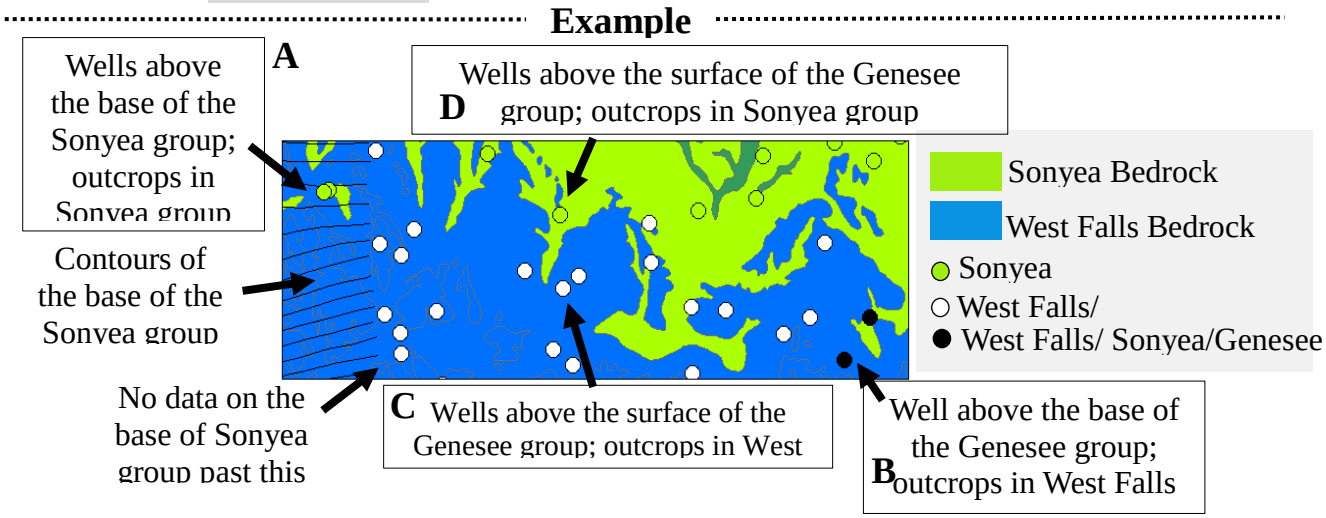

Figure S2. Decision chart for bedrock classification of groundwater wells

References

Boyer, E.W., Swistock, B.R., Clark, J., Madden, M., Rizzo, D.E., 2012. The impact of Marcellus gas drilling on rural drinking water supplies. The Center for Rural Pennsylvania.

Brantley, S. L., Yoxtheimer, D., Arjmand, S., Grieve, P., Vidic, R., Pollak, J., … Simon, C. (2014). Water resource impacts during unconventional shale gas development: The Pennsylvania experience. *International Journal of Coal Geology*, *126*, 140–156.

Davies, R. J. (2011). Methane contamination of drinking water caused by hydraulic fracturing remains unproven. *Proceedings of the National Academy of Sciences of the United States of America*, *108*(43), E871; author reply E872.

Considine, T.J., Watson, R.W., Blumsack, S. (2010). The economic impacts of the Pennsylvania Marcellus shale natural gas play: an update. Pennsylvania State University College of Earth and Mineral Sciences, Department of Energy and Mineral Engineering.

Entrekin, S., Evans-White, M., Johnson, B., & Hagenbuch, E. (2011). Rapid expansion of natural gas development poses a threat to surface waters. *Frontiers in Ecology and the Environment*, *9*(9), 503–511.

EARTHSAT, 1997. Remote Sensing and Fracture Analysis for Petroleum Exploration of Ordovician to Devonian Fractures Reservoirs in New York State. New York State Energy Research and Development Authority, Albany, NY, 35 pp

EIA (2012) Natural gas consumption by end use. U.S. Energy Information Administration. http://www.eia.gov/dnav/ng/ng_cons_sum_dcu_nus_a.htm

EIA (2014) How much natural gas is consumed in the United States? . U.S. Energy Information Administration. http://www.eia.gov/tools/faqs/faq.cfm?id=50&t=8

Eltschlager, K.K., Hawkins, J.W., Ehler, W.C., and Baldassare, Fred, 2001, Technical measures for the investigation and mitigation of fugitive methane hazards in areas of coal mining: U.S. Department of the Interior, Office of Surface Mining Reclamation and Enforcement, 125 p

Fisher, D.W., Isachsen, Y.W., and Rickard, L.V., 1970, Geologic map of New York, Hudson–Mohawk sheet*: New York State Museum and Science Service*, Map and Chart Series no. 15, 1:250,000.

Helsel, D.R., and Hirsch, R.M., 2002, *Statistical methods in water resources: U.S. Geological Survey Techniques of Water Resources Investigations*, book 4, Cpt. A3.

Heisig, P. M., & Scott, T.-M. (2013). Occurrence of methane in groundwater of south-central New York State, 2012- Systematic evaluation of a glaciated region by hydrogeologic setting. *Scientific Investigations Report, 2013-5190*.

Jackson, R. B., Vengosh, A., Darrah, T. H., Warner, N. R., Down, A., Poreda, R. J., … Karr, J. D. (2013). Increased stray gas abundance in a subset of drinking water wells near Marcellus shale gas extraction. *Proceedings of the National Academy of Sciences of the United States of America*, *110*(28), 11250–5.

Jacobi, R. D. (2002). Basement faults and seismicity in the Appalachian Basin of New York State. *Tectonophysics*, *353*(1-4), 75–113.

Jenden, P.D., D.J. Drazan, and I.R. Kaplan. 1993. Mixing of thermogenic natural gases in northern Appalachian Basin. *AAPG Bulletin* 77: 980–998.

Kamakaris, D.G., Van Tyne, A.M., 1980a. Isopach map of black shale in the Java Group (from well sample studies). New York State Museum and Science Service, Geological Survey, Office, *METC/EGSP series 106*,maps.

Kamakaris, D.G., Van Tyne, A.M., 1980b. Isopach map of black shale in the West Falls Group (from well sample studies). New York State Museum and Science Service, Geological Survey, Office, *METC/EGSP series 118*,maps.

Kamakaris, D.G., Van Tyne, A.M., 1980b. Isopach map of black shale in the Sonyea Group (from well sample studies). New York State Museum and Science Service, Geological Survey, Office, *METC/EGSP series 119*,maps.

Kamakaris, D.G., Van Tyne, A.M., 1980b. Isopach map of black shale in the Genesee Group (from well sample studies). New York State Museum and Science Service, Geological Survey, Office, *METC/EGSP series 120*,maps.

Kamakaris, D.G., Van Tyne, A.M., 1980a.. Isopach map of black shale in the Hamilton Group (from well sample studies). New York State Museum and Science Service, Geological Survey, Office, *METC/EGSP series 121*,maps.

Kappel, W. M. (2013). Dissolved Methane in Groundwater, Upper Delaware River Basin, Pennsylvania and New York, 2007-12. *USGS Open File Report 2013-1167.* Retrieved from http://pubs.usgs.gov/of/2013/1167/pdf/ofr2013-1167.pdf

Kappel, W.M., and Nystrom, E.A., 2012, Dissolved methane in New York groundwater, 1999–2011: *U.S. Geological Survey Open-File Report 2012–1162*, 6 p.,

Kargbo, D. M., Wilhelm, R. G., & Campbell, D. J. (2010). Natural gas plays in the Marcellus Shale: challenges and potential opportunities. *Environmental Science & Technology*, *44*(15), 5679–84.

Kramer, D. (2011). Shale-gas extraction faces growing public and regulatory challenges. *Physics Today*, *64*(7), 23.

Kresse, T.M., N.R. Warner, P.D. Hays, A. Down, A. Vengosh, and R. Jackson. 2012. Shallow groundwater quality and geochemistry in the Fayetteville shale gas-production area, North-Central Arkansas, 2011. *USGS Scientific Investigations Report 2012-5273*, U.S. Geological Survey, 31, Reston, Virginia: USGS.

Mathes, M. ., & White, J. . (n.d.). Methane in West Virginia groundwater. Retrieved April 4, 2015, from http://pubs.usgs.gov/fs/2006/3011/pdf/Factsheet2006_3011.pdf

McPherson, W., 1983. Hydrogeology of unconsolidated deposits in Chenango County, New York. *Water Resources Investigations Report 91-4138.*

McPhillips, L. E., Creamer, A. E., Rahm, B. G., & Walter, M. T. (2014). Assessing dissolved methane patterns in central New York groundwater. *Journal of Hydrology: Regional Studies*, *1*, 57–73.

Miller, T.S., Randall, A.D., Belli, J.L., and Allen, R.V., 1982, Geohydrology of the valley-fill aquifer in the Elmira area, Chemung County, New York: U.S. Geological Survey Open-File Report 82–110, 7 sheets, scale 1:24,000.

Molofsky, L. J., Connor, J. A., Wylie, A. S., Wagner, T., & Farhat, S. K. (2013). Evaluation of methane sources in groundwater in northeastern Pennsylvania. *Ground Water*, *51*(3), 333–49.

New York City Department of Environmental Protection, (NYCDEP). (2009). Rapid Impact Assessment Report: Impact assessment of natural gas production in the New York City water supply watershed. *Hazen and Sawyer Environmental Engineers and Scientists*.

New York State Department of Environmental Conservation (NYSDEC) (2011). *Revised Draft Supplemental Generic Environmental Impact Statement.* http://www.dec.ny.gov/energy/75370.html

Osborn, S. G., & McIntosh, J. C. (2010). Chemical and isotopic tracers of the contribution of microbial gas in Devonian organic-rich shales and reservoir sandstones, northern Appalachian Basin. *Applied Geochemistry*, *25*(3), 456–471.

Osborn, S. G., Vengosh, A., Warner, N. R., & Jackson, R. B. (2011). Methane contamination of drinking water accompanying gas-well drilling and hydraulic fracturing. *Proceedings of the National Academy of Sciences of the United States of America*, *108*(20), 8172–6.

Repetski, J.E, Ryder, R.T., Harper, J.A., and Trippi,M.H., 2008. Thermal Maturity Patterns (CAI and %Ro) in the Ordovician and Devonian Rocks of the Appalachian Basin: A Major Revision of USGS Map I-917-E using new subsurface collections. U.S Geological Survey Scientific Investigations Map 3006, one CD-ROM.

Saba, T., & Orzechowski, M. (2011). Lack of data to support a relationship between methane contamination of drinking water wells and hydraulic fracturing. *Proceedings of the National Academy of Sciences of the United States of America*, *108*(37), E663; author reply E665–6.

Schoell, M. (1980). The hydrogen and carbon isotopic composition of methane from natural gases of various origins. *Geochimica et Cosmochimica Acta*, *44*(5), 649–661.

Siegel, D. I., Azzolina, N. A., Smith, B. J., Perry, A. E., & Bothun, R. L. (2015). Methane Concentrations in Water Wells Unrelated to Proximity to Existing Oil and Gas Wells in Northeastern Pennsylvania. *Environmental Science & Technology*. 49, 4106-4112

Soeder, D. J. (2010). The Marcellus Shale: Resources and Reservations. *Eos, Transactions American Geophysical Union*, *91*(32), 277–278.

Van Tyne, A.M., 1983, Natural Gas Potential of the Devonian Black Shales of New York, *Northeastern Geology*, Vol. 5, no 3/4, p. 209-216

Van Tyne, A.M., Kamakaris, D.G., Corbo, S., 1980a. Structure contours on the base of the Dunkirk. New York State Museum and Science Service, Geological Survey, Alfred Oil and Gas Office, *METC/EGSP series 111*, 1 map.

Van Tyne, A.M., Kamakaris, D.G., Corbo, S., 1980b. Structure contours on the base of the Java Formation. New York State Museum and Science Service, Geological Survey, Alfred Oil and Gas Office, *METC/EGSP series 112*, 1 map.

Van Tyne, A.M., Kamakaris, D.G., Corbo, S., 1980c. Structure contours on the base of the West Falls Formation. New York State Museum and Science Service, Geological Survey, Alfred Oil and Gas Office, *METC/EGSP series 113*, 2 maps.

Van Tyne, A.M., Kamakaris, D.G., Corbo, S., 1980d. Structure contours on the base of the Sonyea Group. New York State Museum and Science Service, Geological Survey, Alfred Oil and Gas Office, *METC/EGSP series 114*, 2 maps.

Van Tyne, A.M., Kamakaris, D.G., Corbo, S., 1980e. Structure contours on the base of the Genessee Group. New York State Museum and Science Service, Geological Survey, Alfred Oil and Gas Office, *METC/EGSP series 115*, 2 maps.

Vengosh, A., Warner, N., Jackson, R., & Darrah, T. (2013). The Effects of Shale Gas Exploration and Hydraulic Fracturing on the Quality of Water Resources in the United States. *Procedia Earth and Planetary Science, 7*, 863–866.

Vidic, R. D., Brantley, S. L., Vandenbossche, J. M., Yoxtheimer, D., & Abad, J. D. (2013). Impact of shale gas development on regional water quality. *Science (New York, N.Y.), 340*(6134), 1235009.

Williams, J. H. (2010). *Evaluation of well logs for determining the presence of freshwater, saltwater, and gas above the Marcellus shale in Chemung, Tioga, and Broome Counties, New York. New York: Scientific Investigations Report 2010-5224, 27* (p. p.). Retrieved from http://pubs.usgs.gov/sir/2010/5224/pdf/sir2010-5224_williams_text_508.pdf

Ziemkiewicz, P. F., Quaranta, J. D., Darnell, A., & Wise, R. (2014). Exposure pathways related to shale gas development and procedures for reducing environmental and public risk. *Journal of Natural Gas Science and Engineering*, *16*, 77–84.

Vita

Kayla Christian
Email: kaylamchris@gmail.com

EDUCATION

Syracuse University, Dept. of Earth Sciences
GPA: 3.67
(M.S) Master of Science, Earth Sciences (May 2015)

University of Illinois at Chicago, Dept. of Earth and Environmental Sciences
GPA: 3.69
(B.S) Bachelor of Science, Earth and Environmental Sciences (May 2013)

EXPERIENCE

Teaching Assistant, Syracuse University January 2015-Present

Research Assistant, Syracuse University May 2013-December 2014

Physical Scientist/ Intern U.S Geological Survey, Boulder, CO. Summer 2012

PRESENTATIONS

Christian, K. Lautz, LK., Hoke, G.D., Lu, Z., Siegel, D., and Kessler, J., 2014. Salinity and Dissolved Methane Concentrations In Homeowner Wells Prior to Hydraulic Fracturing. Geological Society of America Northeastern Meeting, March 23-25, 2015: Bretton Woods, New Hampshire, USA

Christian, K. Lautz, LK., Hoke, G.D., Lu, Z., Siegel, D., and Kessler, J., 2014. Spatial Parameters Controlling Salinity and Dissolved Methane Concentrations In Private Wells Prior to Hydrualic Fracturing. Geological Society of America Annual Meeting, October 19-22, 2014: Vancouver, BC, Canada

SKILLS

ESRI ArcGIS, Matlab, Microsoft Office, Adobe Illustrator, Visual Modflow

ACTIVITIES

Graduate Student Organization Department Representative (August 2014-Present)
Project Based GIS Consulting for Environmental Law Firm
RESESS (Earth Sciences) Internship (2012)